LAPPEENRANTA UNIVERSITY OF TECHNOLOGY

SCHOOL OF TECHNOLOGY

LUT Chemtech

Master's Thesis

Anna Kuusiniemi

REVERSE OSMOSIS MEMBRANE SURFACE MODIFICATION: EFFECTS ON MEMBRANE PERFORMANCE

Helsinki 20.5.2014

Examiners: Prof. Mika Mänttäri, Dr. Tech. Arto Pihlajamäki

ABSTRACT

Lappeenranta University of Technology
School of technology
LUT Chemtech

Anna Kuusiniemi

Reverse osmosis membrane surface modification: effects on membrane performance

Master's Thesis

2014

112 pages, 59 figures, 12 tables and 8 appendices

Examiners: Prof. Mika Mänttäri
Dr. Tech. Arto Pihlajamäki

Keywords: reverse osmosis, modification, permeability, salt rejection, surfactants

The aim of this thesis was to study the surface modification of reverse osmosis membranes by surfactants and the effect of modification on rejection and flux. The surfactants included anionic and nonionic surfactants. The purpose of membrane modification was to improve pure water permeability with increasing salt rejection.

The literature part of the study deals with the basic principles of reverse osmosis technology and factors affecting the membrane performance. Also the membrane surface modification by surfactants and their influence on membrane's surface properties and efficiency (permeability and salt rejection) were discussed.

In the experimental part of the thesis two thin-film composite membranes, Desal AG and LE-4040, were modified on-line with three different surfactants. The effects of process parameters (pressure, pH, and surfactant concentration) on surface modification were also examined. The characteristics of the modified membranes were determined by measuring the membranes' contact angle and zeta potentials.

The zeta potential and contact angle measurements indicate that the surfactants were adsorbed onto the both membranes. However, the adsorption did not effect on membrane's pure water permeability and salt rejection. Thereby, the surface modification of the Desal AG and LE-4040 membranes by surfactants was not able to improve the membrane's performance.

TIIVISTELMÄ

Lappeenrannan teknillinen yliopisto
Teknillinen tiedekunta
LUT Kemiantekniikka

Anna Kuusiniemi

Käänteisosmoosikalvon pinnan modifiointi: vaikutukset kalvon suoritustehokkuuteen

Diplomityö

2014

112 sivua, 59 kuvaa, 12 taulukkoa ja 8 liitettä

Tarkastajat: Professori Mika Mänttäri
TkT Arto Pihlajamäki

Hakusanat: käänteisosmoosi, modifiointi, permeabiliteetti, suolan pidätys, pinta-aktiivisuusaineet

Työn tarkoituksena oli tutkia käänteisosmoosikalvojen pinnan modifiointia pinta-aktiivisuusaineilla ja modifioinnin vaikutusta vuohon ja retentioon. Käytetyt pinta-aktiivisuusaineet olivat anionisia ja nonionisia. Kalvon modifioinnin tarkoituksena oli parantaa puhtaan veden permeabiliteettia kasvattaen samalla suolan pidätystä.

Kirjallisuusosa käsitteli käänteisosmoosi-tekniikan perusteita ja tekijöitä, jotka vaikuttavat kalvojen suorituskykyyn. Myös pinnan modifiointia pinta-aktiivisuusaineilla ja niiden vaikutuksia kalvopinnan ominaisuuksiin ja tehokkuuteen (permeabiliteetti ja suolan pidätys) käsiteltiin.

Työn kokeellisessa osassa kahta ohutkomposiittikalvoa, Desal AG ja LE-4040, modifioitiin online-mittauksena kolmella pinta-aktiivisuusaineella. Prosessiparametrien (paine, pH ja pinta-aktiivisuusainepitoisuus) vaikutuksia pinnan modifiointiin myös tutkittiin. Modifioitujen kalvojen ominaisuuksia määritettiin kontaktikulma- ja zeta-potentiaali mittauksilla.

Zeta-potentiaali- ja kontaktikulmamittaukset osoittivat, että pinta-aktiivisuusaineet adsorboituivat molempien kalvojen pinnalle. Pinta-aktiivisuusaineiden kiinnittyminen ei kuitenkaan vaikuttanut kalvojen permeabiliteettiin ja suolan pidätykseen. Täten Desal AG- ja LE-4040-kalvojen pinnan modifioinnilla ei onnistuttu parantamaan kalvojen suorituskykyä.

FOREWORDS

This Master's Thesis was a part of Kemira's research project. I would like to thank D.Sc. Samantha Kiljunen for the chance to work in this very interesting subject. I would also like to thank D.Sc. Mehrdad Hesampour and D.Sc. Tarja Turkki for the guidance. Special thanks for D.Sc. Tom Lundin for all the advices and enthusiasm for my thesis.

I would like to thank my supervisors Prof. Mika Mänttäri and Dr.Tech. Arto Pihlajamäki for the guidance and help during my thesis. I would also like to thank Prof. Heli Sirén for her advices.

The greatest thanks for the support and encouragement during my thesis go to Jari. I would like to thank my family for all the support I have received during my studies. Thanks also for my lovely friends.

Anna Kuusiniemi

Helsinki, May 2014

TABLE OF CONTENTS

TABLE OF FIGURES
SYMBOLS
ABBREVATIONS

1 INTRODUCTION 11
1.1 Study approach and restrictions 11
1.2 Structure of the thesis 13
2 REVERSE OSMOSIS DESALINATION 14
2.1 Separation mechanism of the RO membrane 15
2.2 Transport mechanisms of the RO membrane 17
2.3 RO membrane structures 21
2.4 RO membrane materials for desalination 23
2.5 RO membrane fouling mechanisms 25
2.5.1 Adsorption 27
2.5.2 Scaling 28
2.5.1 Concentration polarization 29
3 FACTORS THAT AFFECT RO MEMBRANE PERFORMANCE 31
3.1 Feed water composition 31
3.1.1 Foulant type 32
3.1.2 Concentration 33
3.1.3 Ionic strength 35
3.1.4 pH 37
3.2 Membrane surface properties 38
3.2.1 Hydrophilicity 39
3.2.2 Charge 39
3.2.3 Roughness 41
3.3 Hydrodynamic conditions 42
3.3.1 Temperature 42
3.3.2 Pressure 44
3.3.4 Cross flow velocity 44
4 SURFACE MODIFICATION OF REVERSE OSMOSIS MEMBRANES 46
4.1 Surfactants 47
4.2 Adsorption of surfactants 48
4.2.1 Adsorption of anionic surfactants 50
4.2.2 Adsorption of cationic surfactants 53

4.2.3 Adsorption of nonionic surfactants 54
5 INFLUENCES OF SURFACTANT ADSORPTION ON MEMBRANE PERFORMANCE 56
5.1 Hydrophilicity of membrane 56
5.2 Changes in membrane charge 58
5.3 Surface roughness 60
5.4 Flux and salt rejection 61
EXPERIMENTAL PART 64
6 AIM OF THE EXPERIMENTAL PART 64
7 MATERIALS AND METHODS 65
7.1 Feed solution chemistries 65
7.2 Selected membranes 66
7.3 Filtration equipment 68
7.4 Membrane pretreatment and modification with surfactants 70
7.5 Filtration experiments 71
7.5.1 Filtration procedure 1 71
7.5.2 Filtration procedure 2 72
7.5.3 Filtration procedure 3 72
7.6 The adsorption test of surfactants onto membrane surface 73
8 ANALYZING METHODS OF WATER SAMPLES AND MEMBRANE SURFACE 74
8.1 Analyses of the water samples 74
8.2 Analyses of the membrane surface 74
9 EQUATIONS 77
10 RESULTS AND DISCUSSION 78
10.1 The filtration of modified Desal AG membrane with surfactant 1 78
10.1.1 Zeta potential measurements of Desal AG membrane 79
10.1.2 Contact angle of Desal AG membrane 80
10.1.3 The effect of applied pressure and surfactant concentration on permeability 81
10.2 The effects of surfactant dosing on PWP 82
10.3 The effect of solution pH on adsorption of surfactants onto LE-4040 membrane by contact angle measurements 84
10.4 The effect of modification pH on PWP and salt rejection of LE-4040 membrane 86
10.4.1 Zeta potential measurements of LE-4040 membrane 86
10.4.2 The effect of anionic surfactants on water permeability in the presence of marine salt 91

10.4.3 The effect of nonionic surfactant on water permeability in the presence of marine salt 93
10.4.4 The effect of modification pH on water permeability in the presence of marine salt 94
10.4.5 The effect of membrane modification on the salt rejection 96
10.3.6 Pure water flux after salt addition 100
11 POSSIBLE SOURCES OF ERROR 102
12 SUMMARY AND CONCLUSIONS 103
REFERENCES 105

TABLE OF FIGURES

Figure 1. The aim of this study 12
Figure 2. Schematic of separation process of RO membrane 15
Figure 3. Separating capacity of pressure-driven membrane processes 16
Figure 4. The effect of applied pressure and osmotic pressure on water flow 18
Figure 5. Fluxes and salt rejection of seawater Film Tec FT-30 membrane 20
Figure 6. Structure of traditional TFC RO membrane 23
Figure 7. The polyamide RO barrier layer 24
Figure 8. Flux decrease due to fouling and concentration polarization 26
Figure 9. The mass transfer resistances in pressure driven membrane processes 27
Figure 10. Concentration polarization under steady-state conditions 30
Figure 11. The salt flux at different feed salt concentrations 34
Figure 12. The Donnan potential of negatively charged membrane 35
Figure 13. The repulsive force of the membrane's negative charge 36
Figure 14. The negatively charged membrane shielded by divalent cations 36
Figure 15. The influence of feed water pH on RO membrane flux 38
Figure 16. The ion transport through polyamide TFC membrane 41
Figure 17. The theoretical effects of temperature 43
Figure 18. The effect of cross flow velocity on flux 45
Figure 19. Schematic illustration of surfactant 47
Figure 20. Surfactant adsorption on non-polar and polar surfaces 49
Figure 21. The effect of SDS on the zeta potential of TFC RO membrane 51
Figure 22. Illustration of the adsorption of SDS onto polymeric surface 52
Figure 23. The effect of SDS on zeta-potential of NF-55 membrane 53
Figure 24. Illustration of the adsorption of DTAB onto polymeric surface 53
Figure 25. The effect of DTAB on zeta potential of NF-55 membrane 54

Figure 26. Schematic illustration of the adsorption of nonionic surfactants 55
Figure 27.The relative flux of NF membranes in the presence of surfactant 57
Figure 28. Illustration of the adsorption of nonionic surfactant adsorption 57
Figure 29. The effect of SDS and DTAB on the zeta potential of RO membrane 59
Figure 30. The permeate flux of the RO membranes during fouling 60
Figure 31. The effect of SDS on flux and salt rejection of TFC RO membrane .. 62
Figure 32. The effect of SDS on flux and salt rejection of CA RO membrane 63
Figure 33. Molecular structures of salts 66
Figure 34. T he zeta-potentials of Desal AG and LE-4040 membranes..... 68
Figure 35. DSS Labstak M20 filtration unit 69
Figure 36. The filtration and permeation plates of DSS filter 70
Figure 37. The flow diagram of DSS filter..... 70
Figure 38. The contact angle measurement of sessile drop method 75
Figure 39. Drawing of electrokinetic analyzer 76
Figure 40. Drawing of measuring cell of electrokinetic analyzer 76
Figure 41. The zeta potential of modified Desal AG membrane..... 80
Figure 42. The permeability of modified Desal AG membrane 82
Figure 43. The permeability of modified LE-4040 membrane with surf. 1,2,3 83
Figure 44. The permeability of modified LE-4040 membrane with surf. 1,2,3 84
Figure 45. The zeta potential of modified LE-4040 membrane with surf. 1,2,3 ... 87
Figure 46. The zeta potential of modified LE-4040 membrane with surf. 1,2 88
Figure 47. The zeta potential of modified LE-4040 membrane with surf. 3 89
Figure 48. The zeta potential of LE-4040 membrane in the presence of salt 90
Figure 49. The zeta potential of modified LE-4040 membrane with surf. 1 91
Figure 50. The permeability of modified LE-4040 membrane with surf. 1,2 92
Figure 51. The permeability of modified LE-4040 membrane with surf. 3 93
Figure 52. The effect of modif. pH on the permeability of LE-4040 membrane .. 95
Figure 53. The effect of modif. pH on the permeability of LE-4040 membrane . 97
Figure 54. The salt rejections of modified LE-4040 membranes 97
Figure 55. The salt rejections of modified LE-4040 membrane with surf. 3 98
Figure 56. The fluxes of modified LE-4040 membrane with surf. 3..... 98
Figure 57. The salt rejections of modified LE-4040 membrane with surf. 1,2 99
Figure 58. The fluxes of modified LE-4040 membrane with surf. 1,2..... 100
Figure 59. The pure water fluxes of modified LE-4040 membranes 101

SYMBOLS

A	the membrane area,	m^2
A_w	water permeability coefficient,	$m^3/ (m^2 s\ bar)$
a	the width of a rectangular cross-section,	m
a_{sp}	the particle specific surface area,	m^2/g
B	solute (salt) permeability coefficient,	m/s
b	the height of a rectangular cross-section,	m
C	the solute concentration,	moles/L
ΔC_s	the salt concentration difference,	kg/m^3
c	the equilibrium concentration,	mg/mL
c_0	the concentration before adsorption	mg/mL
c_m	the salt concentration at the membrane interface,	kg/m^3
c_f	the solute (salt) concentration in the feed stream,	kg/m^3, g/L
c_p	the solute (salt) concentration in the permeate stream,	kg/m^3, g/L
c_w	the concentration of water,	kg/m^3
D	diffusion coefficient,	m^2/s
D_s	solute (salt) diffusion coefficient,	m^2/s
D_w	water diffusion coefficient,	m^2/s
dc	the concentration,	kg/m^3
i	the number of ions,	-
J	permeate flux,	$L/ (h\ m^2)$, m/s
J_s	the solute (salt) flux,	m/s
J_w	the water flux	m/s
K_s	the solute (salt) distribution coefficient,	-
m	the mass of permeate,	kg
m_p	the particle amount,	g
n	the number of channels,	-
P	permeability,	$L/ (h\ m^2\ bar)$
p	pressure,	bar
Δp	transmembrane pressure difference,	bar
R	retention,	%
R_i	ideal gas constant	L bar/ (mol K)
r_{int}	intrinsic retention,	-
T	operating temperature,	K
t	time,	h
U	linear flow velocity,	m/s
V	volumetric flow rate,	m^3/s
V_b	the molar volume of pure water,	L/mole
V_s	the solution volume,	mL
V_w	the water molar volume,	m^3/mole
x_w	the mole fraction of water,	moles/mole
dx	the distance,	m
Δx	the thickness of the membrane,	m
π	the osmotic pressure	bar
$\Delta\pi$	the osmotic pressure difference	bar
θ	the contact angle,	°
ϕ	unitless osmotic coefficient,	-
ρ	the density of water,	$1000\ kg/m^3$
Γ	the amount of adsorption	mg/m^2

γ_{lv}	the surface tension of liquid/gas interface	N/m
γ_{sl}	the surface tension of solid/liquid interface	N/m
γ_{sv}	the surface tension of solid/gas interface	N/m

ABBREVATIONS

BW	brackish water
CDA	cellulose diacetat
CEOP	cake-enhanced osmotic pressure
CMC	critical micelle concentration
CTA	cellulose triacetate
DOC	dissolved organic carbon
DTAB	dodecyl trimethylammonium bromide
ED	electrodialysis
EPS	extracellular polymeric substances
HMC	hemi micelle concentration
MED	multi-effect distillation
MF	microfitration
MPD	m-phenylenediamine
MSF	multi-stage flash distillation
MWCO	molecular weight cut off
NF	nanofiltration
NOM	natural organic matter
PA	polyamide
PWP	pure water permeability
RO	reverse osmosis
SDI	silt density index
SDS	sodium dodecyl sulfate
SW	sea water
TDS	total dissolved solids
TFC	thin-film composite
TMC	trimesoyl chloride
TOC	total organic carbon
UF	ultrafiltration
VCD	vapour compression distillation
WHO	world health organization

1 INTRODUCTION

The production of potable water has become a worldwide concern. The demand of clean drinking water has increased because of population growth. Approximately 41 % of the world population suffers lack of water and over 1 billion people are completely without clean drinking water [1]. Traditional fresh water sources such as rivers, lakes and, groundwater are decreasing or becoming saline because of misuse or overuse of fresh water. The solutions for new water resources are water reuse and salt water desalination. [2]

Desalination processes such as thermal (distillation) and membrane processes have become important methods for drinking water productions. Membrane processes have rapidly developed since the 1960s and now they are more popular in new plant installations than thermal processes. [2]

Usable membrane processes for desalination are reverse osmosis (RO), nanofiltration (NF) and electrodialysis (ED) [2]. Nowadays RO is the most important desalination technology [3]. RO membranes can reject monovalent ions such as chloride and sodium, and salt rejections of seawater can be greater than 99 % [2].

Despite of good performance of RO membrane processes, the main disadvantage is fouling. The fouling of RO membranes declines process productivity by causing flux decline and, therefore, a need of higher pressure, and more energy are needed to achieve the desired throughput. [4] One way to enhance membrane efficiency (permeability and salt rejection) and prevent fouling is to modify the surface of membranes. Generally it is assumed that smooth, more hydrophilic and lower surface charge of membranes provides better anti-fouling properties [5].

1.1 Study approach and restrictions

This thesis was a based on a project conducted and funded by Kemira Oyj. Kemira is a global chemical company with an extensive experience in industrial water treatment. Kemira offers water treatment chemicals and innovative solutions for raw water, process water and wastewater.

The purpose of this thesis was to study the modification of RO membranes by adding surfactants into the feed solution by means to improve the membrane efficiency. The effects of modification were studied by measuring the permeability and salt rejection of membranes. In this thesis the permeability means the pressure normalized flux. Furthermore, the effects of process parameters (pressure, pH, and surfactant concentration) were also evaluated. The characteristics of the modified membranes were defined by measuring the contact angle and zeta potentials of membranes. In this study the contact angle means the contact angle between water and membrane surface. Figure 1 presents the idea of this study.

In the present study, two RO membranes were modified with three different surfactants aiming to increase membrane permeability and salt rejection. The surfactants include two anionic and one nonionic surfactant.

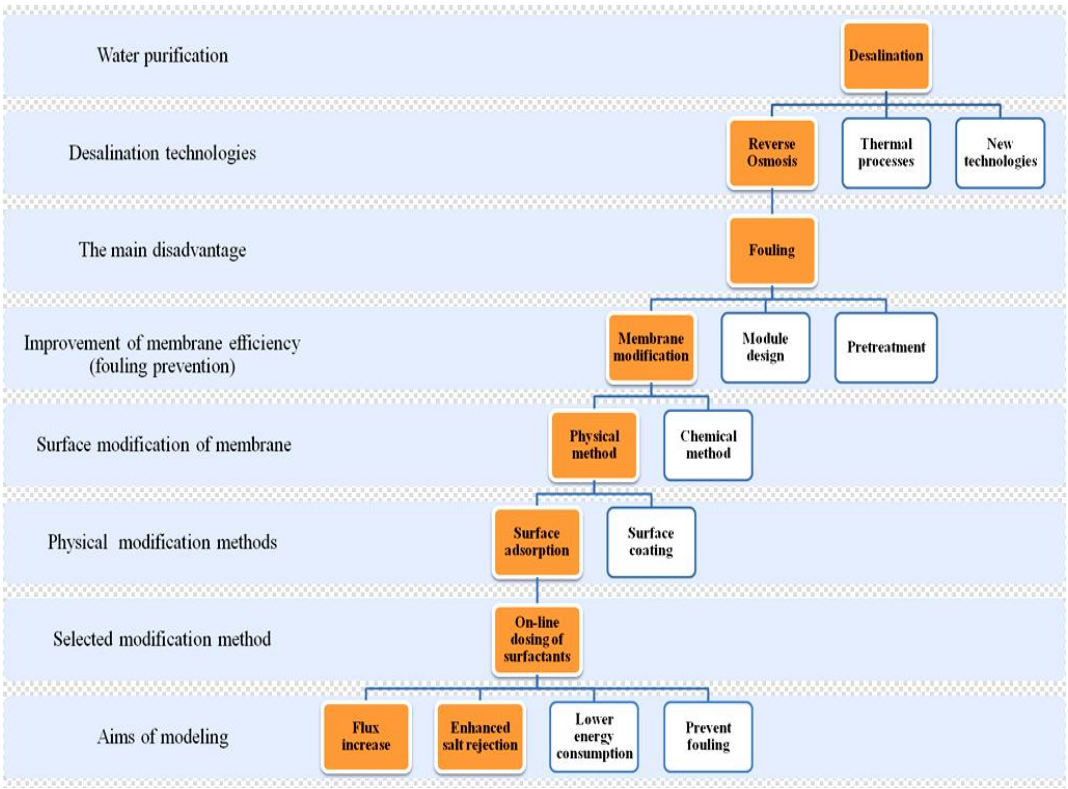

Figure 1. The aim of this study. The colored boxes represent the content of which this study is focused on.

1.2 Structure of the thesis

The literature part of the study deals with the basic principles of RO technology, fouling mechanisms of desalination and factors that affect the RO technology performance and efficiency. In addition, membrane surface modification by surfactants and the influence of modification on membrane surface properties and its efficiency (permeability and salt rejection) is discussed.

The theory part starts with the introduction to the RO membrane process, its transport mechanisms and the membrane structures. As fouling is the main disadvantage of membranes that reduces its efficiency and membrane's operating lifetime, it is therefore discussed at this point also.

In the next chapter, the factors that affect membrane process efficiency like the feed solution properties (foulants, concentration, ion strength, and pH), membrane surface characteristics (hydrophilicity, charge and roughness) and hydrodynamic conditions (temperature, pressure, cross-flow velocity) are discussed. The influence of these factors on fouling is also evaluated, because fouling reduces remarkably membrane efficiency. The following chapter deals with modification of membranes by surfactants. At the end, the influences of surfactants onto membrane surface and efficiency are being dealt.

The experimental part of thesis consists a description of used membranes and compounds and the used filtration and analysis equipment. Also, the filtration and analysis methods are described. Finally, the result of filtrations and analysis of the membrane's character are discussed.

2 REVERSE OSMOSIS DESALINATION

Desalination technologies can be divided into thermal and membrane processes based on their separation mechanisms. Thermal desalination technologies are multi-stage flash distillation (MSF), multi-effect distillation (MED), and vapour compression distillation (VCD). Membrane based desalination technologies are reverse osmosis (RO), nanofiltration (NF), and electrodialysis (ED). From these technologies, RO and MSF are most widely used. [6] Nowadays membrane technologies have overtaken the conventional thermal processes because of their simplicity and efficiency and RO is the leading desalination technology [3, 7–10].

The RO technology has proved to be the lowest energy consuming technique compared to other desalination processes [6]. It consumes about a half of the energy used in thermal processes. Other advantages are low investment cost at low capacities, ease of operation, flexibility in capacity expansion, operation at ambient temperature, and short construction periods. [7] Despite the advantages, thermal desalination can deal more saline waters and deliver higher permeate quality than RO [6]. Table I illustrates the procedure of Fritzmann *et al.* [6], who gathered key operational data for thermal and membrane based desalination technologies.

Table I Comparison of operation data of thermal (MSF) and membrane based (RO, electrodialysis) desalination technologies [11, 12]

	MSF	RO	Electrodialysis
Thermal energy consumption [kWh/m^3]	12	-	-
Electrical energy [kWh/m^3]	35	0.4–7	1
Typical salt content of raw water [ppm]	30 000–100 000	1000–45 000	100–3000
Product water quality [ppm TDS]	<10	<500	<500

It will be expected that RO maintains its leadership in the near future, even if new investigated technologies such as electrodialysis, membrane distillation, capacitive deionization and forward osmosis exists. Commercial interest in RO technology has been increased globally due to continuous process improvements which lead to significant cost reductions. These improvements consist of developments in membrane material, module and process design, feed pre-treatment, and energy recovery or reduction in energy consumption. [3]

2.1 Separation mechanism of the RO membrane

The RO is a pressure driven membrane process that can be used to purify or concentrate a dilute solution. The RO membrane acts as a semi-permeable barrier allowing particular species (water) to pass through the membrane while the others (salt) are partially or completely retained. [8, 10, 13] The solvent stream that passes through the membrane is called permeate, and the stream that is blocked by the membrane is called retentate (see Figure 2) [8, 14]. Membranes can be used either in dead-end filtration, where the feed flows normal to the filter media, or in cross-flow filtration, where the feed flows across to the filter media [2, 8]. Usually RO membranes are operated in cross-flow mode and are most often available in spiral wound modules, where the membrane sheets are wound around an inner tube that collects the permeate [3, 14].

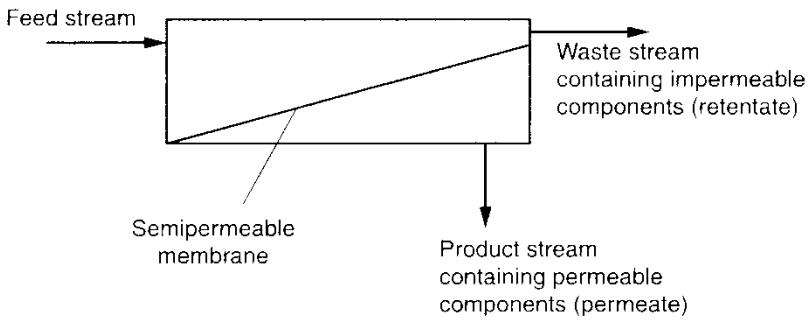

Figure 2. Schematic of separation process of RO membrane [14].

The separation characteristics of membranes depend on their chemical structure [10]. Compared to other pressure driven based membranes, the RO membrane structure is denser, allowing it to separate smaller contaminants such as monovalent ions (see Figure 3). Because of the denser membrane structure, the resistance of the membrane mass transfer is higher. Thus, the applied pressure must be higher in order to get the same amount of flux through the membrane. [8] A comparison between the reverse osmosis (RO, NF) and membrane filtration (microfiltration (MF), ultrafiltration (UF)) is given in Table II.

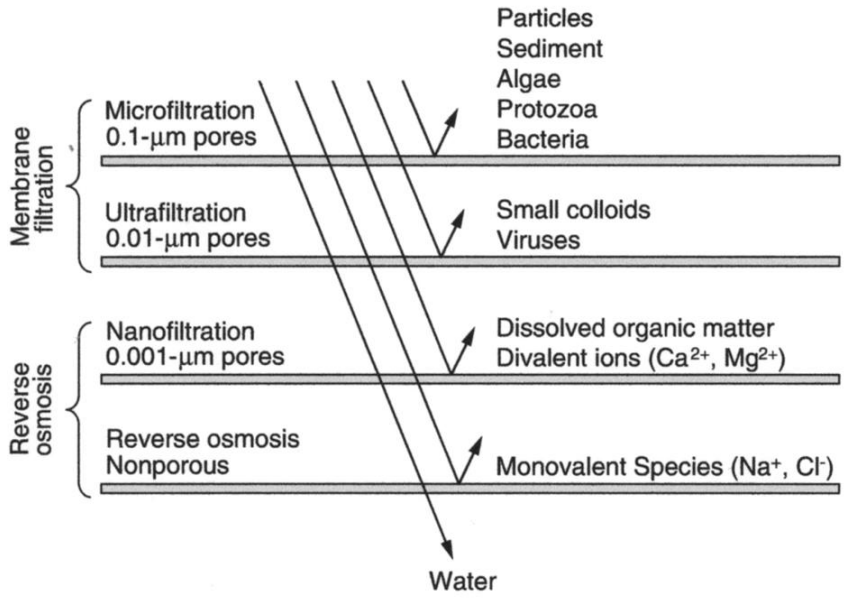

Figure 3. Separating capacity of pressure-driven membrane processes [14].

Table II Comparison between reverse osmosis (RO, NF) and membrane filtration (MF, UF) characteristics [14].

Process Characteristic	Membrane Filtration	Reverse Osmosis
Objectives	Particle removal, microorganism removal	Seawater desalination, brackish water desalination, softening, NOM removal for DBP control, specific contaminant removal
Membranes types	Microfiltration, ultrafiltration	Nanofiltration, reverse osmosis
Typical source water	Fresh surface water (TDS < 1000 mg/L)	Ocean or sea water, brackish groundwater (TDS = 1000–20,000 mg/L), colored groundwater (TOC > 10 mg/L)
Membrane structure	Homogeneous or asymmetric	Asymmetric or thin film composite
Most common membrane configuration	Hollow fiber	Spiral wound
Dominant exclusion mechanism	Straining	Differences in solubility or diffusivity
Removal efficiency of targeted impurities	Frequently 99.9999% or greater	Typically 50–99%, depending on objectives
Most common flow pattern	Dead end	Tangential
Operation includes backwash cycle	Yes	No
Influenced by osmotic pressure	No	Yes
Influenced by concentration polarization	No	Yes
Noteworthy regulatory issue	Integrity monitoring	Concentrate disposal
Typical transmembrane pressure	0.2–1 bar (3–15 psi)	5–85 bar (73–1200 psi)
Typical permeate flux	30–170 $L/m^2 \cdot h$ (18–100 $gal/ft^2 \cdot d$)	1–50 $L/m^2 \cdot h$ (0.6–30 $gal/ft^2 \cdot d$)
Typical recovery	>95%	50% (for seawater) to 90% (for colored groundwater)
Competing processes	Granular filtration	Carbon adsorption, ion exchange, precipitative softening, distillation

2.2 Transport mechanisms of the RO membrane

Transport through the RO membranes is controlled by diffusion. Pore flow cannot exist due to nonporous active layer. [2] This transport mechanism is called solution-diffusion model which was originally described by Londale *et al.* [15]. In the solution-diffusion model, the transport of water across the membrane occurs in three separate steps: absorption onto the membrane surface, diffusion through membrane thickness and, desorption from the membrane permeate surface. When the water molecule is absorbed onto the membrane surface, the concentration gradient of water across the membrane causes the water molecules to diffuse down the concentration gradient to the permeate side of the membrane. Then the water molecules desorb from the membrane to the bulk permeates. [2] The same holds true also for the solutes [16].

The solution-diffusion model predicts that separation occurs because of the solute's diffusivity and solubility or both are much lower than those of water. Thereby the solute concentration in the permeate is lower than in the feed. [14] Thus, the separation performance of the RO membrane is determined by the difference between solvent and solute permeability [17].

The RO membrane process is operated by achieving a hydrostatic pressure that is higher than the osmotic pressure of the solution. The positive difference in the pressure creates a chemical potential difference (concentration gradient) across the membrane that transports liquid through the membrane against natural direction of *osmosis*, while the salts are retained and concentrated onto the membrane surface. Though, some of the salt passes through the membrane which can be increased with salt concentration and temperature. [2]

The *osmosis* refers to the net movement of water through a partially permeable membrane into an area of higher concentration. If the applied pressure is higher than the osmotic pressure, the process can be reversed: water flows from the concentrated solution to the dilute solution. This process is known as reverse osmosis and it is featured in Figure 4 [8]. When the applied pressure is higher than the osmotic pressure, water flows from the concentrated solution to the dilute

solution (from right to left). On the other hand, when the osmotic pressure is higher, water flows from the dilute solution to the concentrated solution (from left to right). From the graph, it can be seen that when the osmotic pressure is equal to the applied pressure, no water flux is formed.

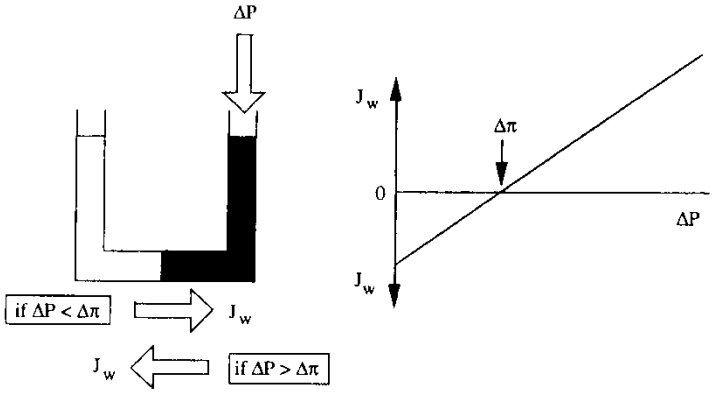

Figure 4. Schematic drawing of the effect of applied pressure (ΔP) and osmotic pressure (Δπ) on water flow (J_W) [8].

In the solution-diffusion model, the transport of solvent and solute are independent [14]. The mass transfer of solvent (in this case water) through RO membrane is linearly proportional to the effective pressure difference across the membrane as it can be seen from the following equation [2, 8, 14, 16]:

$$J_w = A_w(\Delta p - \Delta\pi) \tag{1}$$

where
J_w water flux, m/s
A_w water permeability coefficient, $m^3/(m^2 s\ bar)$
Δp transmembrane pressure difference, bar
$\Delta\pi$ the osmotic pressure difference, bar

The water permeability coefficient depends on the membrane characteristics and can be described by the following equation [8]

$$A_w = \frac{D_w \cdot c_w \cdot V_w}{R_i \cdot T \cdot \Delta x} \quad (2)$$

where
- D_w water diffusion coefficient, m^2/s
- c_w the concentration of water, kg/m^3
- V_w the water molar volume, m^3/mole
- R_i ideal gas constant, L bar/(moles K) or J/(moles K)
- T operating temperature, K
- Δx the membrane thickness, m

The solute flux across the membrane is proportional to the effective solute concentration difference across the membrane [8, 16].

$$J_s = B(c_f - c_p) \quad (3)$$

where
- J_s the solute (salt) flux, m/s
- B solute (salt) permeability coefficient, m/s
- c_f the solute (salt) concentration in the feed stream, kg/m^3
- c_p the solute (salt) concentration in the permeate stream, kg/m^3

The solute permeability coefficient is described by [2, 8]

$$B = \frac{D_S \cdot K_S}{\Delta x} \quad (4)$$

where
- D_s solute (salt) diffusion coefficient, m^2/s
- K_s the solute (salt) distribution coefficient between the solution and membrane phases, -

With highly selective membranes the solute flux can be neglected, thus water flux can be considered as the total flux [8].

$$J_{total} = J_w + J_s \approx J_w \quad (5)$$

Figure 5 shows water and salt fluxes and salt rejection of seawater Film Tec FT-30 membrane as a function of applied pressure [16]. It can be seen that, there is no water flux until the applied pressure exceeds the osmotic pressure in the solution (as well it was seen from the graph in Figure 4). The water flux increases linearly with the increasing pressure, as it was assumed in Equation 1. Unlike the water

flux, the salt flux seems to remain constant while the applied pressure increases. Simultaneously, more water passes through the membrane relative to the salt concentration. This leads to conclusion that the salt concentration in permeate should decrease by increasing the applied pressure and the salt retention should increase as in the lower graph in Figure 5 [16].

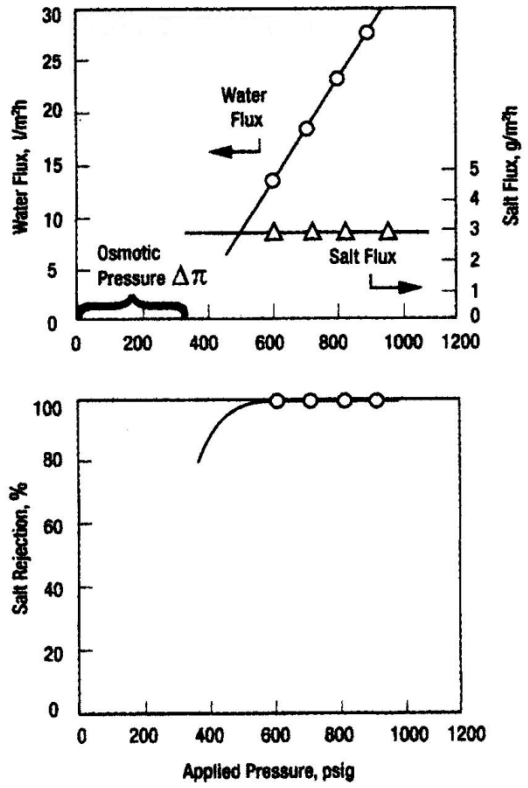

Figure 5. Water and salt fluxes and salt rejection of seawater Film Tec FT-30 membrane in the presence of 35 000 ppm (3.5 %) of sodium chloride (osmotic pressure ~25 bar) [18].

The osmotic pressure depends on the solution temperature and its concentration [2]. Thermodynamically, the osmotic pressure can be defined with the following equation [6, 14]:

$$\pi = -\frac{R_i \cdot T}{V_b} \ln (x_w) \tag{6}$$

where π the osmotic pressure, bar
V_b the molar volume of pure water, L/mole
x_w the mole fraction of water, moles/mole

For an ideal dilute solution, the relationship is described as follows [2, 6, 14]:

$$\pi = CR_iT \tag{7}$$

where C the solute concentration, moles/L

However, the dilute solutions are not often the case with the RO system. To account for the assumption of diluteness, the non-ideal behavior of the concentrated solutions, and the liquid compressibility at high pressure, the non-idealic coefficient must be included into the equation. Dissociation of solutes influences also the mole fraction of water. For example, 1 mole of NaCl produces 2 moles of ions in solution, thus doubling the osmotic pressure compared to a solute that does not dissociate. [14] Incorporating the osmotic coefficient and the dissociation of solutes into the van't Hoff equation (Equation 7) gives [6, 14]

$$\pi = i\phi CR_iT \tag{8}$$

where i number of ions produced during dissociation of solute, -

ϕ unitless osmotic coefficient, -

Typical osmotic pressure for seawater is 2300 kPa (concentration 32g/L) and for brackish water from 100 to 300 kPa (concentration 2–5 g/L) [19].

2.3 RO membrane structures

The membrane structure also has a major effect on the separation mechanism. The flux through the membrane is approximately inversely proportional to the membrane thickness. Thereby, the flux can be increased by reducing membrane thickness. Most of the commercial RO membranes have an asymmetric structure with a thin dense top layer (thickness ≤ 1µm) supported by a porous sub-layer (thickness ≈50–150 µm). The resistance of the membrane mass transfer is mainly determined by the top layer. [8]

Asymmetric membranes can be divided to (integral) asymmetric membranes and composite membranes. Integral asymmetric membranes are prepared by the

phase-inversion. The top layer and a sub-layer are composed of the same material. Composite membranes consist of a top layer and a sub-layer those are composed of different polymeric materials. [8] Thus, each layer can be optimized separately which allows optimization of the overall composite membrane structure, permeability, selectivity, and stability [8, 20]. Composite membranes are produced by preparation of the porous sub-layer, which is then laminated by dip-coating, in-situ polymerization, interfacial polymerization, or plasma polymerization on the top of the sub-layer [8, 21]. The composite membrane's selectivity is determined by the thin top layer, whereas the porous sub-layer acts as a support. The typical support material is an asymmetric membrane manufactured by phase inversion. [8]

For now, the most commercially available RO membranes are thin-film composite (TFC) membranes and asymmetric cellulose type (cellulose acetate, diacetate, triacetate or their blend) membranes [13, 20]. Commonly used TFC RO membranes consist of three layers: an ultra-thin barrier layer on the surface of membrane, a microporous support layer and a polyester web acting as structural support (Figure 6) [22]. The barrier layer is usually made of aromatic polyamide via interfacial polymerization on a microporous support such as polysulfone [3, 23]. The microporous support layer is needed, because the polyester support web is too irregular and porous to provide direct support to the barrier layer [3]. The main advantage of TFC is the ability to achieve the best membrane stability and separation performance by optimizing the thin film and the porous support separately [20].

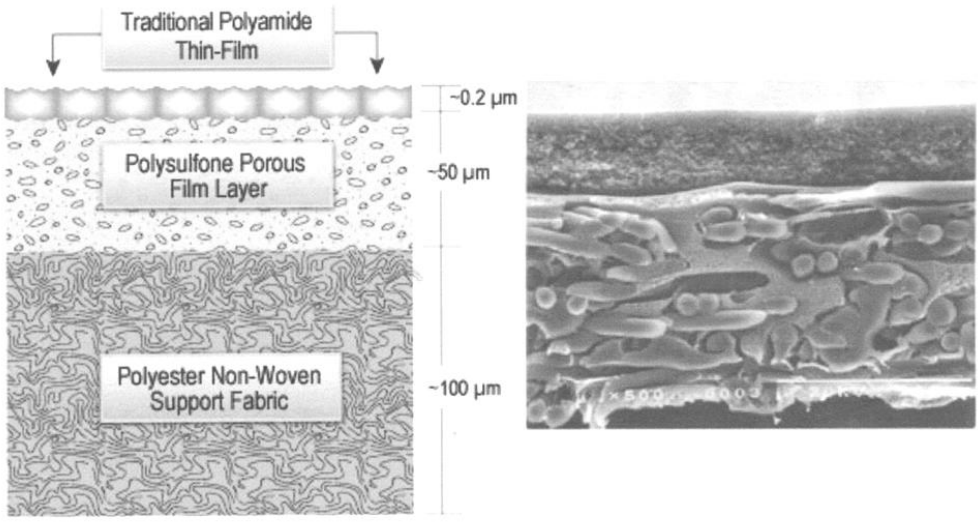

Figure 6. Structure of traditional TFC RO membrane and cross-section of traditional RO membrane's microscopic image [24].

Compared to cellulose membranes TFC polyamide membranes dominate the membrane markets [3, 13]. With the TFC membrane, the salt rejection and water flux are higher, the operating pH and temperature range are wider and pressure compaction resistant is higher. They are also less prone to biological fouling. [25] However, TFC membranes are susceptible to fouling and as a result; researchers have tried to develop new antifouling RO membrane materials [13].

2.4 RO membrane materials for desalination

So far polymeric RO membranes are the most commercially used desalination membranes [3, 13]. Due to technological developments, they are easy to handle, affordable to manufacture, and their selectivity and permeability performance is improvable [3].

Suitable integral asymmetric membrane materials for desalination are cellulose diacetate (CDA) and cellulose triacetate (CTA). These materials have high permeability towards water and low solubility towards salts. [8] Compared to CDA membrane, CTA membrane has a wider pH and temperature application range and higher resistant to chemical and biological attack [3]. Though, CTA suffers severe loss of flux due to its susceptible to compaction [26]. The poor stability against temperature, bacteria and chemicals limits the use of CDA and

CTA membranes [8]. Other problems are susceptibility of acetate group to hydrolysis at acidic and alkaline conditions and poor selectivity of some small organic molecules such as glucose and sucrose [8, 27].

Aromatic polyamide membranes formed from m-phenylenediamine (MPD) and trimesoyl chloride (TMC) are most dominating TFC membranes in commercial reverse osmosis applications [13, 28]. The selectivity of aromatic polyamide towards salt is high, but the water flux is lower. The preferred aromatic polyamide is a completely aromatic polyamide that comprises of an aromatic acid component and an aromatic amine component. [29] The main disadvantage of polyamides is their sensitivity to free chlorine (Cl_2) which causes degradation of the amide group. [3, 8]

The preparation technique of TFC membranes is based on interfacial polymerization (polycondensation) reaction between two monomers (MPD and TMC) dissolved in water and hydrocarbon solvent [13, 21, 30]. The hydrocarbon solvent and water are immiscible [21]. The polymerization reaction takes place predominantly in the organic phase due to the low solubility of acid chlorides in water [21, 31]. Figure 7 presents polyamide barrier layer formed from MPD and TMC via interfacial polymerization [13].

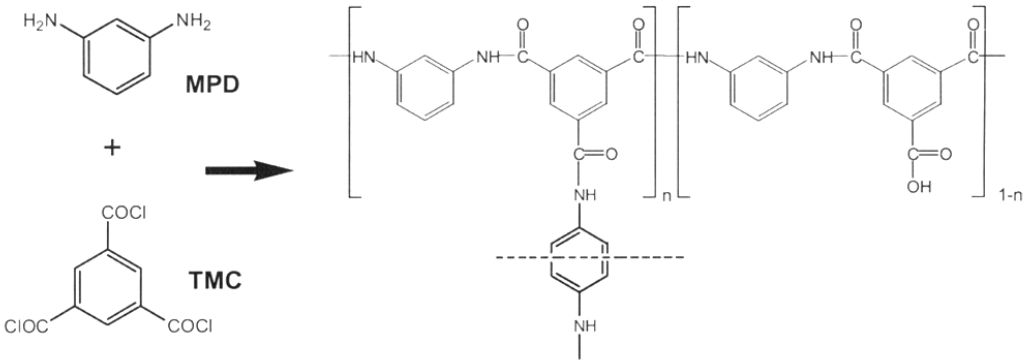

Figure 7. The polyamide RO barrier layer formed of MPD and TMC monomers via interfacial polymerization [13].

Recently used support materials for polyamide composite membranes have been polymers like polysulfone, polyethersulfone, polycarbonate, polyphenylene oxide, polyetherimide, polypropylene, and others by phase inversion techniques [32–35].

However, polysulfone has found to be an optimum material for the support layer due to its stability in acidic conditions, fairly stability against thermal, chemical, mechanical, and bacterial attack, resistance to compaction and its reasonable flux [3, 20]. Moreover, it is relatively cheap, easy to process and widely available. Compared to most of the other polymers, polysulfone is also relatively hydrophobic. [20]

The improvement of membranes has shown the greatest efficiency in RO membrane process development. The RO membrane structure, material and morphology have been modified to improve membrane applicability (mechanical, chemical and biological stability) and functionality (permeability and selectivity). However, the search for multifunctional membrane materials that offer higher permeability, high organic and ion contaminant rejection, and operational robustness is still ongoing. Various nano-structured RO membranes have been proposed to offer desirable permeability characteristics for desalination. Nevertheless, there are still many fundamental scientific and technical aspects that have to be addressed before the potential benefits may be realized. [3]

2.5 RO membrane fouling mechanisms

As the idea of surface modification of conventional membranes is to enhance the antifouling ability, it is important to understand the fouling mechanism. Membrane fouling performance is not exactly known. It depends on the nature of the used membrane and solute [21, 36]. Fouling is the main phenomenon that limits the use of membranes in industrial processes. In desalination processes, besides the water flux decline, fouling causes an increase in salt passage through the membrane. [37]

In pressure driven RO membrane processes, the membrane’s performance can change much with time. Usually the flux through the membrane decreases over time, if the pressure remains constant [8, 16]. If the flux decline is continuous, it is mainly due to membrane fouling. With concentration polarization phenomenon, the flux becomes constant when steady state conditions have been attained (Figure

8) [5, 8]. Unlike fouling, the concentration polarization is a reversible phenomenon; thereby it can be affected by hydrodynamic conditions [8].

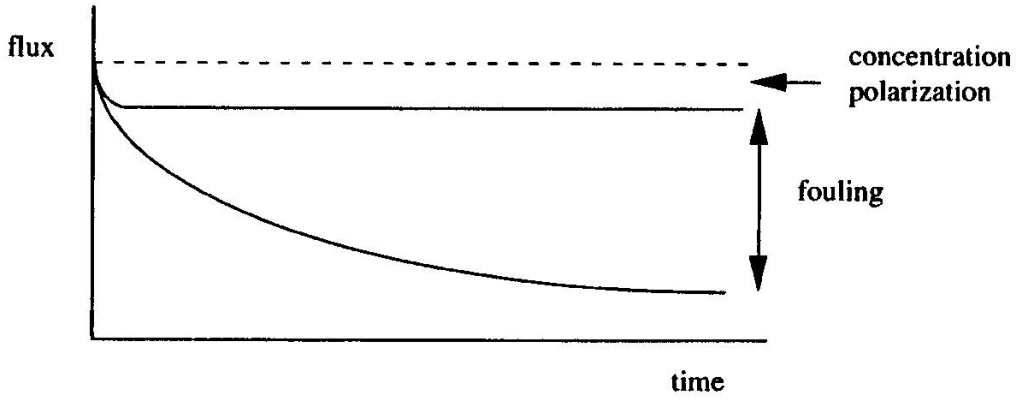

Figure 8. Flux decrease due to fouling or concentration polarization during filtration time [8].

Flux decline of RO membrane can be caused by concentration polarization, adsorption, and gel or cake layer formation. All these factors cause additional resistances on the feed side to the transport across the membrane (Figure 9). With RO membranes, pore-blocking resistant is not considered due to nonporous membranes. In the ideal case however, only the membrane resistance (R_m) exists. [8]

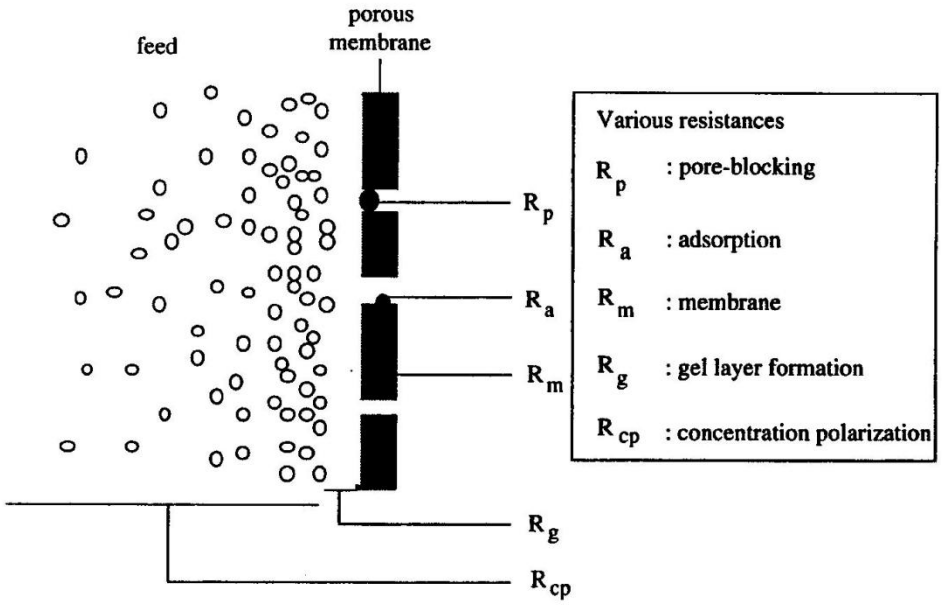

Figure 9. Description of various resistances those affect the mass transfer across the membrane in pressure driven processes [8].

The main types of RO membrane foulants are inorganic salts, organic compounds, colloids, and microbes [13, 16, 38]. Surface fouling mechanisms can be divided into cake, scale, and biofilm formation based on the type of foulants in feed solution [17, 39]. Cake formation is caused by a deposition of colloidal matter onto the RO membrane surface. Scaling is a result from heterogeneous crystallization of sparingly soluble mineral salts on the RO membrane surface. Biofilm formation occurs, when deposited microorganisms proliferate and colonize a membrane module. [17] In this thesis, only the adsorption and scaling are considered as the study focuses on salt filtration and surfactant adsorption.

2.5.1 Adsorption

As the RO membranes are nonporous, solutes can only be adsorbed onto the surface of membrane. The adsorption occurs through different interactions such as hydrophobic or van der Waals interactions, hydrogen bonding, or by electrostatic effects [36].

Depending on the characteristics of the solute and the membrane surface, three kinds of adsorption types have been observed: monolayer adsorption, multilayer

adsorption, and capillary condensation in porous materials. Usually amphiphilic substances like surfactants form monolayers on hydrophobic surfaces and double layers on hydrophilic surfaces. Multilayer adsorption can be formed, when hydrophobic solutes adsorb onto the solid surface. [40] Adsorption of surfactants onto membrane surface will be discussed in more detail in Chapter 4.

2.5.2 Scaling

The scale formation of the RO membrane is a result of precipitation of saturated salts onto the membrane surface. The species commonly causing scale formation are calcium scales (carbonate, fluoride, and phosphate), magnesium scales, sulfate based scales of trace metals (barium and strontium), and reactive silica. [7, 16]

The scaling can be caused by low cross-flow velocity and high membrane flux. Higher flux brings more solutes in boundary layer quicker and if their concentration reaches saturation, the solutes will precipitate on the membrane surface. Lower cross-flow velocity causes a thicker boundary layer which increases the residence time of solutes in boundary layer. This makes saturation more possible and scale will be formed. [16]

Major issues with the scaled membranes are higher operating pressure, higher pressure drop and lower salt rejection. Formed scale creates an additional barrier layer through which water must travel. Thus, additional driving force (pressure) is needed to get the same amount of water through the membrane. Lower salt rejection is a result of concentration polarization, because the concentration of scaled mineral is higher at the membrane surface than in the bulk solution. This leads to lower apparent mineral rejection. [16]

The scale forming potential of the salt can be determined by comparing the ion product of salt with the solubility product for the salt under the conditions in the reject. Normally, scaling will occur when the ion product is higher than the solubility product. Scaling indexes are used to aid in the determination of the scaling potential of salt for RO membranes. Most commonly used indexes for calcium carbonate scale prediction are the Langelier Saturation Index (LSI) and

the Stiff-Davis Saturation Index. For most salts the scaling index is 100 % when ion product equals the solubility constant. [16]

Carbonate scaling can be prevented by maintaining pH of the feed solution at acidic side (pH 4–6). Carbonate, sulphate, and calcium fluoride scaling can be avoided by adding antiscalants such as surfactants. [41]

2.5.1 Concentration polarization

Concentration polarization differs from fouling, because fouling involves the immobile deposition of foulants on the membrane surface [5]. However, these phenomena are closely related to each other. A severe concentration polarization tends to accelerate fouling by producing higher foulant concentration for the membrane [5].

The RO membrane retains the salt with a certain retention, while the water permeates through the membrane more or less freely. Thus, the concentration of the salt in the permeate (c_p) is lower than that in the bulk (c_b). [8] However, the retained salts can accumulate near the membrane surface causing an increase of salt concentration at the membrane surface. Consequently, the concentration of salts near the surface (c_m) is higher than in the bulk. The increase of the salt concentration causes a diffusive back flow to the bulk solution. After a certain time, steady-state condition will be formed: the convective solute flow to the membrane surface will be equal to the sum of the solute diffusive back flow to bulk solution plus the permeate flow (Figure 10). This phenomenon is known as concentration polarization. [5, 8]

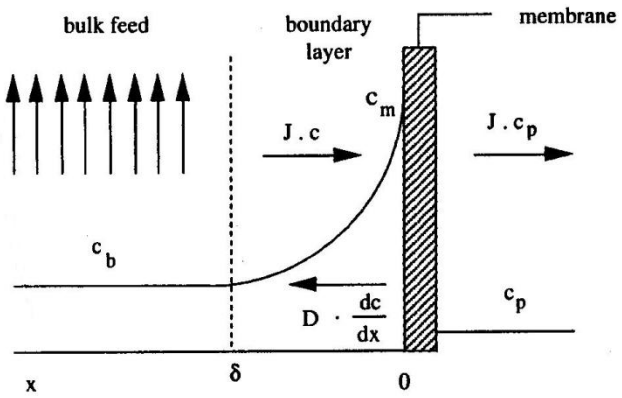

Figure 10. Schematic illustration of concentration polarization under steady-state conditions [8].

The concentration polarization reduces the water flow through the membrane in important ways. Firstly, it acts as a hydraulic resistance to water flow. [16] Secondly, the accumulation of solutes near the membrane surface increases the osmotic pressure at the boundary layer. Thus, it reduces the driving force (in this case pressure) to get the water through the membrane and the permeate flux decreases. [5, 16] Thirdly, the higher concentration of the solutes at the membrane surface than in the bulk solution causes greater solute passage than otherwise would be predicted based on the concentration of feed solution. For example, if the solute concentration in the bulk solution is 10 ppm and 11.5 ppm at the membrane surface, with the rejection of 98 %, the concentrations of solutes in permeate should be 0.20 ppm. However, the RO membrane rejects the solutes based on the concentration at the membrane surface. Thus, the actual solute passage is 0.23 ppm (2 % of 11.5 ppm). So the actual rejection is still 98 %, but the apparent rejection is 97.7 %. [16]

3 FACTORS THAT AFFECT RO MEMBRANE PERFORMANCE

Feed water composition, membrane surface properties and process conditions have a remarkable influence on membrane desalination process. Thus, the influence of these factors on membrane efficiency (permeability and rejection) should be considered.

3.1 Feed water composition

In RO desalination industry all natural waters are usually divided into two types: sea waters (SW) and brackish waters (BW) [42]. Seawater contains total dissolved solids (TDS) 35 000 mg/L or more and in brackish water TDS concentration is from 1000 mg/L to 15 000 mg/L. [7, 42] This study focuses on brackish type of waters.

Brackish waters cannot be consumed by humans directly because of its high salinity (0.2–1 %) in comparison to drinking water salinity, which must be below 500 mg/L (0.05 %) according to World Health Organization (WHO). Thus, brackish waters must be desalinated before it can be used. The composition of brackish waters varies depending on the location. [7] Table III shows two examples of brackish water compositions and some guidelines for drinking water quality from social and health affairs. The existence of contaminants depends on the natural occurrence or human pollution. [3, 43]

Table III Compositions of brackish water from Port Hueneme and Martin County and some guidelines for drinking water quality [2, 44].

Component	Brackish water Port Hueneme, USA mg/L	Brackish water Martin County, USA mg/L	Guidelines for drinking water quality mg/L
Calcium (Ca^{2+})	175	179	100
Magnesium (Mg^{2+})	58	132	100
Barium (Ba^{2+})	<0.10	0.06	1.5
Strontium (Sr^{2+})	-	26.4	
Sodium (Na^{+})	170	905	200
Chloride (Cl^{-})	72	1867	250
Sulphate (SO_4^{2-})	670	384	250
Bicarbonate (HCO_3^{-})	260	146	
TDS	1320	3664	
DOC*	-	1.4	

*Dissolved organic carbon (DOC)

There are two commercially available RO membrane types for all water types: SWRO and BWRO. Water cannot be reliably systematically classified and that is why the selection of proper membrane type and pretreatment method is hard, or even too hard causing technical problems like inorganic scaling. [42] Thus, accurate characterization of the specific feed water is an important factor in brackish water RO system design and crucial for the system pretreatment [2, 7]. Manharawy and Hafez [42] proposed “Water molar classification” to understand the chemical nature of the investigated water type and it possible behavior under pressure-dehydration process that characterizes desalination by RO membrane technology.

The feed water characteristics such as foulant type, concentration, and physiochemical properties (size, charge, functional groups, and conformation) significantly affect membrane separation process and fouling. Whereas, the solution chemistry (pH, ionic strength, ionic fouling) can significantly affect the physiochemical properties of solutes. For example, the conformation of some macromolecules like humic acids, depends on the solution chemistry. [5] In additions, interactions between different components in feed solution have a major effect on membrane fouling, thereby reducing its efficiency [5, 45].

3.1.1 Foulant type

Main species in natural waters that cause RO membrane fouling are organic matter, inorganic salts, colloidal or particulate deposits and micro-organisms such as bacteria, fungi, algae, and viruses [8, 16, 21, 45, 46]. From the foregoing foulants, colloidal matter and dissolved organics are considered the most serious ones [37].

In Table IV, there is a list of generally accepted water quality guidelines to improve membrane efficiency by minimizing RO membrane fouling tendency [16].

Table IV Generally accepted water quality guidelines for minimizing RO membrane fouling [16].

Species	Measure	Value
Suspended Solids	Turbidity	< 1 NTU
Colloids	SDI	< 5
Microbes	Dip Slides	< 1,000 CFU/ml
Organics	TOC Concentration	< 3 ppm
Color	Color units	< 3 APHA
Metals: iron, manganese, aluminum	Concentration	< 0.05 ppm
Hydrogen Sulfide	Concentration	< 0.1 ppm

The abundance of water constituents cannot be fully integrated in a process design exercise. Thus, water quality is characterized by certain key parameters, which give information about its tendency to cause fouling. These feed quality parameters are SDI index (Silt density index), the content of magnesium and calcium (water hardness), the solubility product (scaling potential), conductivity (content of dissolved salts) and TDS). [16]

3.1.2 Concentration

The solute concentration has a major role in separation performance because it affects the osmotic pressure. The relationship between the solute concentration and the osmotic pressure is described by the van't Hoff equation (see Equation 7). The increase of feed concentration causes an increase in osmotic pressure and the flux through the membrane decreases, if other process parameters remain constant. [8]

Hung *et al.* [9] investigated desalination efficiency of salty water using RO process. In their study, the permeate flux decreased due to higher osmotic pressure at higher salt concentration. The higher osmotic pressure decreased the net driving force (Δp-$\Delta \pi$), as shown in Equation 1. In Table V is represented the salt rejection coefficients and permeate fluxes (J_w) at various NaCl concentrations. It can be seen that the salt rejection decreased as the salt concentration increased. Also, when the salt concentration increased, the permeate flux decreased due to higher osmotic pressure.

Table V The effect of feed concentration on salt rejection and permeate flux (J_w) [9].

NaCl conc. (%)	Permeate conc. (%)	J_w (10^{-5} m^3 m^{-2} s^{-1})	J_w (L m^{-2} h^{-1})	Rejection	r_{int}
0.0	0.00	4.92	177	–[b]	–[b]
0.5	0.01	3.67	132	0.984	0.998
1.0	0.04	3.50	126	0.966	0.992
1.5	0.06	2.08	75	0.970	0.987
2.0	0.18	1.83	66	0.910	0.961

[a] Operating condition: pressure = 1960 kPa, elapsed time = 60 min, temperature = 25 °C.
[b] Not applicable.

The intrinsic retention (r_{int}) was calculated as follows [9]:

$$r_{int} = 1 - \frac{c_p}{c_m} \tag{9}$$

Where r_{int} intrinsic retention, -
c_p the solute (salt) concentration in the permeate stream, kg/m^3
c_m the solute (salt) concentration at the membrane interface, kg/m^3

In Figure 11, the salt flux is plotted as a function of the salt concentration difference in the feed and in the permeate (ΔC_s) [9]. The salt flux increased as the salt concentration in the feed increased. Thus, more salt passed through the membrane and the salt retention was lower.

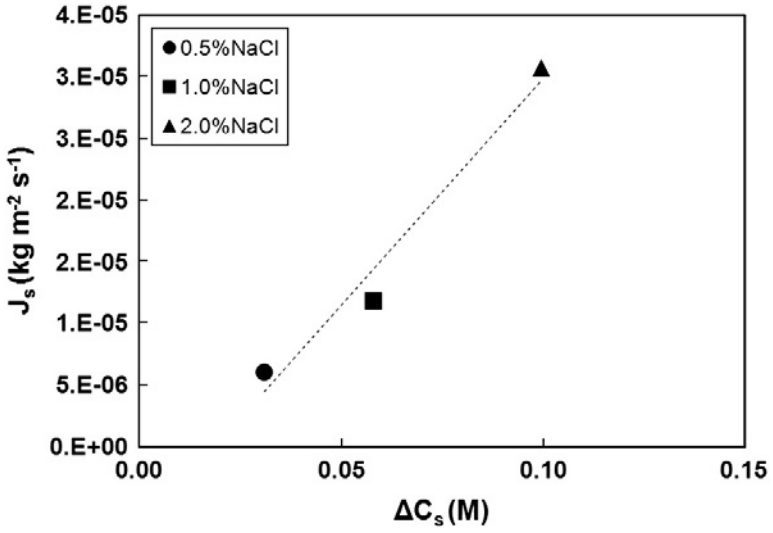

Figure 11. The salt flux at different salt concentration differences in the feed and in the permeate. The RO membrane operation pressure was 1.96 MPa and temperature 25 ˚C [9].

3.1.3 Ionic strength

The combined influence of feed ionic strength and membrane charge has a significant role in salt rejection [47]. When electrolyte solution comes in contact with a charged membrane, the concentration of ions with the same charge as the membrane (co-ions) will be lower in the membrane than in bulk solution. Respectively, the concentration of ions with opposite charge (counter-ions) is higher at the membrane than in the bulk solution. [48] For example, when a feed solution containing positively charged ions (cations) and negatively charged ions (anions) comes in contact with the negatively charged membrane, the concentration of anions in bulk solution will be greater than near the membrane surface (Figure 12). On the contrary, the concentration of cations near the membrane surface will be greater than in the bulk. [47]

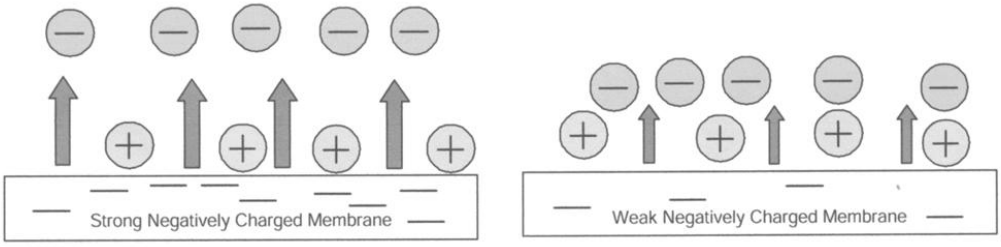

Figure 12. Negatively charged membrane repels anions and attracts cations due to Donnan potential. Strongly negatively charged membrane has greater repulsive force than weakly charged membrane [47].

The concentration difference of ions creates an electrical potential also called as Donnan potential at the boundary between the membrane and the solution. Formed Donnan potential attracts counter ions to the membrane while rejecting co-ions. [47, 48] The concentration of co-ions at the membrane increases when the salt concentration of the solution increases and fixed membrane charge decreases. Decreased co-ion limitation from the membrane often causes lower salt rejection, when rejection of co-ions determines the salt rejection. [48] In the case of Figure 12, the salt rejection is dependent on the anion rejection. This theory implies that higher Donnan potential leads to higher salt rejection of the membrane [48].

The greatest benefit of Donnan potential, based on the increased salt rejection, is from low to mid salinities (1000 mg/L < TDS < 3000 mg/L). At very low salinity it is negligible and at high salinity the Donnan potential becomes weaker and the salt rejection of the membrane decreases. According to this, as the feed concentration increases, the concentration of counter ions at the membrane surface increases causing a shield at the membrane surface. With the negatively charged membranes, this shield prevents the repulsive force of the anions in the bulk solution (Figure 13). [47]

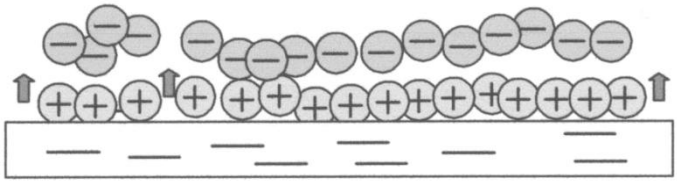

Figure 13. Increase of the concentration of cations at the membrane surface prevents the repulsive force of the membrane's negative charge on the anions in bulk solution [47].

Besides the feed salinity, also the valence of ions in the feed solution affects Donnan potential [47]. Higa *et al.* [49] discovered that the Donnan potential is mainly controlled by the counter ion concentration having the highest valence in the system. Donnan potential becomes weaker with higher concentration of divalent counter ions in a solution. Divalent counter ions shield the repulsive force of membrane's charge on the co-ions in the bulk solution [47]. Figure 14 shows how divalent cations shield the negative charge of the membrane on anions in the solution.

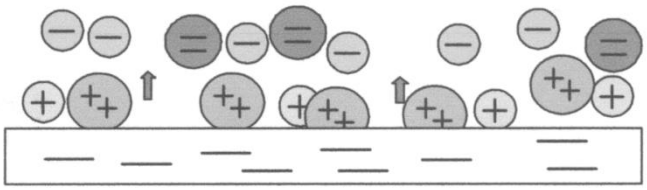

Figure 14. The repulsive force of negative membrane on the anions in bulk solution is shielded by divalent cations [47].

3.1.4 pH

Solution pH has an influence on the nature of species in the solution and the membrane structure. Generally it is known that higher pH values improve the salt rejection of polyamide membranes. At higher pH deprotonation of carboxylic acids occurs and cause an increase of membrane charge density which promotes Donnan exclusion of charged species. [17] Typically, rejection decreases significantly when solution pH decreases below 6 [50].

Nada *et al.* [51] observed in their study that the fouling potential increased with increasing acidity of the feed solution. They examined the effect of pH on the fouling potential of calcium sulfate with polyamide TFC nanofiltration membrane. At higher pH of the feed solution, the retention was higher than at lower pH. This was due to suppression of functional groups at low pH, which caused a lower repulsive force at the membrane surface. They discovered that the formed deposit on the membrane surface was sticky in the filtration of solution at acidic pH and loose in the filtration of solution at alkaline pH. The reason for this is the change of charge density of the membrane as a function of pH. Usually, polyamide TFC membranes are negatively charged at high pH range and positively charged at low pH range (see Figure 21). In their study the pure water flux of fouled membranes increased due to the top polyamide layer thickness shrinking at acidic pH, when usually water flux decreases with fouled membranes. The study implicated that the polyamide membranes are pH-sensitive.

Yu *et al.* [52] investigated the influence of pH on the organic fouling of polyamide TFC RO membranes under surface and seawater conditions. They observed that at low ion strength the feed water pH affect significantly on organic fouling, but at the high ionic strength the impact of pH on the flux was almost negligible (Figure 15). The flux-decline curves at different pH were nearly identical.

Under seawater conditions the overall charge density of organic macromolecules is completely masked. Thus, the charge density characteristics of organic foulants are similar despite pH variation. However, high ion content of seawater induces electrostatic double layer compression and charge screening making membranes

and organic foulants more hydrophobic. Thus, the hydrophobic interactions between membrane and foulants and among foulants are enhanced. Thereby, the feed water pH has not big influence on organic fouling of TFC RO membranes under seawater conditions. [52] Also, Yang *et al.* [53] observed that solution pH has less influence on membrane chemical properties under seawater conditions.

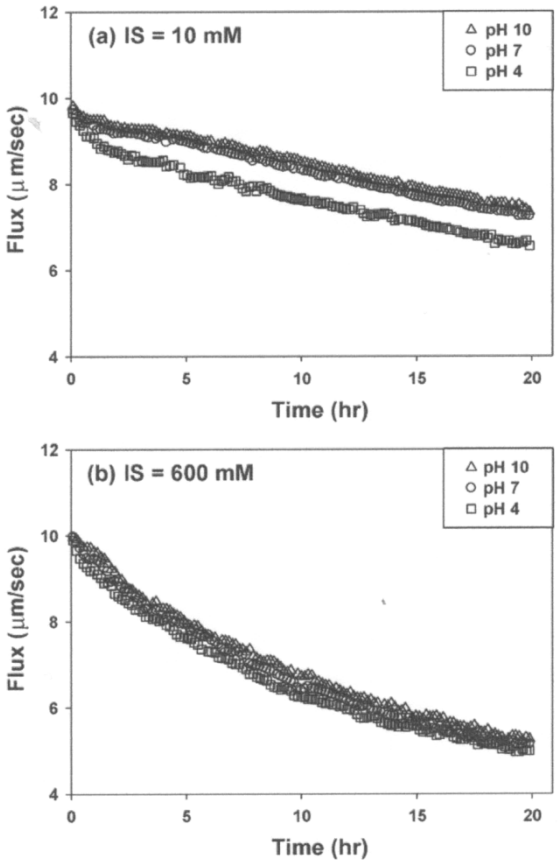

Figure 15. The influence of feed water pH on RO membrane flux under typical surface water ionic strength (10 mM) (a) and a seawater-level ionic strength (600 mM) (b) [52].

3.2 Membrane surface properties

The interactions of substances in water solutions are dependent on the surface properties of membranes, as it was noticed with the relation between ionic species and membrane surface charge in previous Chapter. These surface properties affect the degree of adsorption of dissolved solids [54]. Thus, membrane surface properties are critical to water permeability, salt rejection and fouling performance of membrane [28, 37]. The surface properties contributing to membrane

separation performance are hydrophilicity, roughness, and charge [5, 28, 50, 53–56]. Generally more hydrophilic, smoother and lower surface charge of membranes shows better anti-fouling properties [56, 57].

3.2.1 Hydrophilicity

It is generally known that hydrophobic membranes tend to suffer more severe fouling than hydrophilic ones. An increase in surface hydrophilicity usually prevents fouling because many foulants, such as proteins, are hydrophobic in nature [58]. Increasing wettability of membrane surfaces can reduce fouling by decreasing the adsorption of hydrophobic foulants [53, 58–60]. Enhancing surface hydrophilicity also increases water affinity for the surface groups on the membrane, thus preventing the adsorption and deposition of hydrophobic foulants, thus reducing fouling [13, 59]. However, for hydrophilic foulants, such as natural organic matter (NOM) fouling cannot be prevented by increasing surface hydrophilicity [55, 61]. Thus, prevention of membrane fouling by modifying surface hydrophilicity depends on the nature of existing foulants [55].

Yang *et al.* [53] examined the effect of solution chemistry on the surface property of polyamide TFC RO membranes under seawater conditions. They discovered that under these conditions RO membranes turned to be more hydrophobic. The increased hydrophobicity of membranes at higher TDS concentration can be related to electrostatic screening or osmotic swelling. Electrostatic screening leads to compression of electrostatic double layer at the solid-liquid interface, which cause charge reduction at polymer skin layer of the membrane. Thus, membranes have more non-polar characters. Effect of electrostatic screening and reduced polymer wettability caused by high TDS concentration were greater with more hydrophilic and charged membranes. Thus, desalination even with relatively hydrophilic RO membranes can lead to membrane fouling under seawater conditions. [53]

3.2.2 Charge

Like surface hydrophilicity, the selection of optimal surface charge for fouling prevention depends on existing foulants in feeding solution. Thus, the antifouling

RO membranes should be developed according to the electrostatic character of present foulants [13]. The electrostatic repulsion between the membrane and foulants increases, if they are similarly charged [58, 59]. For example, aromatic polyamide TFC RO membranes are negatively charged under typical operation conditions (pH>4) due to the carboxyl groups on the membrane surface [28]. Thus, they are easily fouled by positively charged foulants [13, 28, 50]. It is usually known that negatively charged RO membranes suffer less fouling because most foulants such as NOMs are negatively charged [53, 58]. Thus, the electrostatic repulsion increases membrane efficiency making membranes less prone to fouling by foulants having the same charge than the membrane surface [28]. More about the interactions between charged membrane and electrolyte solutions are discussed in Chapter 3.1.3.

Zhou *et al.* [28] modified negatively charged polyamide TFC membrane surface charges to improve their fouling resistance to positively charged foulants. They reversed the charges of membrane surface by electrostatic self deposition of polycations (polyethyleneimine) to enhance the electrostatic repulsion between the membrane and foulants.

The unmodified negatively charged TFC membrane repelled anions (Cl^-) and attracted cations (Na^+ and Mg^{2+}) due to Donnan potential (Figure 16 A), while after modification the membrane became positively charged and rejected cations better (Figure 16 B). With negatively charged membrane the attractive force with divalent cation (Mg^{2+}) was stronger than with monovalent cation (Na^+), thus divalent cations passes easier through the membrane (Figure 16 A). Thereby, the rejection of $MgCl_2$ was lower than NaCl. With positively charged modified membrane the rejection of $MgCl_2$ was higher than NaCl due to electrostatic interaction (Figure 16 B). Thereby, the charge reversal on the membrane surface showed an increase in fouling resistance of the membrane to cationic foulants due to electrostatic repulsion. [28]

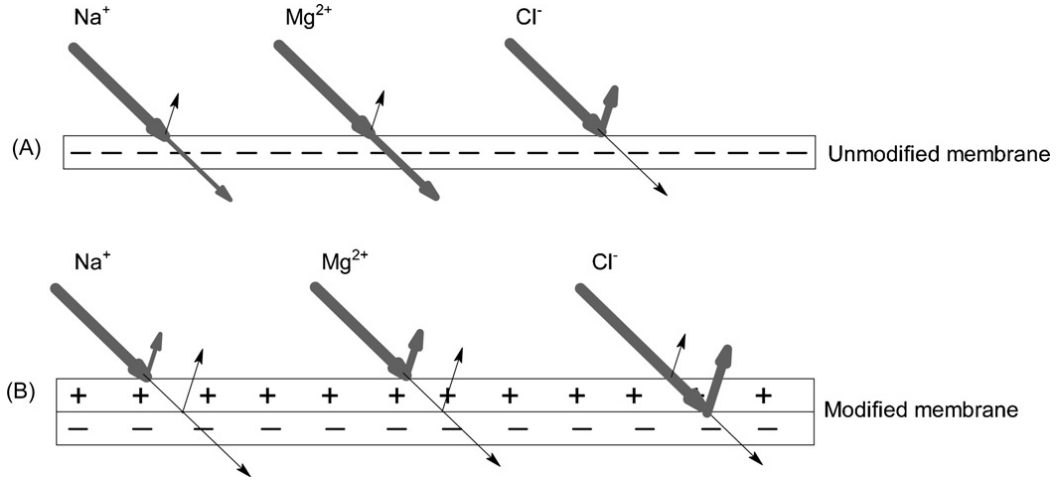

Figure 16. A schematic diagram of ion transport through unmodified (A) and unmodified (B) polyamide TFC membrane [28].

3.2.3 Roughness

A smoother membrane surface is generally expected to experience less fouling because it is assumed that foulant particles are more likely to be entrained by rougher topologies than by smoother membrane surfaces [13, 50, 56]. Elimelech *et al.* [57] found in their experiments that the commercial TFC membranes fouled faster by colloids than the cellulose acetate membranes. They came to a conclusion that higher fouling rate for the TFC membranes related to greater surface roughness. Also Vrijenhoeck *et al.* [56] research results showed that colloidal fouling of RO and NF membranes is strongly correlated with membrane surface roughness. Particles tend to accumulate in the "valleys" of rough membrane, resulting "valley clogging" which can cause more severe flux decline than in smooth membranes [56]. According to these results the decrease of surface roughness can improve antifouling properties of RO membranes.

However, Hirose *et al.* [62] and Kwak *et al.* [63] discovered that a rougher surface of polyamide TFC membranes increases the water flux of the membrane because of the enlargement of effective membrane skin area. Thus, lower surface roughness can be unfavorable to membrane flux. Al-Jeshi and Neville [64] examined also the relationship between flux and roughness of RO membranes. They did not find the linear correlation between surface roughness and flux but they observed up to 33 % variation in surface roughness upon imaging different areas of one membrane. Thereby, more investigations must be done to fully

understand the effect of surface roughness on flux. They also found that surface morphology changes upon exposing the membrane to different environments. Thus, the surface measuring conditions are very important. [64]

Yang *et al.* [53] examined the performance of surface roughness under seawater conditions. They observed that surface roughness increased with more hydrophobic and less charged RO membranes at higher TDS condition. This can be caused by polymer swelling at the membrane surface, which increases so-called peak and walley-structure of membrane. With more hydrophilic and negatively charged membrane, the results were opposite. Roughness decreased at higher TDS conditions. [53]

3.3 Hydrodynamic conditions

The operation parameters such as temperature, pressure and cross-flow velocity have significant influence on separation performance. The permeability and rejection can be increased by optimizing these parameters. Fouling can also be reduced by optimal process parameters.

3.3.1 Temperature

The feed water temperature affects the feed solution properties, the mass transfer of membrane, membrane properties and applied pressure [17]. Thereby, temperature has a significant influence on RO process performance. While feed water temperature increases, the solution viscosity decreases and of flow resistant decreases [8, 14]. Unlike viscosity, solution diffusivity and solution osmotic pressure increases with increasing temperature [14]. Thus, the flux increases as temperature increases. The influence of diffusion coefficient on flux can be described by Fick's law as follows [8]:

$$J = -D\frac{dc}{dx} \tag{10}$$

where J flux, m/s
D diffusion coefficient, m^2/s
dc the concentration, kg/m^3
dx the distance, m

When hydrodynamics are constant, solution rejection decreases and diffusivity increases while feed water temperature increases. As the concentration polarization is a function of permeate flux, solute rejection, and mass transfer which is strongly impacted on solute diffusion, the concentration polarization decreases with increasing temperature. This is notable because concentration polarization affects solute passage, osmotic pressure, and surface fouling. [17]

Jin *et al.* [17] examined the effects of feed water temperature on separation performance and humic acid fouling of brackish water RO membranes. They presented theoretical impacts of temperature on separation performance, which is shown in Figure 17.

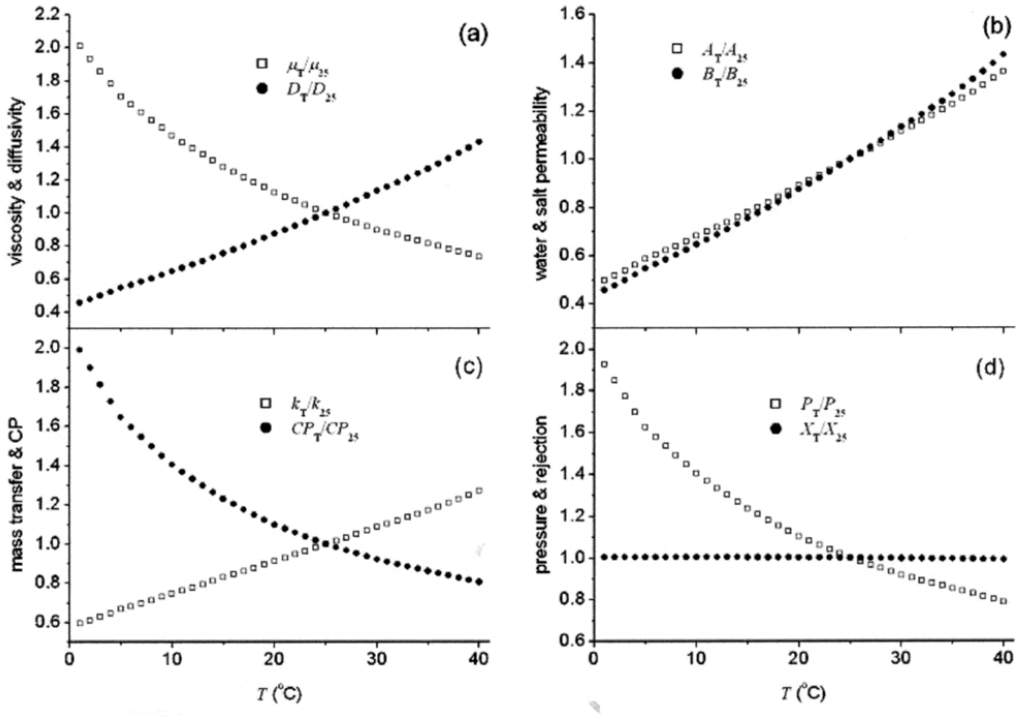

Figure 17. Theoretical effects of temperature for a): water viscosity (μ) and solute diffusivity (*D*), b): water (A) and solute (B) permeability, c): mass transfer coefficient (*k*) and concentration polarization factor (*CP*), and d): applied pressure (*P*) and observed salt rejection (*X*). Data are normalized by corresponding parameter value at 25 ˚C and assumed constant flux of 1.29×10^{-5} m/s. [17]

As assumed, the solute diffusivity increases and viscosity decreases when temperature increases (Figure 17a) and as a result water and solute permeabilities increase (Figure 17b). Temperature increase also enhances the mass transfer

coefficient, where the concentration polarization reduces (Figure 17c). Applied pressure decreases and observed rejection for salt stays constant with increasing the feed water temperature (Figure 17d) due to changes in mass transfer and membrane permeability.

Based on Jin *et al.* [17] experimental results of temperature effects, the applied pressure, salt rejection, and concentration polarization decreased with increasing temperature. They concluded that the changes in polyamide membrane film (with increased diffusivity and decreased viscosity) appeared to dominate the relationship between mass transfer, membrane transport, and feed water temperature. Polyamide membranes swell when they are contacted with water due to the polymer interactions with water. Thermal expansion drives adjacent polymer chains apart, thus enhancing the permeability of water and solute. Thereby, besides the feed water temperature effects on the changes in solute and solvent properties, the impact on RO membrane must be taken into account. [17]

3.3.2 Pressure

As RO membranes are dense membranes the applied pressure must be higher than with looser membranes (NF and UF) to get the same amount of flux through the membrane. Pressure also needs to overcome the osmotic pressure so that flux can be formed. For brackish water initial desalination pressurization ranges from 17 bar to 28 bars, and for seawater desalination 55 to 69 bars. [65]. However, too high a pressure can lead to concentration polarization, thus flux decreases [8]. As the water flux depends on the pressure gradient and the solute flux depends on the concentration gradient, the pressure enhancement increases the water flux while the solute flux is essentially constant. Thereby, as pressure increases the rejection of solute increases (see Figure 5). [14, 16]

3.3.4 Cross flow velocity

The cross flow velocity is important in determining membrane efficiency because it affects the mass transfer rate over the membrane surface [66]. In general, higher

cross flow velocity show better anti-fouling properties due to thinner boundary layer thickness and reduced concentration polarization [5, 66].

Mattaraj *et al.* [67] investigated the effect of cross flow velocity on normalized flux with two ionic strengths (NaCl) during the RO of NOM. In Figure 18 is shown their results of the cross flow velocity effect on the solution flux.

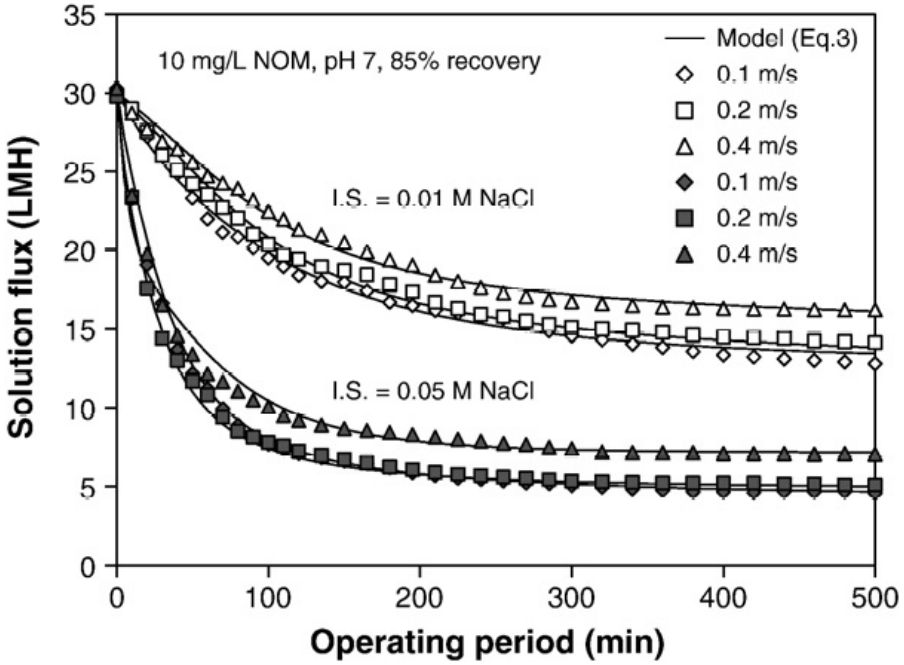

Figure 18. Effect of different cross flow velocities (0.1–0.4 m/s) on solution flux with two NaCl concentrations (0.01 and 0.05 mM) in the presence of 10 mg/L NOM at solution pH 7 [67].

As shown in Figure 18, the effect of increased cross flow velocity on solution flux rate with both ionic strengths was more important at the longer period filtration than in the beginning. The solution flux rates decrease at initial stage were primarily caused by salt concentration polarization and reduction of membrane permeability due to hydraulic resistant enhancement. Their results showed that the solution flux decreased less with higher cross flow velocity with both ionic strengths. Thus, the higher cross flow velocity decreased the solute accumulation at the membrane surface. [67]

4 SURFACE MODIFICATION OF REVERSE OSMOSIS MEMBRANES

The technological and economic efficiency of RO processes are determined by the membranes, making the progress in RO technology significantly dependent on the membrane development. [13] So far, TFC RO membranes have shown good filtration results due to high water flux and high salt rejection and higher resistance to operation parameters (pressure, temperature and pH). However, they are susceptible to fouling [68].

One method to prevent fouling is to use different cleaning methods. Though, cleaning can make membranes only partially restored and the operation becomes more difficult and membrane's life time shorter. Hence, cleaning causes more costs. [13] To reduce this problem different pretreatments such as chemical addition and filtration have been combined [7, 13] Also new membrane modules have been designed. Among these efforts, researchers have paid much attention to development of antifouling membranes. [13] Development of membranes can be done by selection of new interfacial polymerization monomers or improvement of interfacial polymerization process. Another way is a surface modification of conventional RO membranes. [13]

Surface modification techniques have been developed to improve the performance of commercial RO membranes in separation of different solutions and to enhance the fouling resistance [55, 69]. Modification techniques can be divided into chemical and physical methods. The difference between these two is how the modifiers are connected with the membrane surface. In chemical methods, the modifiers are covalently connected making the modification permanent. Thus, it is more suitable for long-term operations. However, it may require special equipment, reagents or complicated operation processes, making it less practical. Chemical methods are hydrophilization treatment, radical grafting, chemical coupling, plasma polymerization or plasma-induced polymerization and initiated chemical vapor deposition. [13]

In physical treatment, modifying agents such as polymers (polyelectrolytes) or surfactants are connected with membrane surface by hydrogen bonding, Van der Waals attraction or electrostatic interaction [13, 59, 69]. Thus, during long-

running operations the coating layer may be leached away and worsen the antifouling properties. [13] The aim of these techniques is to make membrane surface layer more hydrophilic, specifically charged and/or denser. This modification can enhance the rejection; increase the water permeability and improve the antifouling properties. [69] This study concentrates in the surface modification by adsorption of surfactants.

4.1 Surfactants

Surfactants (also known as surface active agents or wetting agents) are organic chemicals that reduce surface tension of water and other liquids [70–72]. They have been used as additives, for example, detergents, defoamers, wetting agents, cleaning agents, emulsifiers, and dispersing agents for industrial and domestic applications [73, 74]. Surfactants are also sometimes present as impurities [74]. They have also been used in filtration applications. Surfactant adsorption on filter surface can lower the energy barrier between the filter surface and the particles. Thus, the deposition of small particles increases on the surface of filter. [75] The denser the surfactant packing is at the interface, the lower is the surface tension [70].

Surfactants are amphiphilic, which means that they consist of two parts, one that is soluble in specific fluid (the lyophilic part) and one which is insoluble (the lyophobic part). When the fluid is water they are usually called as hydrophilic head group and hydrophobic tail (Figure 19). [70]

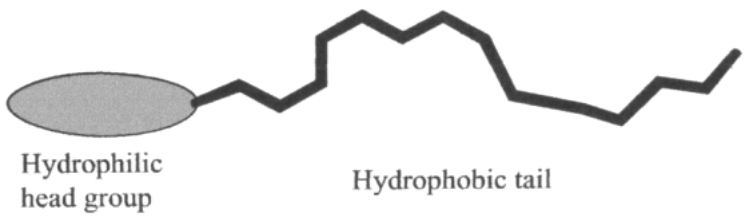

Figure 19. Schematic illustration of surfactant wherein hydrophilic part is referred to as a head group and the hydrophobic part as a tail [70].

Based on the polar head group of surfactants they can be classified into ionic and nonionic surfactants, where ionic surfactants can be further divided into anionics

and cationics. [70] For coatings most used surfactants are nonionic or anionic [76]. Most ionic surfactants are monovalent but there are also divalent anionic amphiphiles. For ionic surfactants the choice of counterions has an influence in the physiochemical properties. The counterion for most anionic surfactants is sodium and for cationic surfactants a halide or methyl sulfate. The typical hydrophobic groups is a hydrocarbon. [70]

The degree of surfactant concentration at a boundary depends on the surfactant structure and the two phases' nature at the interface. Thereby, the suitable surfactant depends on the application. Usually, the stronger the accumulate tendency is, the better the surfactant is. Also, a good surfactant should have low solubility in the bulk. [70]

Surfactants cannot lower the surface tension endlessly. Normally, the surface tension lowering limit is reached when surfactant aggregates (so-called micelles) are formed in bulk solution. The concentration where micelles start to form is known as a critical micelle concentration (CMC). CMC is an important characteristic of the surfactant because only surfactant monomers contribute to surface tension lowering. In a micelle the hydrophobic group of surfactant is oriented towards the interior of the cluster and polar head group is oriented towards the solvent. Thus it has not much surface activity. Thereby, the amount of added surfactant to the solution should never exceed the CMC concentration. [70]

4.2 Adsorption of surfactants

Surfactant adsorption is mainly determined by the interaction of the surfactant with the surface and the hydrophobicity of the surfactant. The latter has been found to be the dominating force in surfactant adsorption in many cases. Surfactants adsorb on hydrophobic surfaces with their hydrophobic part, while hydrophilic part is in contact with solution (Figure 20 a). On the contrary, at very polar surfaces, the surfactants adsorb with their polar head group in contact with the surface due to the interactions between the surface and the surfactant head group (Figure 20 b). [70]

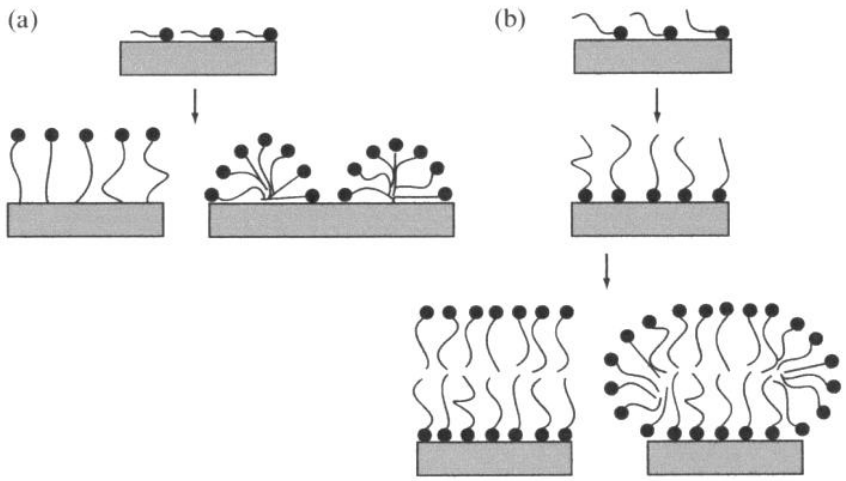

Figure 20. Surfactant adsorption on non-polar surfaces with their hydrophobic tails in contact with the surface (a) and their adsorption on polar surfaces with their polar head groups in contact with surface (b) [70].

As the surfactant concentration increases, two different surface structures are possible. When the attraction between the surfactant head group and the surface is strong, a monolayer, where the surfactant head groups are in contact with the surface and hydrophobic tails are in contact with a solution, is formed. This adsorption form creates a hydrophobic surface. Further adsorption of surfactants creates a surfactant bilayer on surface. This occurs, for example, when the surface and surfactants are oppositely charged. [70]

When the attraction between the surfactant head group and the surface is intermediate in strength, micelles or other surfactant aggregates will be formed as the surfactant concentration increases. This is due to stronger attraction between the hydrophobic tails than the interaction of surfactant head groups with the surface. Thus, the surfactant aggregation at the surfaces is a question of a balance between the interactions of the surfactant head groups with the surface and the interactions between the surfactant hydrophobic moieties. [70]

In dispersed systems, surfactant adsorption can be measured by adding surfactant, allowing time for the system to stabilize, separating the solids and finally determining the surfactant concentration in the solution. The adsorption can be determined by the following equation [70]:

$$\Gamma = \frac{(c_0 - c)V}{ma_{sp}} \quad (11)$$

where,

Γ	the amount of adsorption, mg/m^2
c_0	the concentration before adsorption, mg/ml
c	the equilibrium concentration, mg/ml
V_s	the solution volume, ml
m_p	the particle amount, g
a_{sp}	the particle specific surface area, m^2/g

The adsorption extent varies with the bulk concentration, the nature of surfactant and the presence of salt [75].

4.2.1 Adsorption of anionic surfactants

Earlier studies [37, 57, 77, 78] have investigated the influence of anionic sodium dodecyl sulfate (SDS) surfactant addition on the performance of TFC NF and RO membranes. All studies discovered that the anionic surfactant has significant effect on the charge of membranes. The zeta potential of membranes became more negative in the presence of SDS surfactant. It was assumed that the negatively charged functional groups of the surfactant molecule cause the membrane to become more negatively charged. Childress and Elimelech [78] examined the effect of SDS on the zeta potentials of TFC RO membrane with two SDS concentrations (Figure 21).

As shown in the Figure 21, the addition of SDS makes TFC RO membrane more negatively charged at entire pH range. The effect of SDS on the membrane surface charge changes with the variation of solution pH. This is due to changes in adsorption mechanism at the different solution pH values. At low pH, the unmodified membrane is positively charged, thus, surfactant adsorption results primarily from electrostatic attraction. At higher pH, the unmodified membrane is negatively charged and the adsorption results from the hydrophobic interactions between the membrane and SDS surfactant. As the pH further increases, the surfactant adsorption due to hydrophobic interactions remains constant, but the zeta potential becomes more negative. This is due to the dissociation of membrane functional groups. [78]

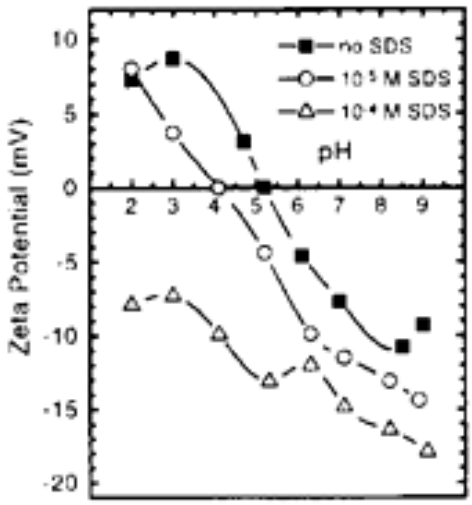

Figure 21. Effect of 10^{-5} M and 10^{-4} M of SDS on the zeta potential of TFC RO membrane. Experiments were carried out in the presence of 0.01 M NaCl. [78]

Whit higher SDS concentration (10^{-4} M) at lower pH (Figure 22 b) the effect on membrane charge is much bigger than with lower SDS concentration (Figure 22 a). This can be due to possible hemi micelle formation [78]. Hemi micelles are formed, when surfactant ions associates with each other in order to reduce the free energy of the system by removing hydrocarbon chains from the bulk water [79]. They are formed at the solid-solution interface when the hemi micelle concentration (HMC) has been exceeded [77]. At that point, the surfactant adsorption increases sharply due to the transfer of surfactant monolayer adsorption to bilayer adsorption [79]. At higher pH-values, the membrane becomes more negatively charged and surfactants adsorb onto the membrane surface by hydrophobic interaction. Thus hydrophobic moieties are attached to the membrane surface and hemi micelles cannot be formed (Figure 22 b). This leads to decline in surfactant adsorption [78].

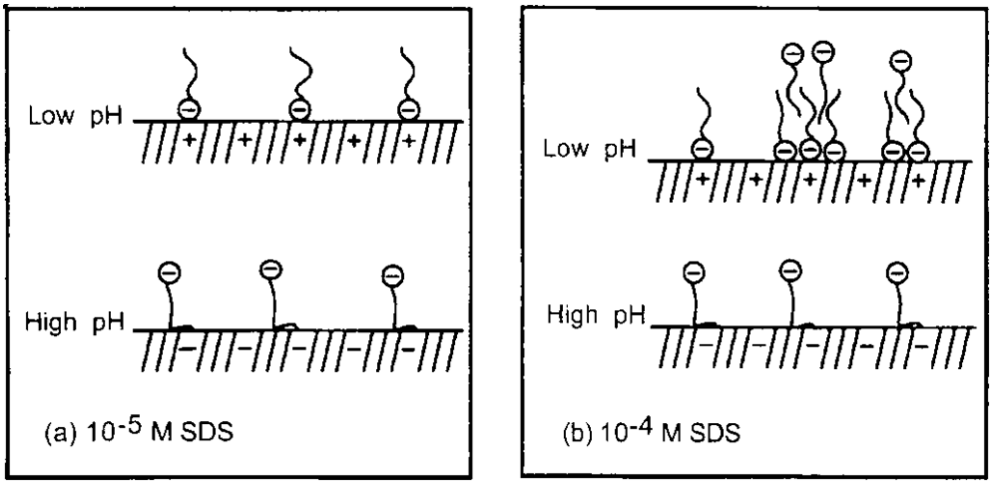

Figure 22. Illustration of the adsorption of SDS onto polymeric surface at two different SDS concentrations (a) 10^{-5} M and (b) 10^{-4} M at high and low solution pH [78].

The differences in SDS adsorption at low and high pH can also be seen from the other investigation results of Childress and Elimelech [77]. They compared the zeta potential of aromatic TFC nanofiltration membrane in the presence of SDS at two pH conditions (Figure 23). At pH 3, the adsorption occurs by electrostatic attraction. As the surfactant concentration increases they associates with each other forming surfactant aggregates or supposedly hemi micelles. Based on the Figure 23, the HMC appears to occur around 0.01mM of SDS, where there is a dramatic change in the slope of zeta potential curve. In that point, individual ion adsorption changes to surfactant association. At pH 8, the adsorption occurs due to hydrophobic interactions. As the SDS concentration increases, the membrane becomes only slightly more negative due to increased surfactant adsorption.

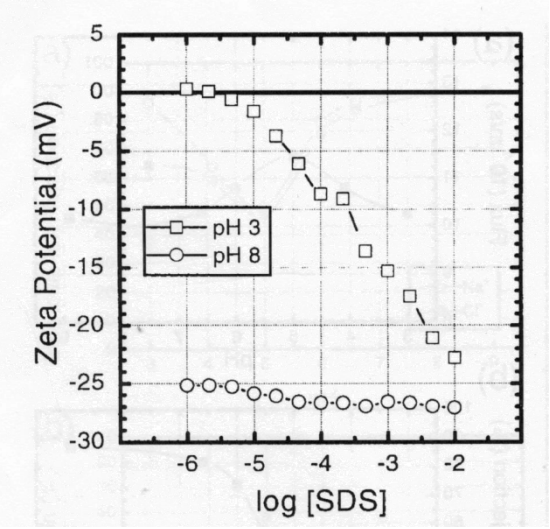

Figure 23. Comparison of zeta-potential of NF-55 membrane in the presence of SDS surfactant at pH 3 and 8. The experiments were carried out with 0.01 M NaCl as a background electrolyte. [77]

4.2.2 Adsorption of cationic surfactants

Childress and Elimelech [77, 78] investigated also the effect of cationic dodecyl trimethylammonium bromide (DTAB) surfactant adsorption onto TFC NF and RO membranes. They discovered that at low pH the hydrophobic interaction (Figure 24) is dominated, because the membrane and surfactant molecules are both positively charged. As the adsorption of DTAB increases, membrane becomes more positively charged (Figure 25).

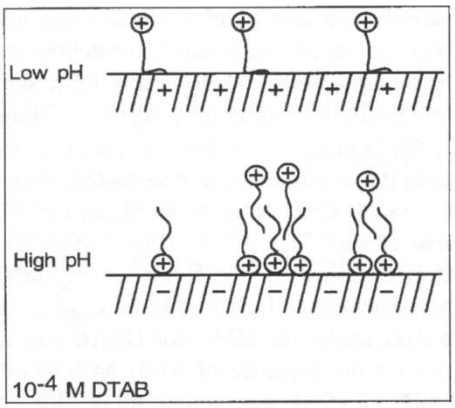

Figure 24. Illustration of the adsorption of dodecyl trimethylammonium bromide (DTAB) at concentration 10^{-4} M onto polymeric membrane surfaces at high and low pH [78].

Above the isoelectric point, the electrostatic interaction becomes more dominate due to opposite charges of the surfactant and the membrane. Thus, the adsorption at higher pH is more significant due to possible hemi micelle formation (Figure 24). Hence, the adsorption behavior with the cationic surfactant is contrary to the adsorption with anionic surfactants.

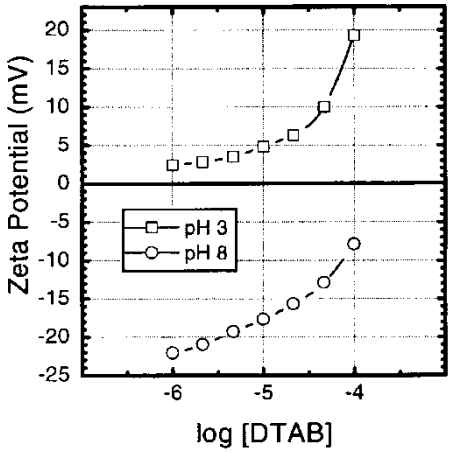

Figure 25. Comparison of Zeta potential of NF-55 membrane in the presence of cationic DTAB surfactant at pH 3 and 8. The experiments were carried out with a background electrolyte of 0.01 NaCl. [77]

4.2.3 Adsorption of nonionic surfactants

Nonionic surfactants are more preferably adsorbed physically than electrostatically adsorbed or chemisorbed. Unlike other surfactants, quite small changes in temperature, concentration, or molecular structure of the surfactant can have a large effect on the adsorption. This is because of surfactant-surfactant and surfactant-solvent interactions, which causes surfactant aggregation in bulk solution and leads to changes in backing and orientation of surfactants at the surface. [75]

Nonionic surfactants adsorb onto neutral membrane by hydrophobic and hydrophilic interactions as a basic function of surface wettability [71]. When contact angle increases, in other words hydrophobicity increases, the hydrophobic binding becomes dominant [80].

Maartens *et al.* [81] used commercial nonionic surfactants Triton X-100 and Pluronic F108 for porous UF membrane pretreatment by means to reduce fouling by NOM. The adsorption of these surfactants onto a hydrophobic membrane surface and its pores is presented in Figure 26.

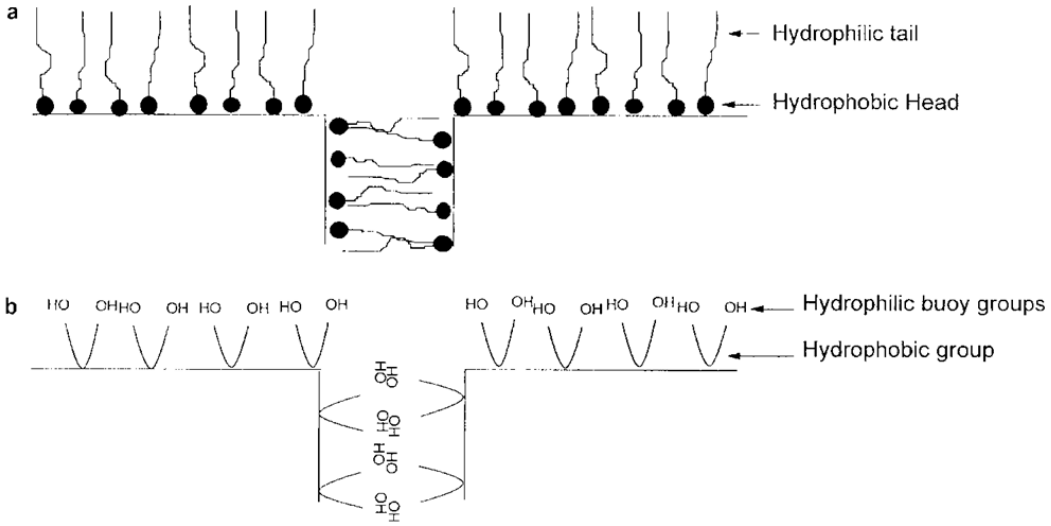

Figure 26. Schematic illustration of the adsorption of nonionic surfactants Triton X-100 (a) and Pluronic F108 (b) onto hydrophobic membrane surface and its pores [81].

It is assumed that nonionic surfactant' micelles do not adsorb on hydrophilic surfaces. They are expected to contribute to the adsorption only by releasing monomers during the diffusive transport [75].

5 INFLUENCES OF SURFACTANT ADSORPTION ON MEMBRANE PERFORMANCE

The aim of surfactant adsorption is to modify membrane surface by means to increase membrane efficiency and prevent membrane fouling tendency. Thus, the influences of surfactant adsorption on membrane surface characteristics (hydrophilicity, charge and roughness) and separation performance (flux and rejection) must be evaluated.

5.1 Hydrophilicity of membrane

Cornelis *et al.* [80] investigated the effect of contact angle on flux behavior in nanofiltration of nonionic surfactants. The used membranes were Desal 5 DL (Ge Osmonics), NF270 (Dow/Filmtec), UTC-20 (Toray), N30F (Nadir) and NTR-7450 (Ditto-Denko). Based on their results, the surfactant adsorption to the hydrophobic groups of the membrane led to flux increase and the surfactant adsorption to the hydrophilic groups led to flux decrease.

The flux increase above the pure water flux was observed with UTC-20 and Desal 5DL membrane (Figure 27). Cornelis *et al.* [80] assumed that increased flux was a result of improved wetting of the membrane surface due to adsorption of surfactants. Nonionic surfactants interact with hydrophobic groups of membrane surface mainly with Van der Waals and London interactions [80]. Thus, hydrophobic tails of surfactants will adsorb onto hydrophobic groups of the membrane while the hydrophilic heads are oriented to the bulk solution (Figure 28 c). Same kind of adsorption assumptions were made by Maartens *et al.* [81] with nonionic Triton X-100 surfactants (Figure 26). Cornelis *et al.* [80] supposed that the flux increase was most obvious with more hydrophobic membranes, such as UTC-20, due to the stronger attraction of surfactants.

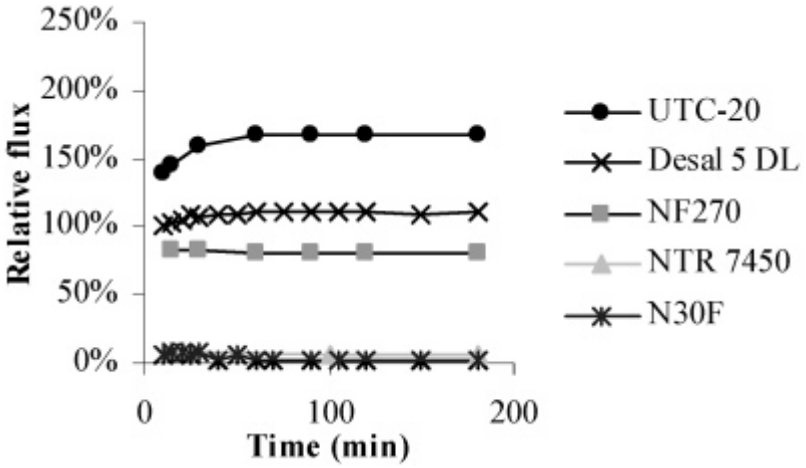

Figure 27. The flux relative to pure water flux of five nanofiltration membranes during the filtration of 200 ppm of synthetic surfactant solution (Fasavin CA 73 solution) at certain time period [80].

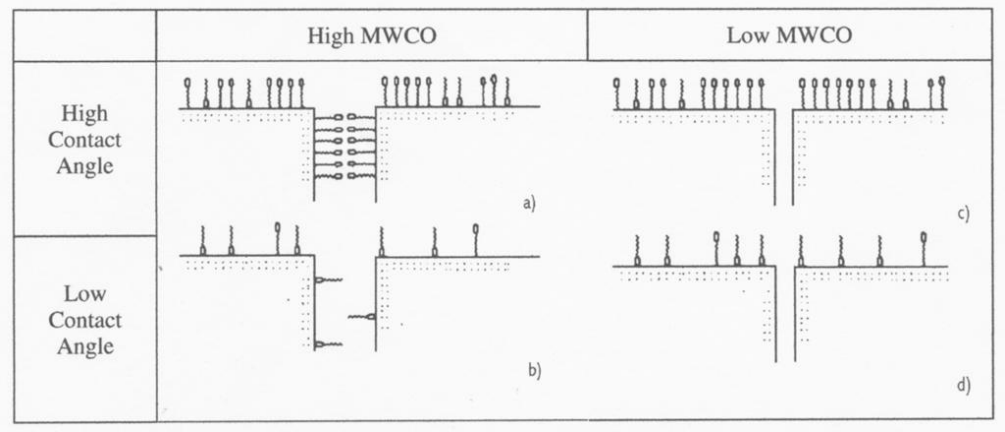

Figure 28. Overview of the possible nonionic surfactant adsorption onto the membrane surface with high MWCO (a,b) and low MWCO (c,d) and membrane with high contact angle (a, c) and low contact angle (b, d) [80].

Cornelis *et al.* [80] hypothesized that with more hydrophilic membranes, such as NF270, the flux decrease was caused by the decreased wettability of the membrane surface. Presumption was made based on assumptions that neither the adsorption in pores due to low molecular weight cutoff of NF270 nor improved wettability due to low contact angle occurred. Used nonionic surfactants were relatively hydrophilic, thus it was supposed that adsorption of surfactant head groups to hydrophilic groups of membrane surface is possible. Thereby, the hydrophobic moieties will be tangled out into the bulk solution (Figure 28 d), which makes membrane more hydrophobic and consequently decreases the flux.

Adsorption of nonionic surfactants to hydrophilic membranes is also quite weak due to low free energy of this construction, hence, the adsorption and flux decline will be reversible [80].

From Figure 28 a and b is shown that when the molecular weight cut off (MWCO) of membrane is high, monomers can also penetrate into the pores. When the membrane is relatively hydrophobic, monomers are strongly adsorbed onto the membrane surface and into the pores, thus the pore radius is reduced, leading to flux loss (Figure 28 a). With more hydrophilic membranes, the adsorption is much less strong, thus, flux decline is limited. However, when the MWCO is much lower than the monomer size, the pore blocking cannot occur and only the changes in the membrane surface affect the flux (Figure 28 c and d). [80] This is also in the case of nonporous RO membranes.

McCutcheon and Elimelech [82] demonstrated that also improving the wetting of the membrane support layer results in a significant increase in water flux for osmotically driven membrane processes. In their study they used cellulosic brackish water RO membrane and TFC RO membrane. SDS surfactants were added to the deionized feed solution after the equilibration procedure.

5.2 Changes in membrane charge

Earlier studies [37, 57, 77, 78] revealed that in the presence of anionic surfactants membranes become more negatively charged. Contrary, with cationic surfactants membrane became more positively charged [77, 78]. The effect of an anionic and cationic surfactant on the zeta potential of TFC polyamide RO membrane is presented in Figure 29.

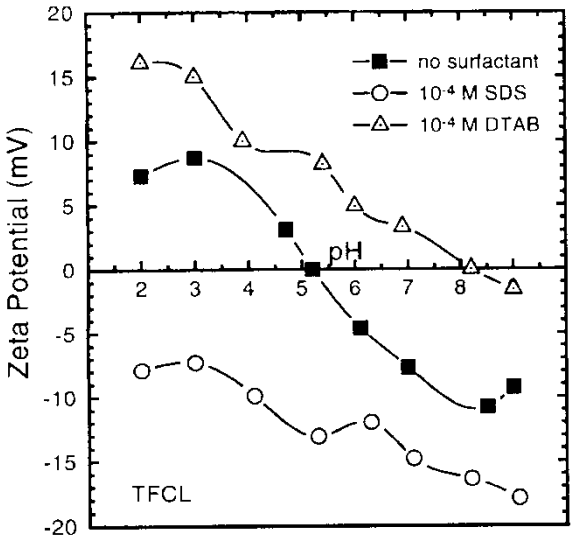

Figure 29. Effect of an anionic surfactant, sodium dodecyl sulfate (SDS) and cationic surfactant, dodecyl trimethylammonium bromide (DTAB), on the zeta potential of the TFC polyamide RO membrane over the pH range 2–9. Experiments were carried out in the presence of 0.01 M NaCl. [78]

Elimelech *et al.* [57] added anionic surfactants (SDS) to mask variations in chemical and electrokinetic surface characteristics of aromatic polyamide TFC membranes and cellulose acetate membranes. The zeta potential results showed that the membranes became negatively charged at entire pH range. As the membrane was negatively charged under used operating pH (pH 5.4–5.6 for cellulose acetate membrane and 7.8 for TFC membrane), it is assumed that SDS surfactant was adsorbed onto membrane surface with hydrophobic moieties. Thereby, their negatively charged polar heads dominate the membrane surface charge [57]. However, there was only small flux increase in the presence of SDS (Figure 30) due to increased electrostatic repulsion between membrane surface and colloidal particles, thus fouling was still significant.

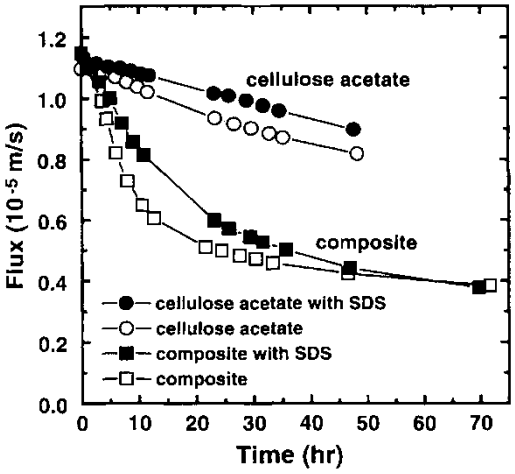

Figure 30. Permeate flux of the composite and cellulose acetate RO membrane as a result of fouling. Fouling experiments with 0.01 M NaCl are represented with open symbols and closed symbols represent fouling at 0.01 M NaCl plus 0.3 mM SDS. Silica colloid concentration was 90 mg/L and used temperature was 20 ˚C. Experiments with the composite membrane were carried out at pH 7.8 and at pH 5.4–5.6 with cellulose acetate membrane. [57]

The big difference in fouling/flux decline behaviors between cellulose acetate and composite membranes is explained by their differences in surface roughness [57]. Therefore, the surface roughness should be considered.

5.3 Surface roughness

Figure 30 shows Elimelech *et al.* [57] results of colloidal fouling behavior of cellulose acetate and composite membranes in the presence of 0.01 M NaCl and a mixture of 0.01 NaCl plus 0.3 mM SDS. In their experiments, the flux of composite membrane dropped sharply during the first 12 hours while the flux of cellulose acetate membrane decreased slowly throughout the whole fouling test. They assumed that the difference in colloidal fouling between the membranes is a result from the surface roughness. As earlier studies, they indicate that TFC membranes exhibits large surface roughness of ridge-and-valley structure, while the surface of cellulose acetate membrane is relatively smooth. The roughness of the composite membrane may produce tangential colloidal forces which can attach colloidal particles on the membrane surface [83].

5.4 Flux and salt rejection

Childress and Deshmukh [37] examined the effect of SDS on water flux and salt rejection of RO membranes. Based on their study SDS had significant effect on the flux and salt rejection of TFC polyamide RO membrane and asymmetric cellulose acetate membrane.

Unlike the results of Elimelech *et al.* [57], the flux of both membranes decreased when SDS was introduced to the system. For both membranes (FT-30 and CG), the flux was lower over the entire pH range (Figure 31 a and 32 a), although the operating pressure of FT-30 membrane was increased to maintain sufficient flux. The effect of SDS on flux was most apparent at low pH. Also, at low pH the salt rejection of both membranes increased significantly in the presence of SDS while at high pH it was almost the same than without SDS (Figure 31 b and Figure 32 b). Differences between the membranes can be explained by the differences in the membrane surface layer structure (see previous Chapter 5.3).

The greater effect of SDS on salt rejection and flux at lower pH is a result of the membrane's positive charge at low pH. Thus, the adsorption occurs due to electrostatic attraction of negatively charged head groups of the surfactants onto the membrane surface and hydrophobic moieties are dangled in bulk solution (Figure 22 a). Thermodynamically this formation is not favorable for hydrocarbon moieties and they start to associate hydrocarbon chains in the bulk forming hemi micelles (Figure 22 b) [79]. Formed hemi micelles will create a secondary filtration layer that decrease flux and increase salt rejection of the membrane. At higher pH values, the adsorption occurs due to hydrophobic interaction and negatively charged head groups are tangled in bulk solution (Figure 22 b). Hence, the hydrocarbon chains are thermodynamically favorable formation and hemi micelles are not formed even at higher filtration concentration.

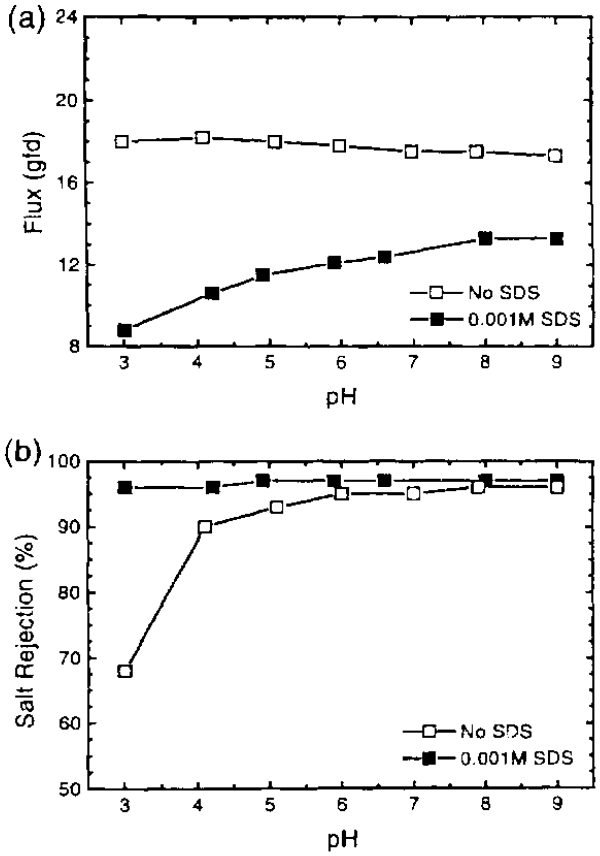

Figure 31. Flux (a) and salt rejection (b) of TFC polyamide RO membrane (FT-30) with and without 0.001 mM SDS. The used pressure was around 17.2 bar, temperature 20 ˚C, flow rate 1.9 L/min and with background electrolyte 0.01 M NaCl. [37]

Childress and Elimelech [77] got similar results with TFC nanofiltration membranes. They also assumed that the SDS addition may result in the formation of a secondary filtration layer on the membrane surface at low pH which causes the flux decline and increased rejection of the membrane. However, the investigated nanofiltration membrane was loose, so also the pore size of the membrane influenced on the flux and rejection unlike the cases observed with RO membranes.

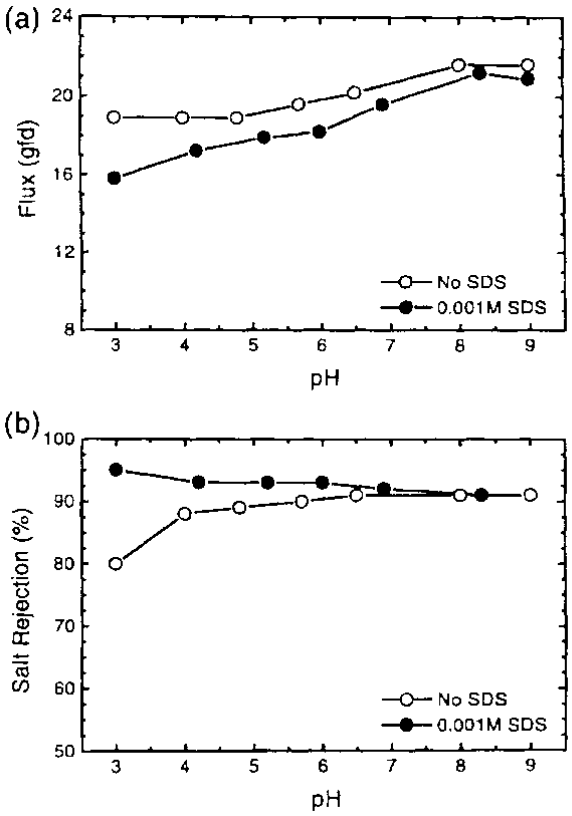

Figure 32. Flux (a) and salt rejection (b) of asymmetric cellulose acetate RO membrane (CG) with and without SDS. The used pressure was around 20.7 bar, temperature 20 ˚C and flow rate 1.9 L/min and with background electrolyte 0.01 M NaCl. [37]

EXPERIMENTAL PART

6 AIM OF THE EXPERIMENTAL PART

The aim of the experimental part of thesis was to investigate how the surfactant addition into the feed water affects membrane efficiency. Here the membrane process efficiency was measured through water permeability and salt rejection. The adsorption of surfactant on membrane surface was also studied by measuring membrane surface hydrophilicity and charge. Moreover, the effects of dynamic conditions on filtration experiment and surfactant adsorption were studied.

7 MATERIALS AND METHODS

Two commercial TFC RO membranes were modified by adding three individual surfactants in the feed solution. The experiments were carried out with DSS Labstak M20 filter. The filtration experiments were divided into three methods based on their differences in pressurization and the surfactant adding stage.

7.1 Feed solution chemistries

Two anionic (surfactants 1 and 2) and one nonionic surfactant (surfactant 3) were added into the feed water below their CMC by means to increase the water permeability and salt rejection. Each surfactant was added separately into the feed water. The properties of used surfactants are presented in Table VI.

Table VI The properties of used surfactants in this study.

Surfactant	Type	CMC w-%
Surfactant 1	Anionic	0.2
Surfactant 2	Anionic	0.07
Surfactant 3	Nonionic	0.01

The used feed water was purified water with Centra-R 60/120 by Elga. This water is called as pure water in this work. The salt was added into the feed water to demonstrate the desalination process. The used model salt was commercial marine salt by Risetti Oy that consists of one additive, anti-caking agent (E5353). The commercial marine salt is mainly composed of sodium chloride (Figure 33 b). Ion chromatography results indicate that besides sodium chloride it contains calcium, magnesium, potassium, and sulphates. The added marine salt concentration was 2 g/L (2000 ppm). The sodium chloride is used in the production of chemicals, metallurgy, food preservative, soap manufacture and home water softeners [84]. Other possible components composed of present ions are shown in Figure 33 and in Table VII. Besides these salts, also sodium sulphate (Na_2SO_4) can be formed.

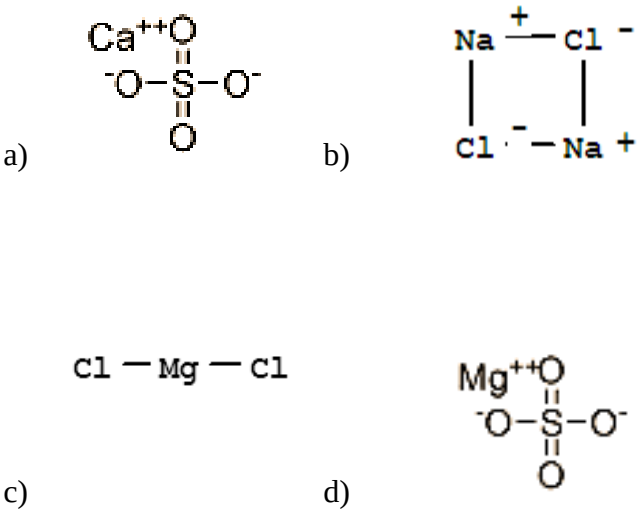

Figure 33. Molecular structure of calcium sulphate (a), sodium chloride (b), magnesium chloride (c) and magnesium sulphate (d) [85a–d, 93].

Table VII Properties of salts in sea water [85a–e].

Compound	Formula	Molar mass, g/mol	Solubility in water (20 ˚C), g/L
Sodium chloride	NaCl	58.44	360
Magnesium chloride	$MgCl_2$	95.21	400
Magnesium sulphate	$MgSO_4$	120.37	255
Calcium sulphate	$CaSO_4$	136.14	2.1

7.2 Selected membranes

Two commercial TFC polyamide (PA) membranes, Desal AG from GE Osmonics and LE-4040 from Dow Filmtec, were used in the experiments. The membranes were selected based on their good salt rejection ability and similarity. The properties of these membranes are summarized in Table VIII.

Table VIII The characteristics of TFC membranes in the study [86, 87].

Trade name	Manufacturer	Material	Maximum temperature, ˚C	Maximum pressure, bar	pH range	Surface charge at pH 6	Salt rejection, %
DESAL AG	GE Osmonics	TFC:PA	50	41	4–11	Negative	99.5
LE-4040	Dow Filmtec	TFC:PA	45	41	2–11	Negative	99.0

The zeta potentials of pretreated AG and LE-4040 membranes as a function of pH are shown in Figure 34. The membrane pretreatment method is described in Chapter 7.4. Zeta potential curves of both membranes are quite similar and typical for TFC polyamide membranes; the membranes are negatively charged at higher pH and positively charged at lower pH values. LE-4040 membrane is slightly more positively charged almost at entire pH range having IEP at pH 4.4, while the IEP of Desal AG membrane is at pH 4.

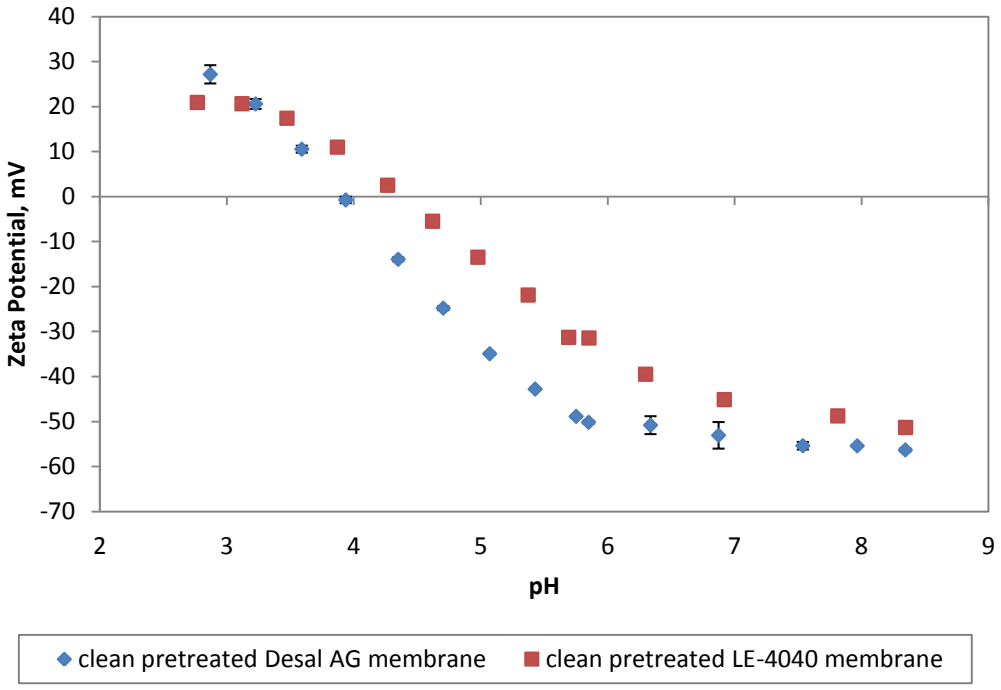

Figure 34. Zeta potentials of pretreated TFC polyamide Desal AG and LE-4040 membranes at different pH values.

7.3 Filtration equipment

The first filtrations were made with three-cell filtration unit. However, the pressure at low cross-flow velocity was not stable enough. Thereby, the rest of filter experiments were made with a DSS LabStak M20 filtration unit that gave more stable pressure at low cross-flow velocity.

The flat sheet DSS Labstak M20 filter can be used for example in comparison of different membranes and in filtrations that need high pressures. With the DSS filter up to 20 membranes can be used at the same time [89]. The membranes are placed on the top of each other and the membrane area of each membrane is 360 cm^2. Here, only one membrane was investigated at a time. The filtration equipment is presented in Figure 35. The membrane was placed on the both side of permeation plate. The filtration and permeation plates of DSS filter are presented in Figure 36.

The temperature was kept constant with cooling coil inside the feeding tank. The cross-flow velocity was calculated on the based on membrane thickness (Equation 16). The experiment runs were carried out with a feed volume of 12–16 dm^3 at the

beginning of each run. The cross-flow was kept constant during the whole filtration. It was 0.32 m/s in first filtrations and 0.14 m/s in the rest of filtrations. The temperature of feed solution was kept around 25±3 ˚C. The permeate and retentate were recycled back to the feeding tank and the permeate volume was measured by taking samples periodically. The flow diagram of DSS Labstak M20 filtration unit is presented in Figure 37.

Figure 35. DSS Labstak M20 filtration unit.

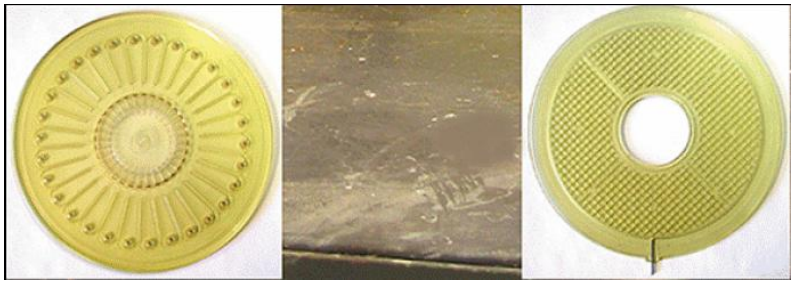

Figure 36. The filtration plate (on the left) and permeation plate (on the right) of DSS filter. The membrane is placed on both sides of the permeation plate and filtration plates are placed on the top of the membrane.

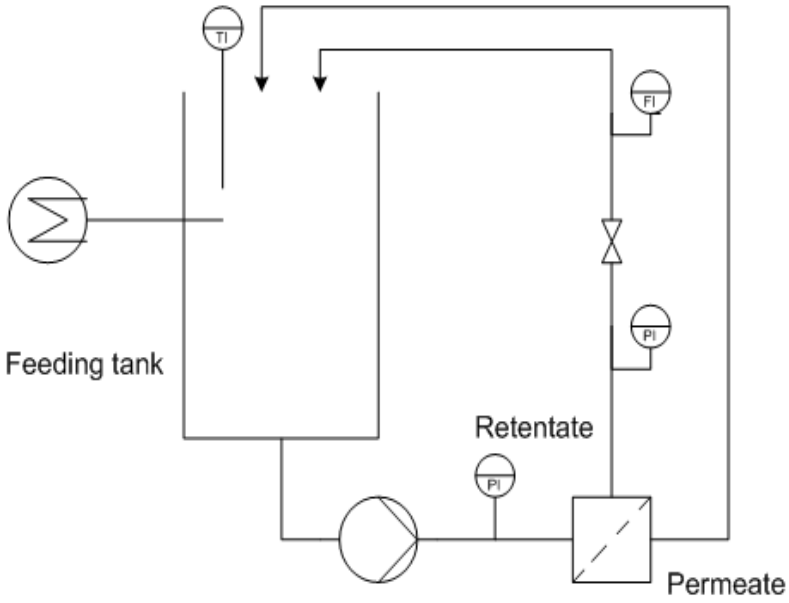

Figure 37. The flow diagram of DSS Labstak M20 filtration equipment.

7.4 Membrane pretreatment and modification with surfactants

All the membrane pieces were pretreated before the filtrations experiments. The used pretreatment method included the following steps:

1. Rinsing of membrane pieces with pure water
2. Shaking of the membranes rigorously three times (each time for one minute with new pure water) by hand in decanter filled with pure water
3. Soaking/storing the membranes in pure water for overnight
4. Rinsing the membrane pieces a last time with pure water before placing them in filtration equipment and pressurized

The membranes were modified with three surfactants whose properties are shown in Table VI. The surfactants were diluted to 1000 ppm solutions and then dissolved into the feed water at predetermined concentrations from 2 to 5 ppm. The idea was to add surfactant under their CMC. Only one surfactant was added into the feed solution at the time. The surfactant addition was performed by taking 2 liters of the feed water from the feeding tank and mixing it with a certain amount of 1000 ppm of surfactant solution. Then the mixed solution was poured at once into the feeding tank while the process was ongoing. Thereby, the surfactant addition was carried out by online dosing.

7.5 Filtration experiments

The filtration experiments can be divided in three parts. In the first part, the effect of surfactant concentration and applied pressure on water permeability was examined. This was done only with surfactant 1. In the second part, the effect of single surfactant addition to water flux with all three surfactants was studied. In the third part, besides the effect of surfactant addition on the water permeability, the effect on the salt rejection was also examined.

7.5.1 Filtration procedure 1

The first filtration experiments were performed with the three-cell filter. However, there were some problems with the filtration equipment; thus these results are not discussed in more detail. The flow diagram of the three-cell filter is shown in Appendix I and the filtration results in Appendix II. The rest of filtrations were carried out with DSS Labstak M20 filter. The used membrane was Desal AG membrane and only surfactant 1 was used. The filtration procedure followed the next steps:

The first filtration procedure

1. Stabilization/pure water flux measurements for 2.5 hours
2. Surfactant dosing into the feed water
3. Flux measurements of the water-surfactant solution for 4 h

Details of these filtrations are presented in Appendix III. Temperature, pH and flow rate were kept constant, while the operating pressure (3.5 and 7 bar) and the surfactant concentration (2 and 5 ppm) varied.

7.5.2 Filtration procedure 2

In the second filtration procedure, the idea was to examine quickly if some of the three surfactants can increase the pure water permeability (PWP). The filtration experiments were carried out with two different flow rate velocities (0.42 and 0.14 m/s) while other parameters remained constant. Details of these filtrations are presented in Appendix IV. The used membrane was LE-4040 and the used surfactant concentration was 2 ppm.

After the surfactant addition and water-surfactant solution flux measurement, the filtration equipment was rinsed with pure water and the feed water was changed to pure water. Then the pure water flux was measured and other surfactant was dosed. The whole filtration procedure was carried out using the same membrane piece. The procedure followed the next steps:

The second filtration procedure

1. Pressurization at 15 bar for 2 hours
2. Compression at 25–30 bar for 2 hours
3. Stabilization at 15 bar for overnight
4. **Surfactant 1** addition at 15 bar and the flux measurements for 2 hours
5. Pure water flux measurements at 15 bar for 2 hours
6. **Surfactant 2** addition at 15 bar and flux measurements for 2 hours
7. Pure water flux measurements at 15 bar for 2 hours
8. **Surfactant 3** addition at 15 bar and flux measurements for 2 hours
9. Pure water flux measurements at 15 bar for 2 hours

7.5.3 Filtration procedure 3

In the third filtration procedure the effect of surfactant addition at different pH to water permeability and salt rejection was studied. The experiments were carried out with LE-4040 membrane. All three surfactants were studied separately at the same concentration (2 ppm). Only the water-surfactant feed solution pH varied while other filtration parameters remained constant. The solution pH was adjusted either with 1 M KOH or with 1 M HCl. In comparison, the filtration procedure

was also carried out without surfactant. Details of these filtrations are presented in Appendices V–VIII.

The difference compared to other filtration procedures was the surfactant dosing in the beginning of filtration. After that the membrane was pressurized. Then the surfactant-water solution was replaced by pure water, where the marine salt (2 g/L) was later added. At the end, the salty water was replaced to pure water. The filter equipment was rinsed with pure water every time before the new feed water was changed. The filtration procedure contained the following steps:

The third filtration procedure

1. Stabilization at 1 bar with surfactant 1, 2 or 3 at different solution pH (4.4; 6; 11) for overnight
2. Compression at 25–30 bar for 2 hours
3. Pure water flux measurements at 15 bar for 2 hours
4. Salt addition and flux measurements at 15 bar for 2 hours
5. Pure water flux measurements at 15 bar for 2 hours

7.6 The adsorption test of surfactants onto membrane surface

The adsorption of the three used surfactants at different modification pH on LE-4040 membrane was examined by measuring the contact angles of membrane pieces. The membranes pieces were kept in the pure water over the weekend. Then they were placed for two weeks into the solution that contained 100 ppm of surfactant 1, 2 or 3 at three different pH:

1. pH 3
2. pH 4.4 (IEP)
3. pH 7

For comparison, the same method was used with the membrane pieces which were placed in pure water without a surfactant at these three pH-values. After two weeks, the membrane pieces were kept two hours in water at the same pH than they were earlier kept. Then they were dried for three days at room temperature before the contact angle measurements. The pH adjustments were made with 1 M KOH and 1 M HCl solutions.

8 ANALYZING METHODS OF WATER SAMPLES AND MEMBRANE SURFACE

From each water sample, the pH and conductivity were measured. The concentration of anions and cations in the feed water and the permeate were analyzed with ion chromatography. The membrane surface characteristics were analyzed with contact angle meter and zeta potential analyzer.

8.1 Analyses of the water samples

Conductivity and pH were measured from the feed solution and permeation samples after the filtration experiments. The temperature of samples was around 23–25 ˚C for pH determination and 25 ˚C for conductivity determination. pH was measured with Orion pH meter (model 410A) and it was calibrated using commercial buffer solutions (pH 4, 7 and 10). Conductivity of the samples was measured with Knick 702 conductivity meter. Cations and anions of water samples were determined with Dionex DX-120 and Metrohm MIC 12 EDU ion chromatographies.

8.2 Analyses of the membrane surface

The membrane surface hydrophilicity was determined by contact angle measurement with CAM 100 contact angle meter. The contact angles of dry membranes were measured using a sessile drop method where a drop of pure water was placed on the membrane surface. The camera took three pictures of one droplet and the contact angles of both side of the droplet were measured and averaged. Ten droplets were placed on different points of each membrane piece and measured. Thus, the total number of measurements for one membrane piece was 30. The contact angle of membrane was the calculated average of these measurements. Figure 38 shows the measurement with sessile drop method. If the contact angle is greater than 90˚ the surface is hydrophobic, and if it is smaller than 90˚ the surface is hydrophilic.

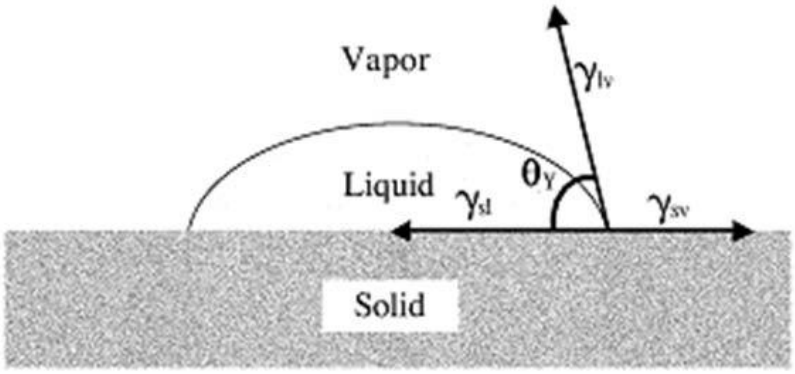

Figure 38. Contact angle measurement with sessile drop method. θ represents the contact angle and $\gamma_{sv,}$ γ_{sl} and γ_{lv} represent the "surface tensions" of the interface solid/gas, solid/liquid and liquid/gas, respectively. [90]

The surface tensions of interfaces and contact angle are linked together based on Young's equation [90]:

$$\gamma_{sv} = \gamma_{sl} + \gamma_{lv} cos\theta \tag{12}$$

where
γ_{sv} the surface tensions of the solid/gas interface, N/m
γ_{sl} the surface tensions of the solid/liquid interface, N/m
γ_{lv} the surface tensions of the liquid/gas interface, N/m
θ the contact angle, ˚

The surface charge was determined by membrane zeta potential. The zeta potential of RO membranes was measured by an electrokinetic analyzer (SurPASS, Anton Paar, Austria) (Figure 39). Before the measurements, the membrane pieces were stored in pure water in a coldroom (about 5˚C). Two pieces of one membrane were placed in the measuring cell (adjustable gap cell). In Figure 40 is shown the clamping cell which operating principle is same with adjustable gap cell. The gap height was adjusted to around 100 μm by flow rate. The streaming potential was detected by Ag/AgCl electrodes installed at the electrolyte inlet and outlet of the measuring cell. The electrolyte was circulated through the measuring cell alternatively from both sides, thereby creating a differential pressure and the corresponding streaming potential signal. [91] The used background electrolyte was 1 mM KCl solution and the solution pH varied from 3 to 8. The operating pressure was around ±300 mbar and the temperature was about 25˚C.

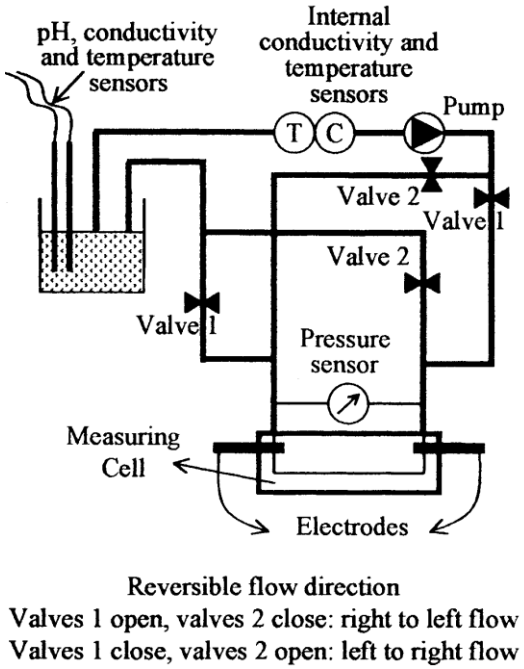

Figure 39. Schematic drawing of electrokinetic analyzer [92].

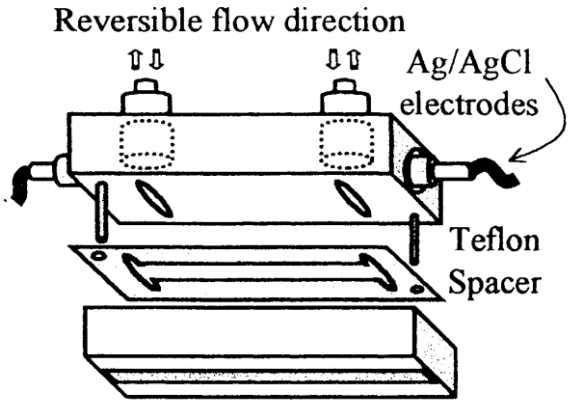

Figure 40. Schematic drawing of the measuring cell (clamping cell) of electrokinetic analyzer [92].

9 EQUATIONS

The permeate flux *J* was calculated from the filtration results by following equation:

$$J = \frac{\frac{m}{\rho} \cdot 1000\, L/m^3}{t \cdot A} \tag{13}$$

where *J* permeate flux, L/h m^2
m the mass of permeate, kg
ρ the density of water, 1000 kg/m^3
t time, h
A membrane area, m^2

The pressure normalized flux which was called as the permeability of membrane *P* was calculated as follows

$$P = \frac{J}{p} \tag{14}$$

where *P* permeability, L/h m^2 bar
p pressure, bar

The salt retention of membrane was calculated by following equation

$$R = \left(1 - \frac{c_p}{c_f}\right) \cdot 100\ \% \tag{15}$$

where *R* retention, %
c_p the concentration of the solute in the permeate, g/L
c_f the concentration of solutes in the feed, g/L

The cross-flow velocity of DSS Labstak M20 filtration unit was calculated as follows

$$U = \frac{V}{a \cdot (b - x) \cdot n} \tag{16}$$

where *U* linear flow velocity, m/s
V volumetric flow rate, m^3/s
a the width of a rectangular cross-section, m
b the height of a rectangular cross-section, m
x the thickness of the membrane, m
n the number of channels

10 RESULTS AND DISCUSSION

The filtration experiments in this study are divided in three parts. In the first part, the effect of surfactant 1 concentration and the applied pressure on PWP of Desal AG membrane was examined. The effect of modification on membrane surface was also measured with contact angle and zeta potential measurements.

In the second part, the idea was to study quickly the effect of single surfactant on PWP of LE-4040 membrane. This was done with all three surfactants. In the third part, the effect of surfactant addition on PWP and the salt rejection of LE-4040 membrane were examined. The surface of the modified membrane was characterized with contact angle and zeta potential measurements.

The surfactant dosing method varied between these three filtration procedures. In the first part the surfactant was added after the water stabilization and in the second part after the compression and overnight lasting pressurization. In the third part the surfactant was added at the beginning of the filtration and the surfactant-water solution was recycled in the filter equipment overnight and compressed before changing the solution to pure water. The filtration procedures are described more detailed in the Chapter 7.5.

10.1 The filtration of modified Desal AG membrane with surfactant 1

Desal AG membrane was modified with one surfactant at two different concentrations and applied pressures. The filtration method is described at Chapter 7.5.1 and the results of these filtrations are presented in Appendix III. The filtrations experiments of the first part are shown in Table IX. The zeta potential and contact angle measurements were carried out with the membranes used in the filtrations.

Table IX. The filtration experiments with DSS Labstak M20 filter. The used membrane was Desal AG membrane modified with two different concentrations of surfactant 1 at two operating pressures.

Filtration equipment	Surfactant 1 concentration, ppm	Operating pressure, bar
DSS Labstak M20-filter	2	7
DSS Labstak M20-filter	5	7
DSS Labstak M20-filter	5	3.5

10.1.1 Zeta potential measurements of Desal AG membrane

In Figure 41 the zeta potential of Desal AG membrane as a function of pH, in the presence and absence of surfactant 1 is presented. All the membranes were pretreated before filtrations (see Chapter 7.4). More specifically, the membranes in the presence with surfactant were used in the filtration experiments and the membranes in the absence of surfactant were pretreated, one of which was also pressurized in the filtration equipment. The zeta potentials showed the basic character of thin film composite membranes. The membrane was positively charged at low pH and negatively charged at high pH having IEP around four.

As shown in Figure 41, the anionic surfactant 1 did not have significant influence on the charge of membranes i.e. the zeta potentials of the membranes modified with surfactant 1 were quite similar than the membranes without modification.

The effect of surfactant 1 on membrane charge was greater at lower pH compared to membrane with no surfactant. The higher surfactant concentration gave slightly more negative charge. At low pH the Desal AG membrane is positively charged, thereby the adsorption occurs due to electrostatic attraction between the negatively charged polar heads of surfactant ions and the membrane surface (Figure 22). Thus, negatively charged surfactants dominate the surface charge. As the concentration increases the adsorption of anionic surfactant molecules onto the membrane surface enhances which gives more negative charge for the membrane.

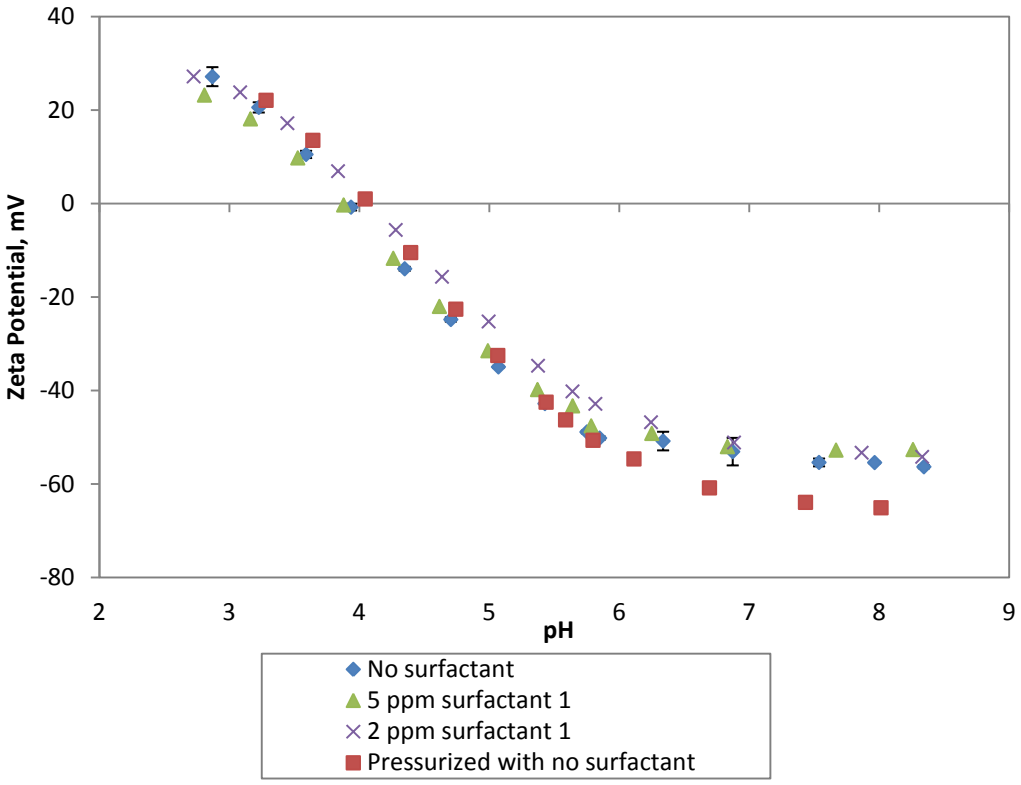

Figure 41. Zeta potential of modified and unmodified Desal AG membrane at pH range 3–8. The modification was carried out with 2 and 5 ppm of surfactant 1 with DSS Labstak M20 filter.

At high pH, the membrane is negatively charged as the surfactant 1, thus, the adsorption occurs due to hydrophobic interactions between the membrane surface and hydrophopic tail of surfactant (Figure 22). Thereby, the negatively charged polar head of the surfactant is tangled in the bulk solution and do not have as great effect on the surface charge than surfactants at low pH. At high pH, the zeta potentials between the modified and the unmodified membrane (without pressurization) were almost the same. However, there was a big difference between the unmodified membranes at higher pH. The zeta potential of the unmodified, pressurized membrane was much more negative than with the membrane without pressurization.

10.1.2 Contact angle of Desal AG membrane

The contact angles of unmodified and modified Desal AG membranes with anionic surfactant 1 are presented in Table X. From the Table X can be seen that

only with higher concentration of surfactant 1 the membrane surface became more hydrophilic i.e. the contact angle decreased.

Table X The contact angles of unmodified and modified Desal AG membrane with 2 and 5 ppm of anionic surfactant 1 with DSS Labstak M20 filter.

Membrane	No surfactant, °	2 ppm surfactant 1, °	5 ppm surfactant 1, °
Desal AG	50±5	48±5	36±5

10.1.3 The effect of applied pressure and surfactant concentration on permeability

The effects of surfactant concentration and the applied pressure on PWP of Desal AG membrane are shown in Figure 42. The addition of surfactant 1 did not increase the PWP. The membrane modified with 2 ppm of surfactant 1 gave greater permeability than modification with 5 ppm. However, the contact angle measurement results showed increased hydrophilicity with higher surfactant concentration (Table X). Also, the zeta potential results showed slightly more negative membrane charge with higher surfactant concentration. Thus, higher surfactant adsorption may have decreased the permeability.

The increased hydrophilicity with surfactant can be explained by the adsorption mechanism. At operating pH, the membrane was negatively charged, thus similarly charged surfactant adsorbed on hydrophobic groups of membrane with hydrophobic moieties and hydrophilic head groups were tangled in bulk solution. This adsorption mechanism has found to increase the water flux with anionic surfactants in the presence of foulants [57].

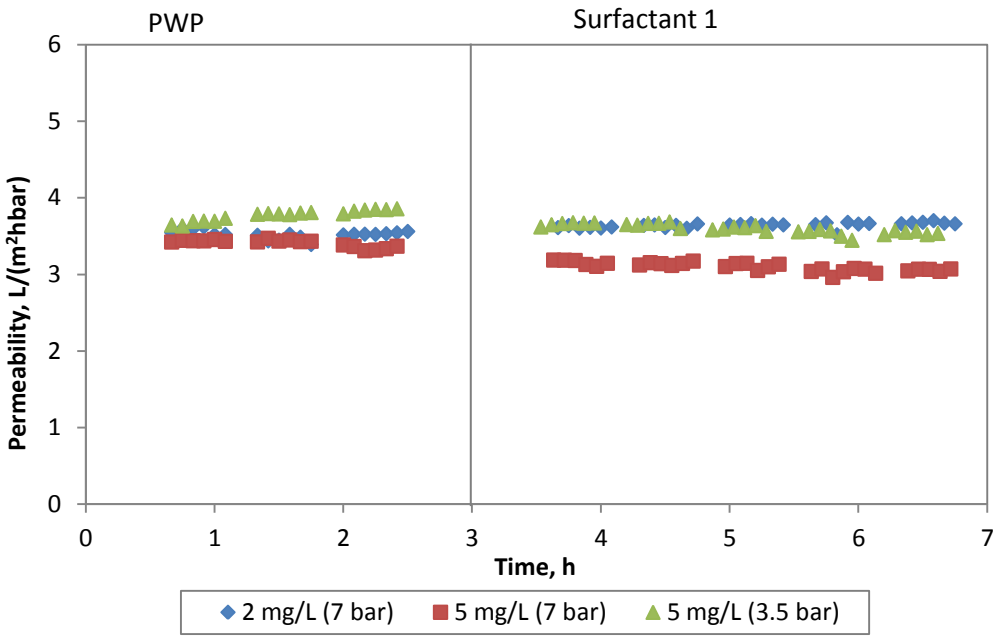

Figure 42. The permeability of Desal AG membrane with pure water (PWP) and pure water with surfactant 1 at two concentrations (5 and 2 ppm) at two operating pressures (3.5 and 7 bar) DSS Labstak M20 filter (pH 6.5, 25 ˚C, 0.32 m/s).

Figure 42 also shows that the permeability of Desal AG membrane was slightly greater at lower pressure when it was modified with 5 ppm of surfactant 1. This can be due to increased CP at higher operating pressure which reduced the permeability.

10.2 The effects of surfactant dosing on PWP

The idea of this filtration test was to investigate quickly if the addition of any of the three surfactants can increase the PWP of LE-4040 membrane. In Figures 43 and 44 are shown the effect of surfactants on PWP of LE-4040 membrane as a function of time. The filtration procedure is described in more detail in Chapter 7.5.2.

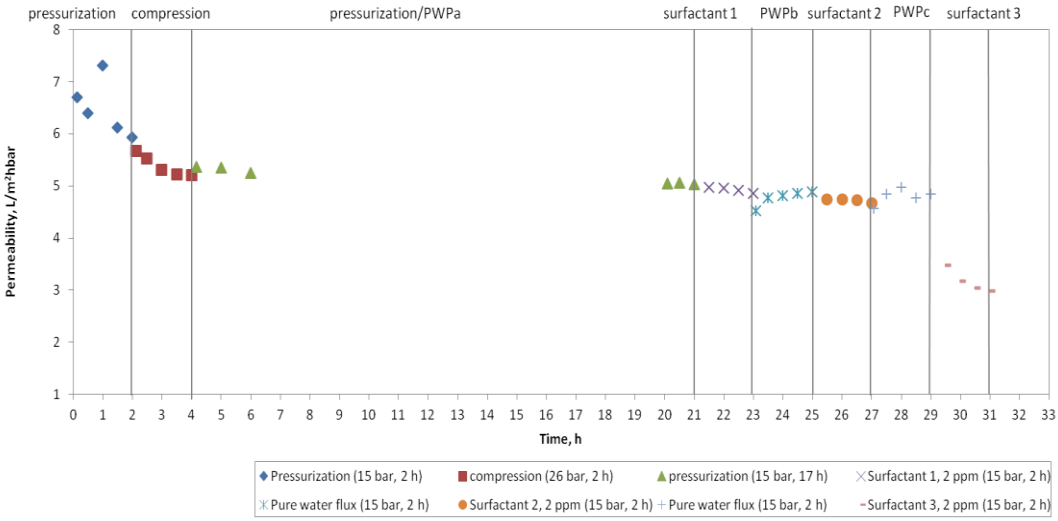

Figure 43. Permeabilities of LE-4040 membrane during the membrane pressurization (0–2 h), compression (2–4 h), pure water filtration PWPa (4–21 h), pure water filtration with 2 ppm of surfactant 1 (21–23 h), pure water filtration PWPb (23–25 h), pure water filtration with 2 ppm of surfactant 2 (25–27 h), pure water filtration PWPc (27–29 h) and pure water filtration with 2 ppm of surfactant 3 (29–31 h). Filtration was carried out with DSS Labstak M20 filter (20–24 ˚C, pH~6, 0.42 m/s, 15 bar and compression 25–30 bar).

The Figure 43 shows that none of the three surfactants increased the water permeability. The pure water permeabilities (PWPa, PWPb and PWPc) were higher before the addition of surfactants 1, 2 and 3. The same filtration procedure was carried out with a smaller flow rate (Figure 44) assuming that surfactants can adsorb more easily with lower flow rate. However, the results were similar. In both cases, there was a slight permeability decline with anionic surfactants (surfactant 1 and 2) and a more severe decline with the nonionic surfactant 3. This indicates that nonionic surfactants may have adsorbed more strongly onto membrane surface decreasing the PWP.

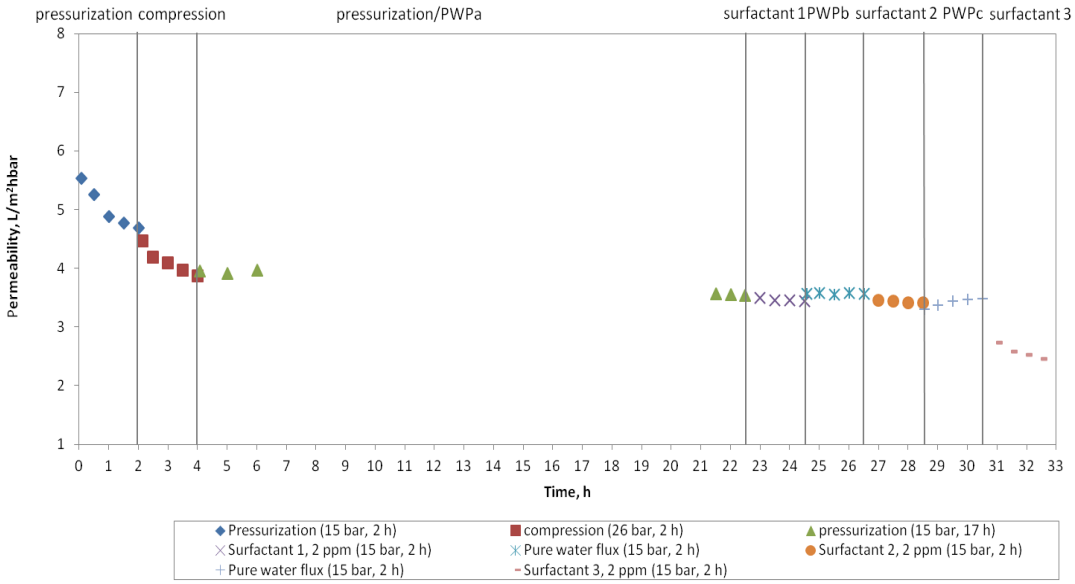

Figure 44. Permeabilities of LE-4040 membrane during the membrane pressurization (0–2 h), compression (2–4 h), pure water filtration PWPa (4–22.5 h), pure water filtration with 2 ppm of surfactant 1 (22.5–24.5 h), pure water filtration PWPb (24.5–26.5 h), pure water filtration with 2 ppm of surfactant 2 (26.5–28.5 h), pure water filtration PWPc (28.5–30.5 h) and pure water filtration with 2 ppm of surfactant 3 (30.5–32.5 h). Filtration was carried out with DSS Labstak M20 filter (20–24 ˚C, pH~6, 0.14 m/s, 15 bar and compression 25–30 bar).

10.3 The effect of solution pH on adsorption of surfactants onto LE-4040 membrane by contact angle measurements

Table XI shows the contact angles of membranes pretreated in 100 ppm of surfactant solutions and pure water at pH 3, 4.4 and 7. The pretreatment method is described in more detail in Chapter 7.6. The membrane contact angles increased i.e. the hydrophobicity increased with anionic surfactants when the modification pH increased from 3 to 7. The unmodified membrane was the most hydrophobic at pH 4.4 (IEP). At this point, the membrane without surfactant was more hydrophobic than modified membranes with surfactant 2 and 3. At pH 4.4, the LE-4040 membrane is electrically neutral, thus the adsorption occurs by hydrophobic interactions where hydrophilic head groups are tangled in bulk solution making the membrane more hydrophilic.

Table XI The contact angles of pretreated LE-4040 membrane with 100 ppm of surfactant 1, 2 and 3 and without surfactant at pH 3, 4.4 and 7.

Modification	Contact angle at pH 3, °	Contact angle at pH 4.4, °	Contact angle at pH 7, °
Surfactant 1	47±2	50±3	63±3
Surfactant 2	42±3	42±3	50±2
Surfactant 3	34±5	37±4	43±5
No surfactant	42±3	54±2	47±3

At pH 3, there were no clear hydrophilicity changes with surfactant modification. It seems that the surfactant 1 made the membrane slightly more hydrophobic. At this pH, the membrane and anionic surfactant 1 are oppositely charged, thus the adsorption occurs primarily because of the attractive electrostatic forces. This means that the hydrophobic parts of the surfactant are oriented in the bulk solution making the membrane more hydrophobic. However, with anionic surfactant 2, there was not change in hydrophilicity. Unlike with anionic surfactants, the nonionic surfactant 3 seems slightly increased the membrane hydrophilicity. Thereby, it can be assumed that hydrophobic parts of surfactants adsorbed on hydrophobic groups of the membrane and the hydrophilic head groups were oriented in bulk solution increasing the hydrophilicity.

At pH 7, the membrane is negatively charged so it can be assumed that the adsorption of anionic surfactants is a result from hydrophobic interactions as with nonionic surfactant. However, anionic surfactant 1 increased hydrophobicity, while wettability stayed constant or slightly decreased with nonionic surfactant. The surfactant 2 did not significantly influence the membrane hydrophilicity.

The differences between anionic surfactants effect on the membrane surface hydrophilicity can be also explained by hydrocarbon chain length of surfactant. The hydrocarbon chain length of surfactant 1 is longer than surfactant 2's, making the surfactant 1 more hydrophobic. The hydrocarbon chain length is shortest with nonionic surfactant; thereby surfactant 3 seems to made the membrane slightly more hydrophilic. Surfactants with longer hydrocarbon chain have greater driving force for the aggregation in water [75]. This may explain the greater change of membrane hydrophilicity with surfactant 1 than with surfactant 2 at pH 7.

10.4 The effect of modification pH on PWP and salt rejection of LE-4040 membrane

After the quick filtration tests, the surfactant addition was done at the beginning of filtrations at low pressure before compression. The filtration procedure is described more detailed in Chapter 7.5.3. Also, unlike in the earlier filtrations, the salt rejection was investigated. The filtration conditions and salt rejections are shown in Table XII.

Table XII The filtration experiments carried out with DSS Labstak M20 filter unit. The used membrane was LE-4040 membrane modified with 2 ppm of surfactant 1, 2 and 3 at different modification pH. Filtrations were made in the presence of marine salt (2 g/L). The salt rejections are calculated mean values determined by ion chromatography.

Surfactant	Surfactant concentration, ppm	Modification pH	Salt rejection %
Surfactant 1	2	6.0	90.92
Surfactant 1	2	11.0	91.19
Surfactant 2	2	6.0	90.21
Surfactant 3	2	6.0	91.28
Surfactant 3	2	11.0	86.69
Surfactant 3	2	4.4	91.44
No surfactant	-	6.0	90.66

10.4.1 Zeta potential measurements of LE-4040 membrane

The zeta potentials were measured from the membranes those were used in filtration experiments. Figure 45 shows the zeta potentials of the modified and the unmodified LE-4040 membranes as a function of pH. With anionic surfactants 1 and 2 the membrane became more negatively charged at the entire pH range. With nonionic surfactant 3 the membrane became more positively charged at low pH and more negatively charged at high pH.

Figure 45 shows that anionic surfactant 1 had greater influence on zeta potential at low pH than at high pH. At the low pH, the negatively-charged groups of surfactant adsorb onto the membrane surface and neutralize the membrane positive charge. At the high pH, the anionic surfactant 1 do not adsorb onto the

similarly charged membrane, thus there is no change in surface charge of membrane. However, the effect of anionic surfactant 2 on zeta potential was greater at higher pH.

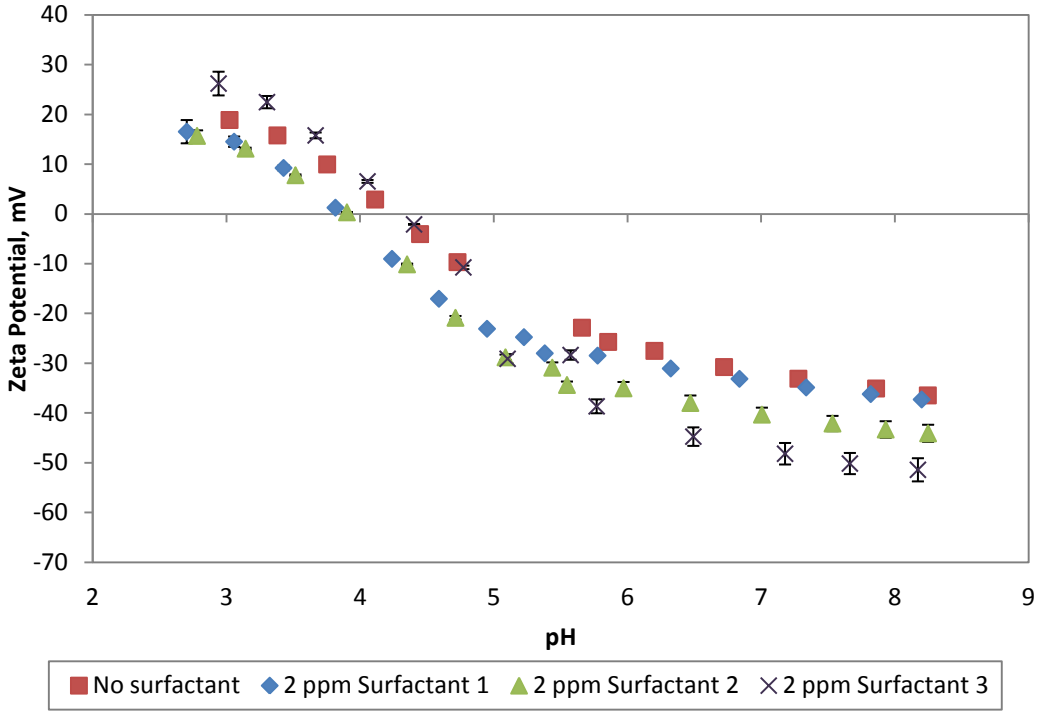

Figure 45. Zeta potential of modified and unmodified LE-4040 membrane at pH range 3–8. The modification was carried out with 2 ppm of surfactant 1, 2 or 3 in the feed water at pH 6 with DSS Labstak M20-filter in the presence of 2 g/L of marine salt.

The effect of anionic surfactants on membrane zeta potential is presented in Figure 46. In the filtrations, surfactant 1 was added at pH 6 and 11 and surfactant 2 at pH 6. At low pH, the modification with surfactant 1, added at pH 11, made the membrane slightly more negatively charged than at pH 6. Thereby, the surfactant 1 may have adsorbed more greatly at higher modification pH. At high pH, the modification with surfactant 1 at pH 6 and 11 did not affect the charge of membrane. The effect of surfactant 2 at low pH was quite similar than with surfactant 1 at pH 6.

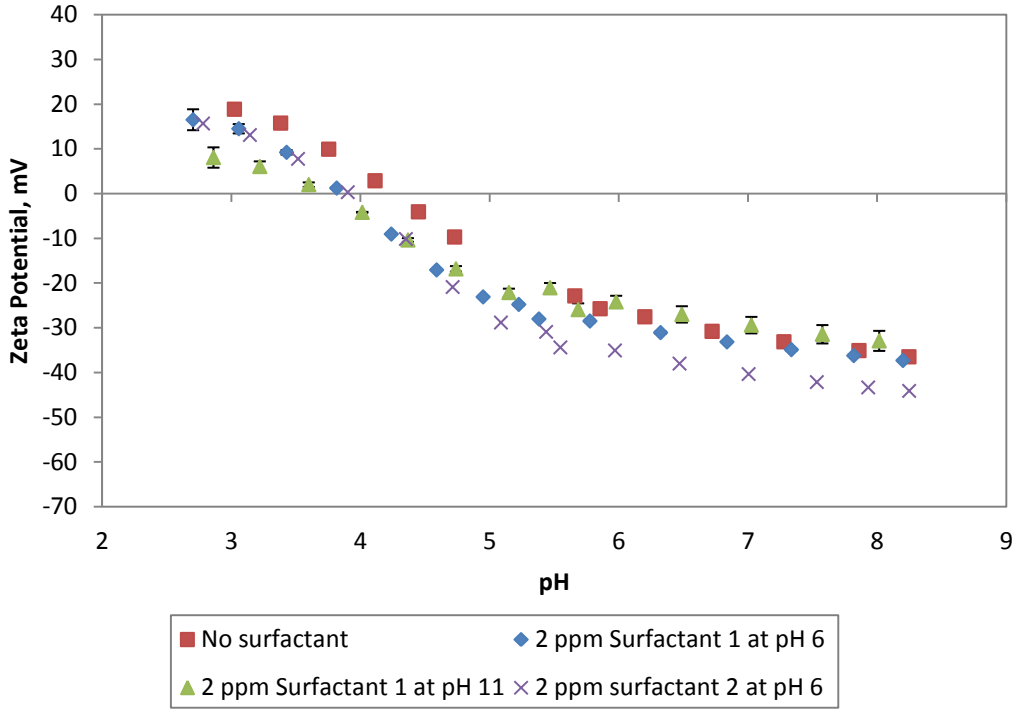

Figure 46. Zeta potential of modified and unmodified LE-4040 membrane at pH range 3–8. The modification was carried out with 2 ppm of surfactant 1 at pH 6 and 11 and 2 ppm of surfactant 2 at pH 6 with DSS Labstak M20-filter in the presence of 2 g/L of marine salt.

Figure 47 shows the effect of modification pH with nonionic surfactant 3 on the membrane surface charge. At low pH, unlike with anionic surfactants, the membrane became slightly more positively charged with surfactant 3. At high pH, the modification made the membrane more negatively charged as with the anionic surfactants. The modification pH did not have significant influence on membrane surface charge.

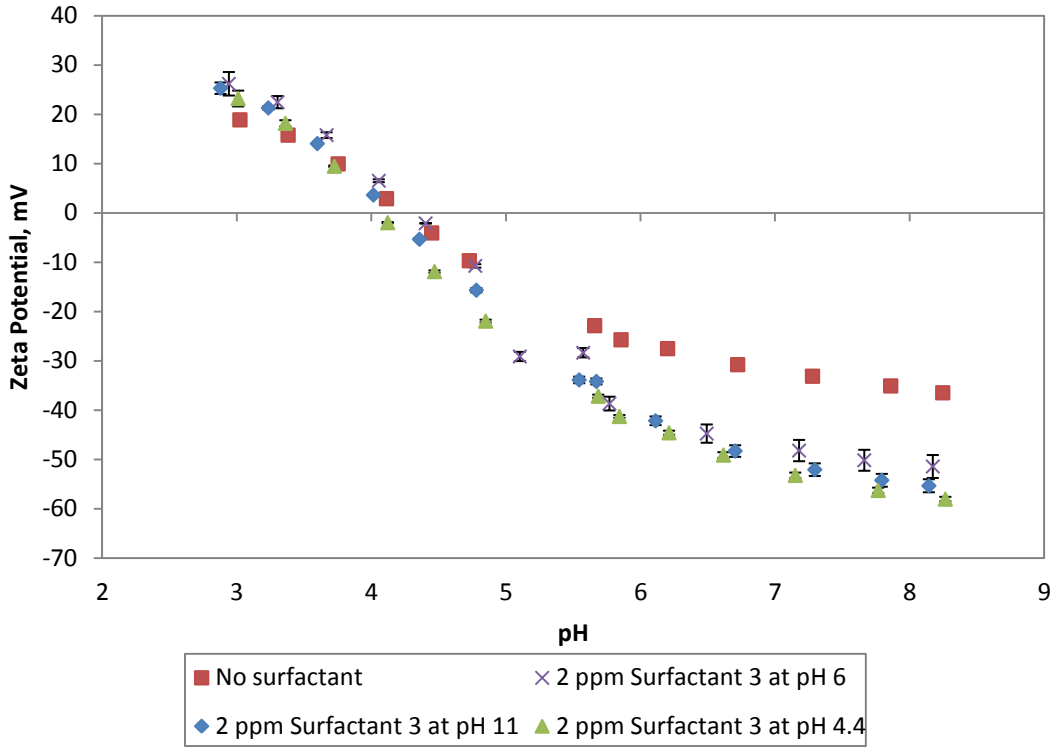

Figure 47. Zeta potential of modified and unmodified LE-4040 membrane at pH range 3–8. The modification was carried out with 2 ppm of surfactant 3 at pH 4.4, 6 and 11 with DSS Labstak M20-filter in the presence of 2 g/L marine salt.

The zeta potential measurements were made with membranes those were used in filtration of commercial marine salt which may have affected to the zeta potentials. Figure 48 shows the zeta potentials of clean LE-4040 membrane and membrane that has been used in marine salt filtration without surfactants.

It can be noticed that at low pH the presence of marine salt made the membrane a slightly more negatively charged decreasing the isoelectric point of membrane from 4.4 to 4.2. At high pH the presence of marine salt made the membrane less negatively charged. Thereby, the membranes could have been even more negatively charged at high pH in the absence of marine salt. The less negative surface charge of membrane at high pH in the presence of marine salt is explained by adsorption of divalent cations. Since the membrane is negatively charged above isoelectric point, the adsorption of divalent cations (Ca^{2+} and Mg^{2+}) is electrostatically more favorable making the membrane surface more positively charged (see Figure 14).

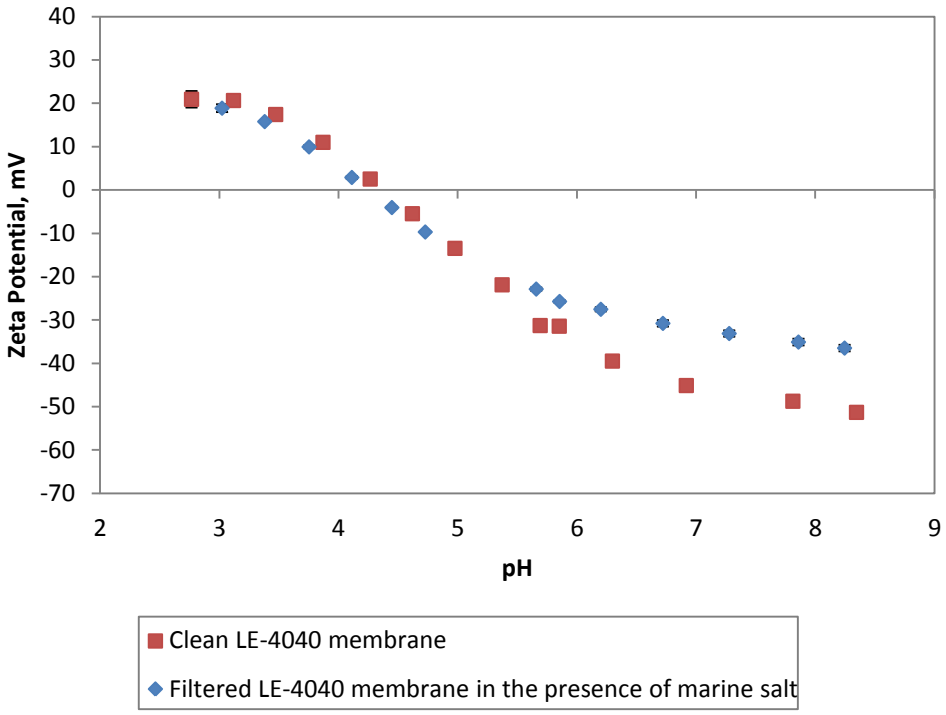

Figure 48. Zeta potentials of pretreated clean LE-4040 membrane and used pretreated LE-4040 membrane with no surfactant in the presence of 2 g/L of marine salt at different pH values.

Figure 49 presents the effect on solution pH and anionic surfactant 1 on the membrane charge. The membranes were pretreated for 48 hours at pH 11 with KOH solution and at pH 11 with KOH plus 100 ppm of anionic surfactant 1. At low pH, the pretreatment with KOH made the membrane more positively charged increasing the IEP from 4.4 to 4.8. Thereby, the surfactant 1 affected the membrane surface charge also above the IEP unlike with the modification of 2 ppm of surfactant 1 at pH 6 and 11 in the presence of marine salt (Figure 46). When 100 ppm of the anionic surfactant 1 was added to the solution the membrane became more negatively charged. At higher pH, the pretreatment with KOH made membrane charge more negative and as surfactant 1 was added the charge became even more negative.

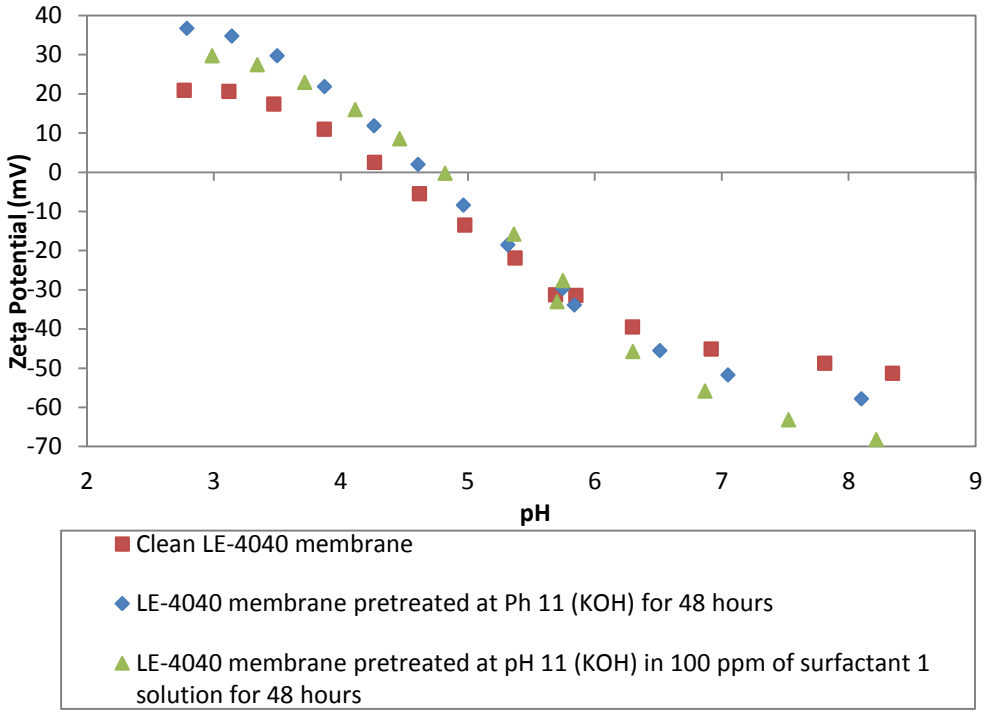

Figure 49. Zeta potentials of LE-4040 membrane pretreated at pH 11 for 48 hours and membrane pretreated in 100 ppm of surfactant 1 solution at pH 11 for 48 hours.

10.4.2 The effect of anionic surfactants on water permeability in the presence of marine salt

Figure 50 shows the effect of anionic surfactants 1 and 2 on water permeability as a function of filtration time. It can be seen that neither surfactant 1 nor 2 increased the permeability.

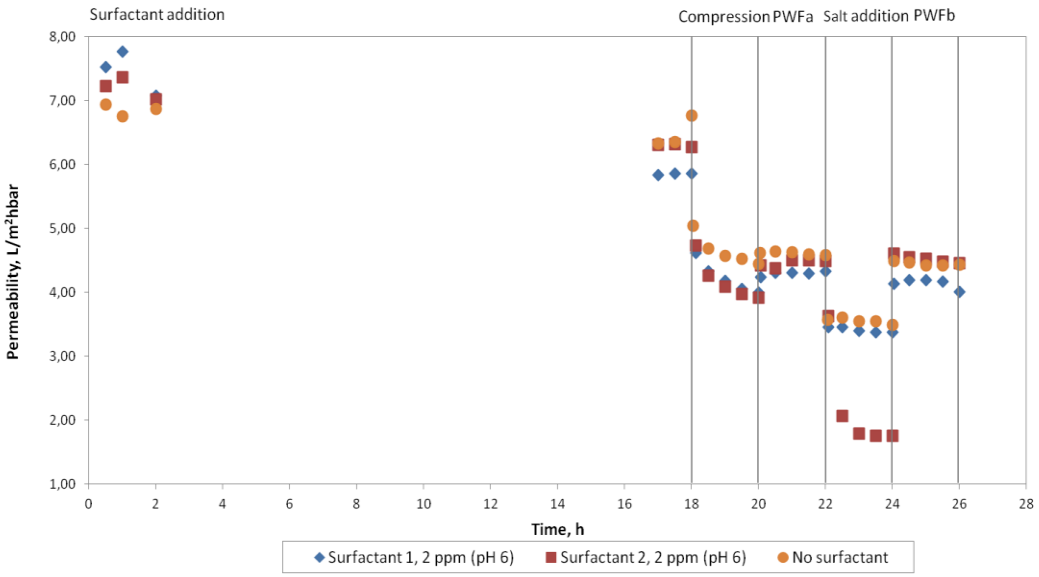

Figure 50. Permeability of modified LE-4040 membrane with 2 ppm of surfactant 1 or 2 at pH 6 (0–18 h) and the membrane permeabilities during the membrane compression (18–20 h), in the filtration of pure water before salt addition PWPa (20–22 h), in the filtration of pure water with marine salt (2 g/L) (22–24 h) and in the filtration of pure water after salt addition PWPb (24–26 h). Filtration is carried out with DSS Labstak M20 filter (19–24 ˚C, pH~6, 0.14 m/s, 15 bar and compression 25–30 bar).

The modification with surfactant 2 gave a slightly higher permeability than surfactant 1. However when the marine salt was added, the modification with surfactant 1 resulted in higher permeability. Based on the contact angle measurements, the membrane surface was more hydrophilic with surfactant 2 than with surfactant 1 at pH 7. Thus, this may explain the higher permeability with surfactant 2. The contact angle measurements also showed that at pH 7 anionic surfactant 1 increased the membrane hydrophobicity, while surfactant 2 did not have significant influence on hydrophilicity. Thereby, surfactant 1 may have adsorbed more greatly at the membrane surface causing lower permeability than surfactant 2. However, the contact angle measurements were made with much higher surfactant concentrations. Moreover, the permeability differences were too small for clear conclusions.

10.4.3 The effect of nonionic surfactant on water permeability in the presence of marine salt

The effect of modification with nonionic surfactant on membrane permeability as a function of time is presented in Figure 51. The membrane PWP decreased remarkably in the presence of surfactant 3.

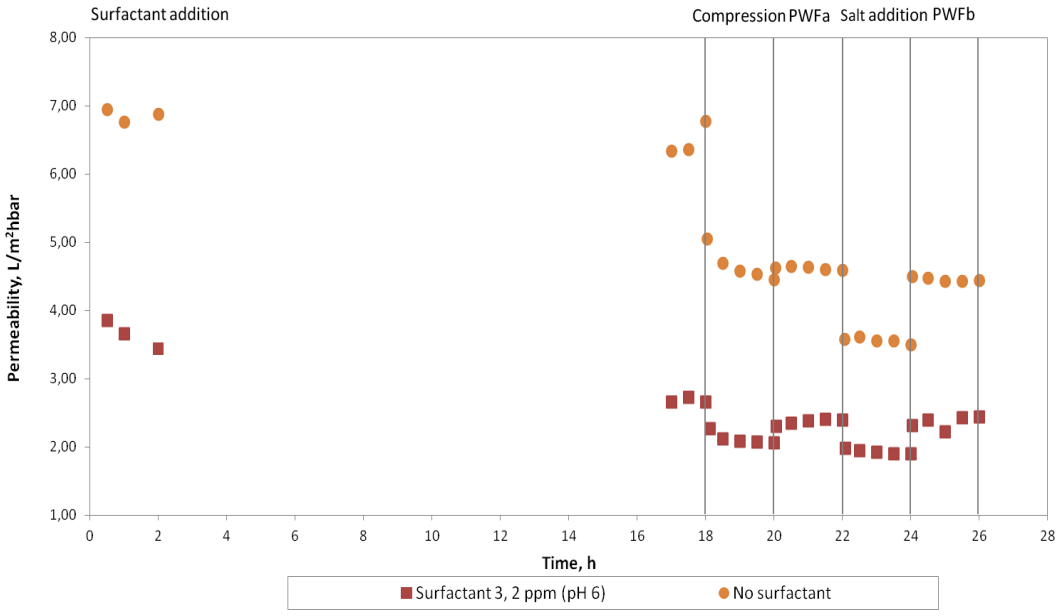

Figure 51. Permeability of modified LE-4040 membrane with 2 ppm of surfactant 3 pH 6 (0–18 h) and the membrane permeabilities during the membrane compression (18–20 h), in the filtration of pure water before salt addition PWPa (20–22 h), in the filtration of pure water with marine salt (2 g/L) (22–24 h) and in the filtration of pure water after salt addition PWPb (24–26 h). Filtration is carried out with DSS Labstak M20 filter (19–24 ˚C, pH~6, 0.14 m/s, 15 bar and compression 25–30 bar).

Comparing the effects between nonionic and anionic surfactants (Figure 50 and 51), it can be noted that the membrane permeability decrease with nonionic surfactant was more significant. Thus, the results were similar than with the quick filtration test (Figure 44). This may indicate that nonionic surfactants were more greatly adsorbed at the membrane surface than anionic surfactants decreasing the PWP more. However, the contact angle measurements indicated that the membrane was more hydrophilic with nonionic surfactant than with anionic surfactant 1 at pH 7.

10.4.4 The effect of modification pH on water permeability in the presence of marine salt

The solution pH affects the membrane surface charge whereas the surface charge affects the surfactant adsorption. The pure water pH, where the surfactant was added, was changed with 1 M KOH and 1 M HCl solutions to see if it could affect positively to surfactant adsorption causing the permeability to increase. With the anionic surfactant 1, the feed water pH was changed from 6 to 11 with KOH solution. Figure 52 shows the effect of the modification pH of surfactant 1 on the membrane permeability.

The increase in modification pH to 11 did not enhance the permeability at any stage of filtration. Also the zeta potential measurement of filtered membranes indicated that the membrane modified with surfactant 1 at pH 11 did not affect the membrane charge at high pH (Figure 46). On the other hand, the measurements with the unfiltered membranes indicated that the increase of solution pH with KOH reduced the membrane surface charge at high pH (Figure 49). When the surfactant 1 was added, the charge became even more negative. This indicates greater adsorption at higher modification pH and thus reduced permeability with higher modification pH of surfactant 1. However, it should be noticed that with the unfiltered membranes the pretreatment time was longer and surfactant concentration was remarkably higher (100 ppm) than with filtered membranes. The contact angle measurements with surfactant 1 resulted in an increased membrane hydrophobicity at higher pH (pH 7), which may explain the reduced permeability with modification pH 11.

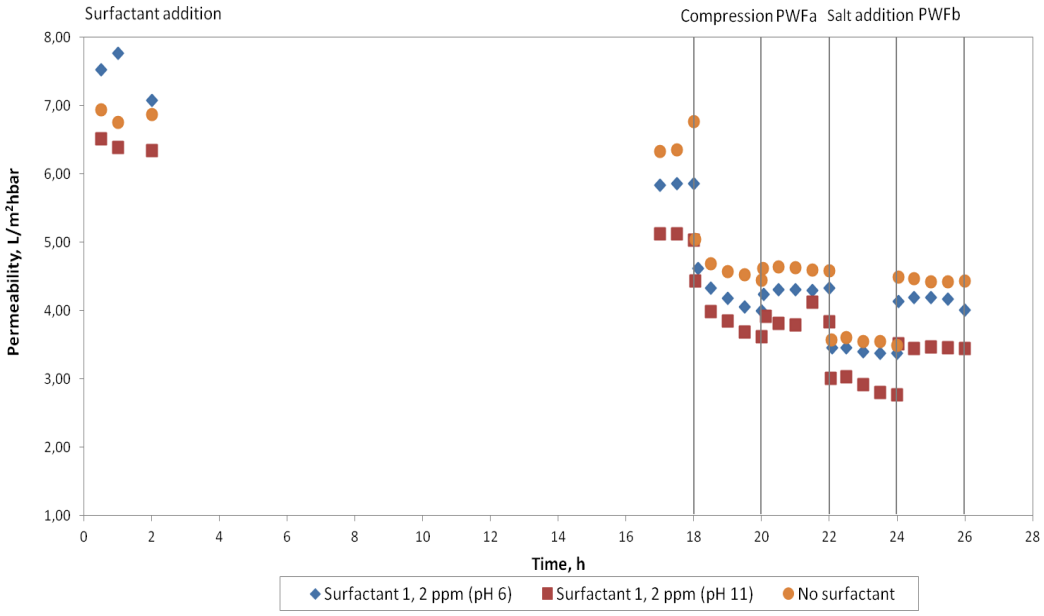

Figure 52. Permeability of modified LE-4040 membrane with 2 ppm of surfactant 1 at pH 6 and 11 (0–18 h) and the membrane permeabilities during the membrane compression (18–20 h), in the filtration of pure water before salt addition PWPa (20–22 h), in the filtration of pure water with marine salt (2 g/L) (22–24 h) and in the filtration of pure water after salt addition PWPb (24–26 h). Filtration is carried out with DSS Labstak M20 filter (19–24 ˚C, pH~6, 0.14 m/s, 15 bar and compression 25–30 bar).

With nonionic surfactant 3 the feed water pH was altered from 6 to 4.4 with HCl solution and from 6 to 11 with KOH solution. Figure 53 presents the effect of the nonionic surfactant 3 addition, at different solution pH, on the membrane permeability. The membrane permeability did not increase with surfactant 3 at any of modification pH. The modification pH did not affect to water permeability. This indicates that the nonionic surfactant adsorption is dominated by hydrophobic interactions. Thus, it seems that the surface charge does not have a significant influence on nonionic surfactant adsorption.

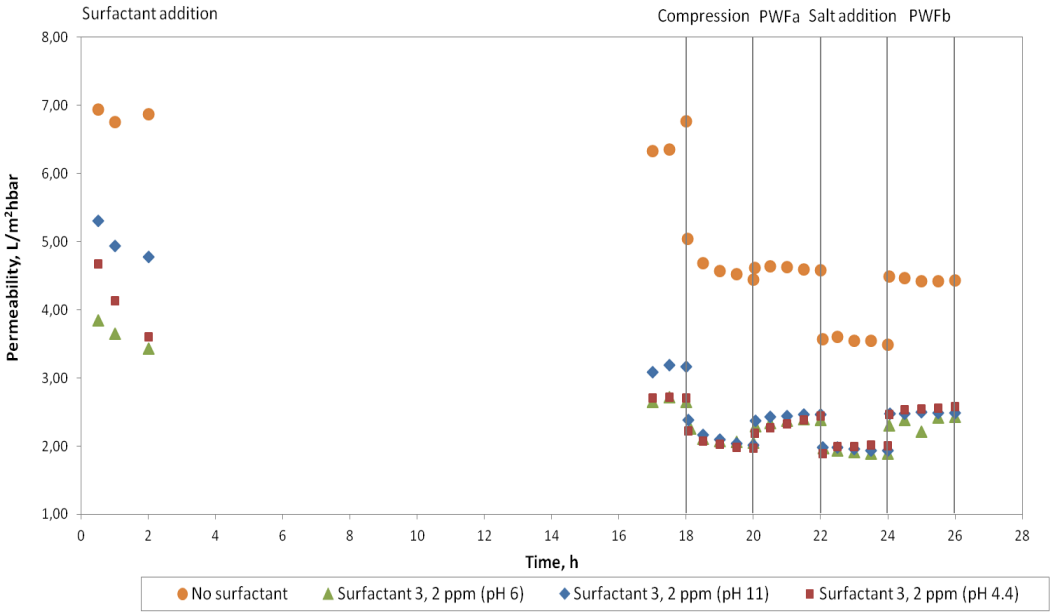

Figure 53. Permeability of modified LE-4040 membrane with 2 ppm of surfactant 3 at pH 4.4 (IEP), 6 and 11 (0–18 h) and the membrane permeabilities during the membrane compression (18–20 h), in the filtration of pure water before salt addition PWPa (20–22 h), in the filtration of pure water with marine salt (2 g/L) (22–24 h) and in the filtration of pure water after salt addition PWPb (24–26 h). Filtration is carried out with DSS Labstak M20 filter (19–24 ˚C, pH~6, 0.14 m/s, 15 bar and compression 25–30 bar).

10.4.5 The effect of membrane modification on the salt rejection

The used model salt was commercial marine salt which was added after the modification with surfactant, membrane compression and PWP measurement. Figure 54 shows the salt rejections of modified membranes with all three surfactants added at different solution pH. The salt rejections are also presented in Appendices V–VIII.

The modification with surfactants did not effect significantly on the salt rejection except with surfactant 3 at pH 11 where the rejection was significantly lower. The modification with the surfactant 3 at pH 4.4 and 6 gave much higher salt rejections. This can also be seen from the Figure 55. The flux during the salt addition is presented in Figure 56. It seems that salt rejection increases with low modification pH. The effect of nonionic surfactant on flux during salt filtration seems to be quite similar despite the variation in modification pH.

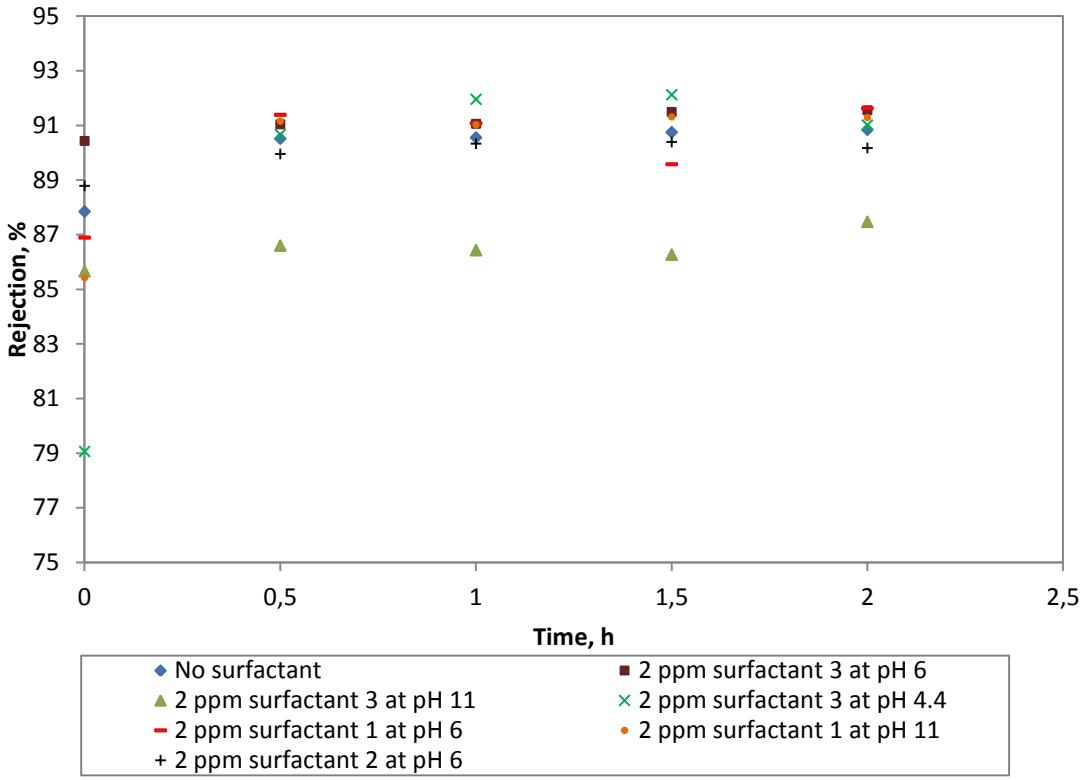

Figure 54. Salt rejection of LE-4040 membrane modified with 2 ppm of surfactant 1 at pH 6 and 11, surfactant 2 at pH 6, surfactant 3 at pH 4.4, 6 and 11) in the filtration of marine salt (2g/L) with DSS Labstak M20 filter (19–24 ˚C, ~pH 6, 0.14 m/s,15 bar).

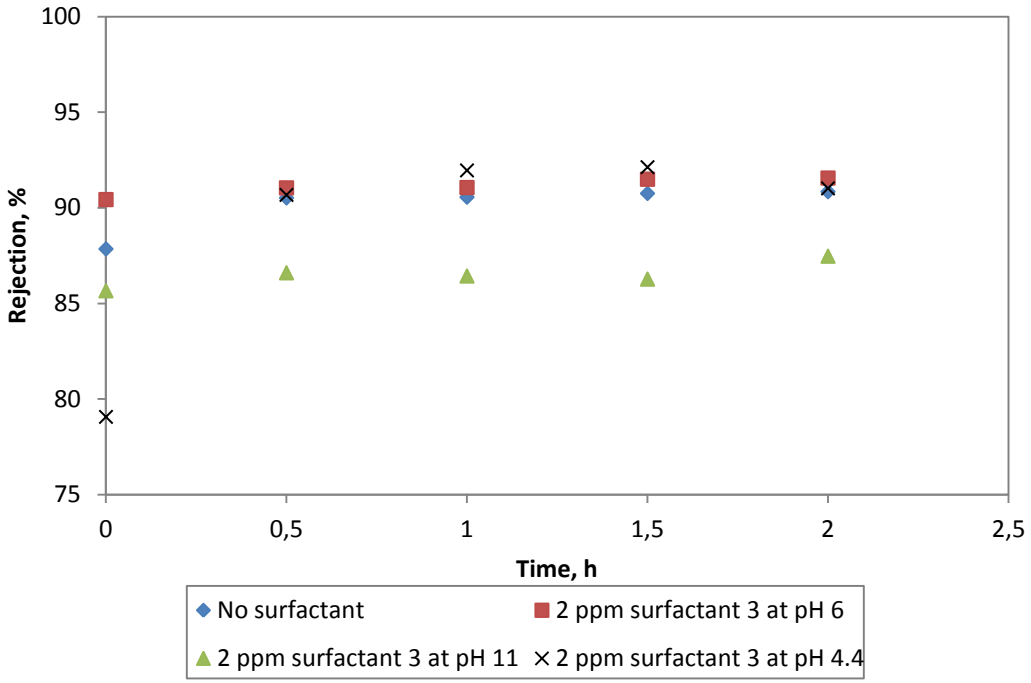

Figure 55. Salt rejection of LE-4040 membrane modified with 2 ppm of surfactant 3 at pH 4.4, 6 and 11 in the filtration of marine salt (2g/L) with DSS Labstak M20 filter (19–24 ˚C, ~pH 6, 0.14 m/s,15 bar).

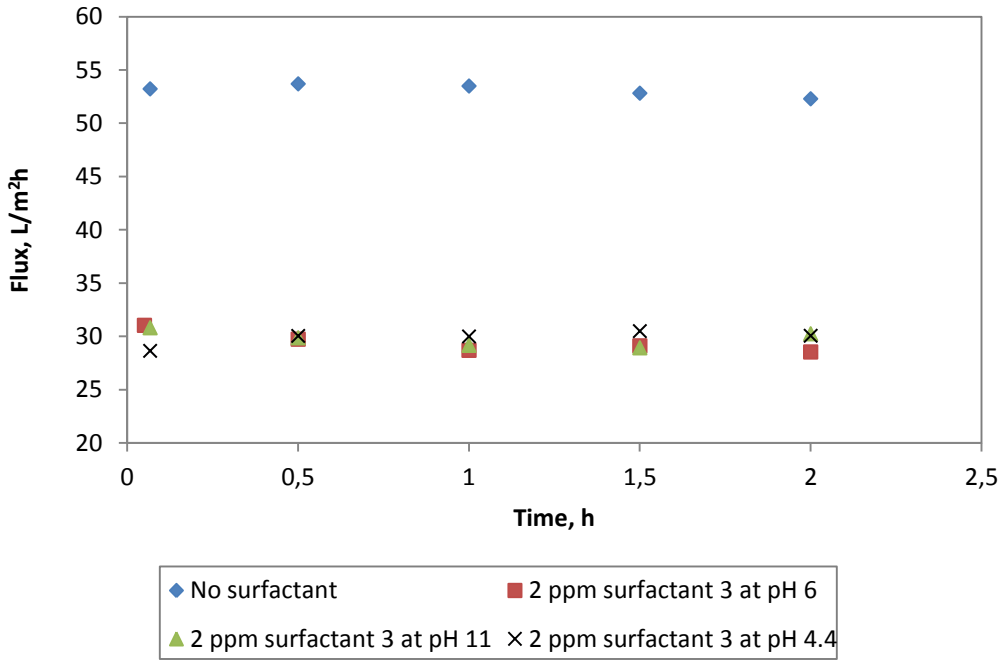

Figure 56. Flux of LE-4040 membrane modified with 2 ppm of surfactant 3 at pH 4.4, 6 and 11 in the filtration of marine salt (2g/L) with DSS Labstak M20 filter (19–24 ˚C, ~pH 6, 0.14 m/s,15 bar).

The effect of anionic surfactants on membrane salt rejection and flux are shown in Figure 57 and 58. The surfactant 2 at pH 6 slightly decreased the rejection. Surfactant 1's effect on salt rejection was similar at modification pH 6 and 11.

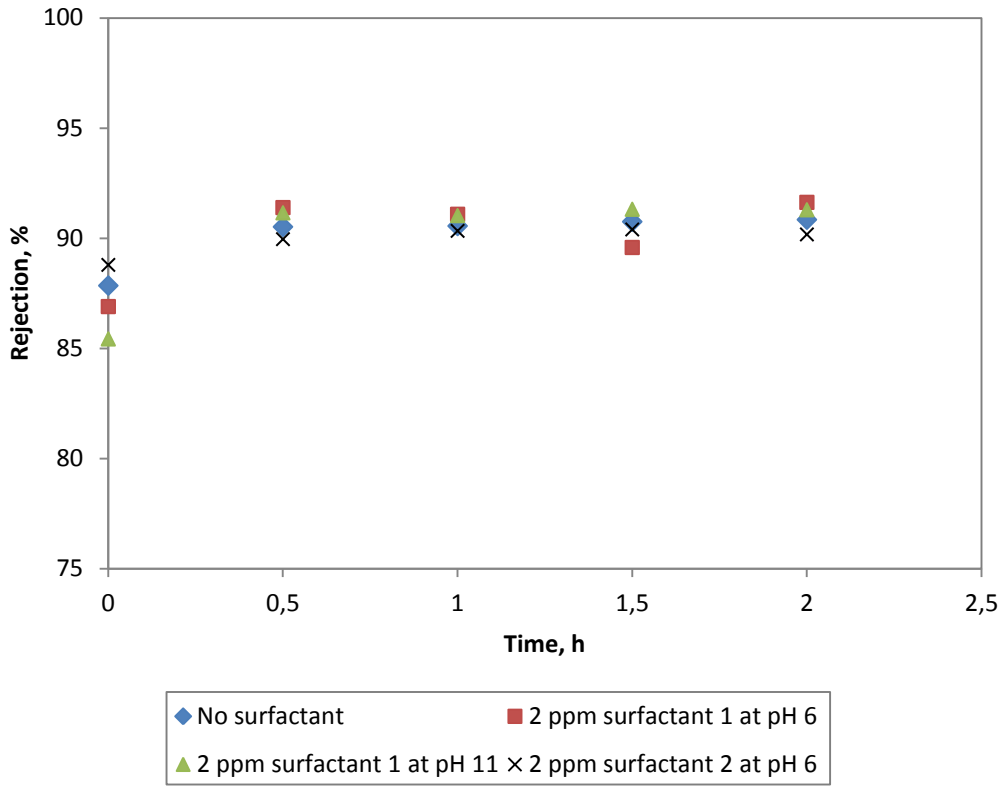

Figure 57. Salt rejection of LE-4040 membrane modified with 2 ppm of surfactant 1 at pH 6 and 11 and surfactant 2 at pH 6 in the filtration of marine salt (2g/L) with DSS Labstak M20 filter (19–24 ˚C, ~pH 6, 0.14 m/s, 15 bar).

The membrane flux during the salt filtration was reduced with anionic surfactants. The flux was remarkably lower with surfactant 2 than with surfactant 1. The flux with anionic surfactant 1 at pH 6 was quite similar with the unmodified membrane. As the modification pH increased to 11, the flux decreased.

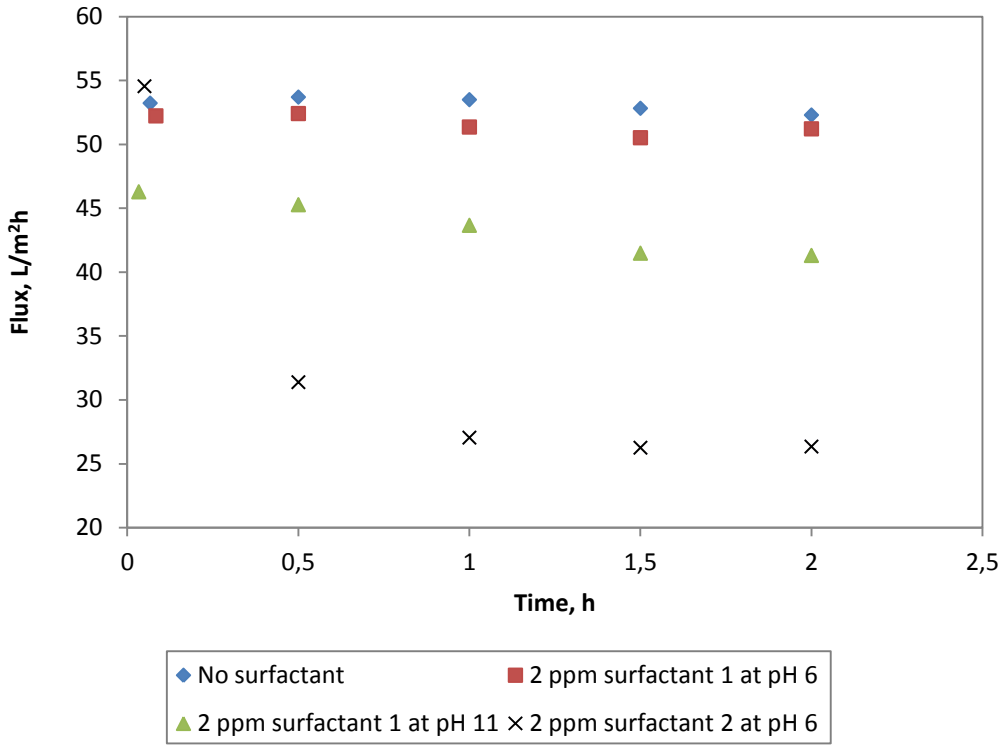

Figure 58. Flux of LE-4040 membrane modified with 2 ppm of surfactant 1 at pH 6 and 11 and surfactant 2 at pH 6 in the filtration of marine salt (2g/L) with DSS Labstak M20 filter (19–24 ˚C, ~pH 6, 0.14 m/s,15 bar).

10.3.6 Pure water flux after salt addition

Figure 59 presents the effect of modification with surfactants on membrane PWP after salt addition. The membrane modification decreased the PWPW of membrane. The fluxes with anionic surfactants were much higher than with nonionic surfactant 3. With the nonionic surfactant, the modification pH did not have as great influence on PWP than with anionic surfactants. The modification with anionic surfactant 1 at pH 6 gave higher flux than modification at pH 11.

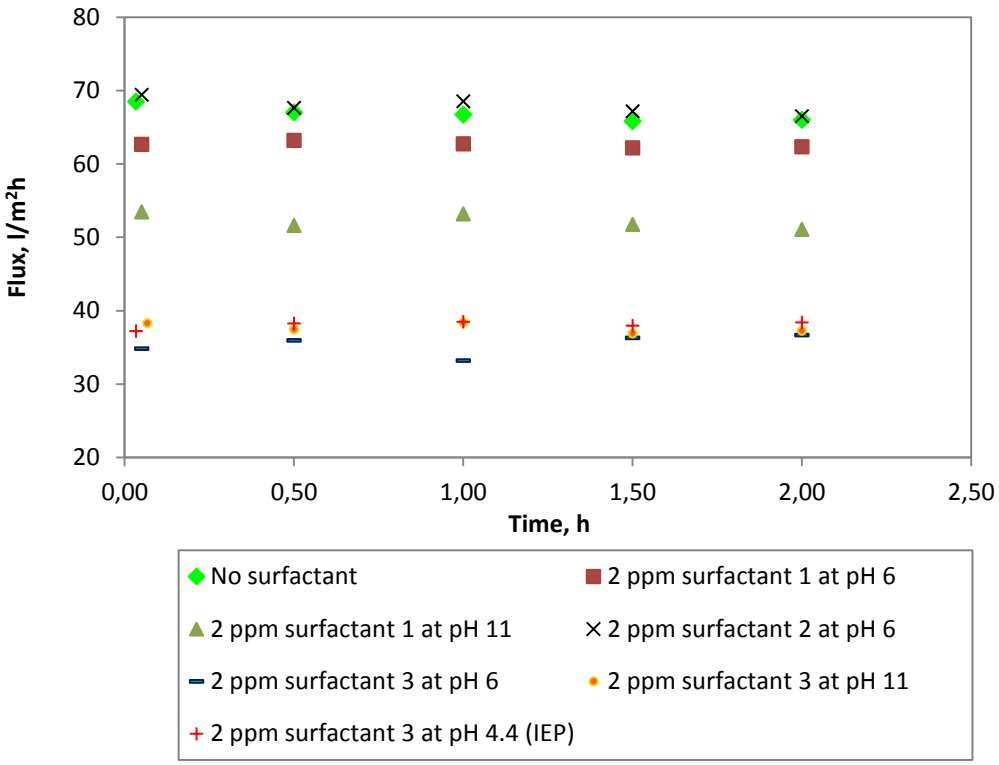

Figure 59. Pure water flux of LE-4040 membrane modified with 2 ppm of surfactant 1 at pH 6 and 11, surfactant 2 at pH 6 and surfactant 3 at pH 4.4, 6 and 11 after the filtration of marine salt (2g/L) with DSS Labstak M20 filter (19–24 ˚C, ~pH 6, 0.14 m/s,15 bar).

11 POSSIBLE SOURCES OF ERROR

The amount of water in the piping system of filter equipment was not accurately known so it was estimated. Thus, this may have caused some errors in the feed concentrations of surfactant. In addition, there might have been some dirt in the filter equipment from the earlier filtrations, even if the equipment was always rinsed with pure water before and after the experiments.

The analyzing equipments may have caused errors, thus it should have been better to analyze samples with different methods. Also with the zeta potential and contact angle measurements only the small area of the used membrane was analyzed. Therefore, these measurements can not characterize the whole membrane completely. In addition, the membrane pieces were dried for the contact angle measurements, which may have caused changes in membrane material. Thus, the contact angle measurement can characterize membrane surface only relatively. As the membrane pieces of the same material can vary from each other, this may have also caused some variations to the permeability results.

12 SUMMARY AND CONCLUSIONS

The aim of the work was to study the effect of surface modification on membrane performance. Two TFC RO membranes, Desal AG and LE-4040, were modified by adding three single surfactants into the feed water. Two of the surfactants were anionic and one was nonionic. The goal of modification was to improve membrane's pure water permeability (PWP) and salt rejection.

With Desal AG membrane the surfactant 1 at the concentrations of 2 and 5 ppm was added to feed water after stabilization. The surfactant addition did not increase the PWP. However, the contact angle and zeta potential measurements indicated that the surfactant adsorption was occurred. The membrane was more hydrophilic at higher surfactant concentrations and the surfactant 1 made membrane surface more negatively charged at low pH.

With LE-4040 membrane 2 ppm of the single surfactant was added to the feed water after compression and overnight lasting stabilization. Nevertheless, the PWP decreased with each surfactant. After this same amount of surfactant was added into the feed water at the beginning of the filtrations and recycled in the filter equipment overnight before compression. The salt was added to pure water after the modification. The filtration results showed that neither the modification with anionic surfactants nor the nonionic surfactant increased the PWP. Moreover, the surfactants did not affect significantly on salt rejection. The altered modification pH of surfactant 1 and 3 did not enhance the PWP. Also, the salt rejection did not increase with altered modification pH.

The PWP decrease of LE-4040 membrane was more severe with the modification of nonionic surfactant than with anionic surfactants. This indicates that nonionic surfactants may have adsorbed more greatly onto the membrane surface. However, the contact angle measurements showed that the membrane was more hydrophilic with nonionic surfactant than with anionic surfactant 1.

The zeta potential measurements showed that the anionic surfactants made membrane more negatively charged, which indicate that the surfactants were adsorbed. With nonionic surfactant the membrane charge became more positive at low pH and more negative at high pH. However, the contact angle measurements

with LE-4040 could not truly explain the surfactant adsorption of filtration experiments because the used surfactant concentration with contact angle measurements was much higher. Also, the zeta potential measurements were not able to describe thoroughly the adsorption of surfactants onto the membrane surface because the used marine salt affected the charge of membrane.

Even though, the zeta potential and contact angle measurements indicate that the surfactants were adsorbed, the adsorption did not effect on membrane's pure water permeability and salt rejection. Thereby, the modification of Desal AG and LE-4040 was not successful to improve membrane's performance.

In further research, the contact angle measurements should be done with same surfactant concentration as in the filtration experiments. In addition, filtration measurements should be done in absence of salt to see the effect of surfactant alone on the membrane surface. Also NaCl could be used instead of marine salt in order to make the retention analysis easier. The membrane surface morphology should also be investigated because the membrane contact angle cannot completely describe the surface hydrophilicity. Also it would be interesting to examine the antifouling properties of surfactants by adding foulants to the feed water.

REFERENCES

1. Service, R.F., Desalination freshens up, *Science* **313**(2006), 1880–1090.

2. Greenlee, L.F., Lawler, D.F., Freeman, B.D., Marrot, B., Moulin, P., Reverse osmosis desalination: Water sources, technology, and today's challenges, Water Research, **43**(2009), 2317–2348.

3. Lee, K.P., Arnot, T.C., Mattia, D., A review of reverse osmosis membrane materials for desalination–Development to date and future potential, *Journal of Membrane Science*, **370**(2011), 1 –22.

4. Ba, C., Ladner, D.A., Economy, J., Using polyelectrolyte coatings to improve fouling resistance of a positively charged nanofiltration membrane, *Journal of Membrane Science* **347**(2010), 250–259.

5. Tang, C.Y., Chong, T.H., Fane A.G., Colloidal interactions and fouling of NF and RO membranes: A review, *Advances in Colloid and Interface Science* **164**(2011) 126–143.

6. Fritzmann, C., Löwenberg, J., Wintgens, T., Melin, T., State-of-the-art of reverse osmosis desalination, *Desalination* **216**(2007), 1–76.

7. Alghoul, M.A., Poovanaesvaran, P., Sopian, K., Sulaiman, M.Y., Review of Brackish water reverse osmosis (BWRO) system designs, *Renewable and Sustainable Energy Reviews*, **13**(2009), 2661–2667.

8. Mulder, M., *Basic Principles of Membrane Technology*, 2nd ed., Kluver Academic Publisher, Netherlands, 2003.

9. Hung, L.-Y., Lue, S.J., You, J.-H., Mass-transfer modeling of reverse-osmosis performance on 0.5–2% salty water, *Desalination* **265**(2011), 67–73.

10. Matin, A., Khan, Z., Zaidi, S.M.J, Boyce, M.C., Biofouling in reverse osmosis membranes for seawater desalination: Phenomena and prevention, *Desalination* **281**(2011), 1–16.

11. Wangnick, K., IDA Worldwide Desalinating Plants Inventory, 2004.

12. Ladorde, H.M., Franca, K.B., Neff, H., Lima, A.M.N., Optimization strategy for small-scale reverse osmosis water desalination system based on solar energy, *Desalination* **133**(2001), 1–12.

13. Kang, G. and Cao, Y., Development of antifouling reverse osmosis membranes for water treatment: A review, *Water Research* **46**(2012), 584–600.

14. Crittenden, J.C., Trussell, R.R., Hand, D.W., Howe, K.J., Tchobanoglous, G., *Water treatment – Principles and Design*, 2nd ed., John Wiley & Sons, 2005, 955–1030, 1430–1503.

15. Lonsdale, H.K., Merten, U., Riley, R.L., Transport properties of cellulose acetate osmotic membranes, *Journal of Applied Polymer Science* **9**(1965), 1341–1362.

16. Kucera, J., *Reverse Osmosis - Design, Processes, and Applications for Engineers*, John Wiley & Sons – Scrivener Puplishing, New Jersey – Massachusetts, 2010, 21–40, 41–84, 255–261.

17. Jin, X., Jawor, A., Kim, S., Hoek, E.M.V., Effects of feed water temperature on separation performance and organic fouling of brackish water RO membranes, *Desalination* **239**(2009), 346–359.

18. Baker, R.W., *Membrane Technology and applications*, John Wiley & Sons, England, 2004.

19. Baker, R.W., Cussler, E.L., Eykamp, W., Koros, W.J., Riley, R.L., Strathmann, H., *Membrane separation systems – Recent developments and future directions*, Williams Andrew Publishing/Noyes Data Corporation, New Jersey, 1991, 276.

20. Ghosh, A.K., Hoek, E.M.V., Impacts of support membrane structure and chemistry on polyamide–polysulfone interfacial composite membranes, *Journal of Membrane Science*, **336**(2009), 140–148.

21. Tarboush, B.J.A., Ranaa, D., Matsuura,T., Arafat, H.A., Narbaitz, R.M., Preparation of thin-film-composite polyamide membranes for desalination using novel hydrophilic surface modifying macromolecules, *Journal of Membrane Science*, **325**(2008), 166–175.

22. Petersen, R.J. and Cadotte J.E., Thin film composite reverse osmosis membrane in: Porter M.C., *Handbook of Industrial Membrane Technology*, Noyes Publication, New Jersey, 1990, 307–329.

23. Cadotte, J.E., Reverse Osmosis Membrane, Patent Application No. 4039440, 1977.

24. Burk, R., New Technology Spotlight, CarbDA News, **2**(2012), 4, p. 6, http://www.nanoh2o.com/company/news/2012/74, 25.10.2013.

25. Li, D. and Wang, H.T., Recent developments in reverse osmosis desalination membranes, *Journal of Materials Chemistry* **20**(2010), 4551-4566.

26. Sudak, R.G., Reverse osmosis, in: Porter, M.C., *Handbook of Industrial Membrane Technology*, Noyes Publication, New Jersey, 1990, 260–285.

27. Edgar, K.J., Buchanan, C.M., Depenham, J.S., Rundquist, P.A., Seiler, B.D., Shelton, M.C., Tindall, D, Advances in cellulose ester performance and application, *Progress in Polymer Science*, **26**(2001), 1605–1688.

28. Zhou, Y., Yu, S., Gao, C., Feng, X., Surface modification of thin film composite polyamide membranes by electrostatic self deposition of polycations for improved fouling resistance, *Separation and Purification Technology*, **66**(2009), 287–294.

29. Hachisuka, H. and Ikeda, K., Composite reverse osmosis membrane having a separation layer with polyvinyl alcohol coating and method of reverse osmosis treatment of water using the same, U.S. Patent No. 6177011 B1, January 23, 2001.

30. Matsuura, T., Progress in membrane science and technology for seawater desalination – a review, *Desalination*, **134**(2001), 47–54.

31. Ghosh, A.K., Jeong, B-H., Huang, X., Hoek, E.M.V., Impacts of reactions and curing conditions on polyamide composite reverse osmosis membrane properties, *Journal of Membrane Science*, **311** (2008) 34–45.

32. Wei, J., Jian, X.G., Wu, C.R.,, S.H., Yan, C., Influence of polymer structure on thermal stability of composite membranes, *Journal of membrane science*, **256**(2005), 116–121.

33. Kim, I.-C., Jegal, J., Lee, K.H., Effect of aqueous and organic solutions on the performance of polyamide thin-film composite nanofiltration membranes, *Journal of polymer science Part B: Polym. Phys*. **40**(2002), 2151–2163.

34. Verissimo S., Peinemann, K.-V., Bordado, J., Thin-film composite hollow fiber membranes: an optimized manufacturing method, *Journal of membrane science*, **254**(2005), 48–55.

35. Korikov, A.R., Kosaraju, R., Sirkar, K.K., Interfacially polymerized hydrophilic microporous thin film composite membranes on porouspolypropylene hollow fibers and flat films, *Journal of membrane science*, **279**(2006), 588–600.

36. Jönsson , A.-S. , Lindau, J., Wimmerstedt, R., Brinck, J., Jönsson, B., Influence of the concentration of a low-molecular organic solute on the flux reduction of a polyethersulphone ultrafiltration membrane, *Journal of Membrane Science* **135**(1997), 117–128.

37. Childress, A.E., Deshmukh, S.S., Effect of humic substances and anionic surfactants on the surface charge and performance of reverse osmosis membranes, *Desalination* **118**(1998), 167–174.

38. Herzberg, M., Elimelech, M., Biofouling of reverse osmosis membranes: Role of biofilm-enchanced osmotic pressure, *Journal of Membrane Science*, **295**(2007) 11–20.

39. Kent, F.C., Farahbakhsh, K., Mahendran, B., Jaklewicz, M., Liss, S.N., Zhou, H., Water reclamation using reverse osmosis: Analysis of fouling propagation given tertiary membrane filtration and MBR pretreatments, *Journal of Membrane Science*, **382**(2011) 328–338

40. Shaw, D.J., *Introduction to colloid and surface chemistry*, Butterworths, London, 1980.

41. Dudley, L.Y and Baker, J.S., The Role of Antiscalants and Cleaning Chemicals to Control Membrane Fouling, http://www.derwentwatersystems.co.uk/chemical-treatments/paper-nine.pdf, 20.4.2014.

42. El-Manharawy, S. and Hafez, A., Water type and guidelines for RO system design, *Desalination* **139**(2001), 97–113.

43. Mickley, M.C., *Membrane concentrate disposal: practices and regulation*, 2nd ed., Mickley & Associates, 109.

44. Social and healt ministry's regulation for drinking water quality requirement and control study, http://www.finlex.fi/fi/laki/alkup/2000/20000461, 13.5.2013

45. Peng, W., Escobar, I.C., White, D.B., Effects of water chemistries and properties of membrane on the performance and fouling – a model development study, *Journal of Membrane Science*, **238**(2004) 33–46.

46. Schäfer, A.I., Testing of a hybrid membrane system for groundwater desalination in an Australian national park, *Desalination* **183**(2005), 55–62.

47. Bartels, C., Franks, R., Rybar, S., Schierach, M., Wilf, M., The effect of feed ionic strength on salt passage through reverse osmosis membranes, *Desalination* **184**(2005) 185–195.

48. Peeters, J.M.M., Boom, J.P., Mulder, M.H.V., Strathmann, H., Retention measurements of nanofiltration membranes with electrolyte solutions, *Journal of Membrane Science* **145**(1998) 199–209.

49. Higa, M., Tanioka, A., Kra, A., A novel measurement method of Donnan potential at an interface between a charged membrane and mixed salt solution, *Journal of Membrane Science* **140**(1998), 213–220.

50. Sagle, A.C., Van Wager, E.M., Ju, H., McCloskey, B.D., Freeman, B.D., Sharma, M.M., PEG-coated reverse osmosis membranes: desalination properties and fouling resistance, *Journal of Membrane Science*, **340**(2009), 92–108.

51. Nanda, D., Tung, K-L., Li, Y-L., Lin, N-J., Chuang, C-J., Effect of pH on membrane morphology, fouling potential, and filtration performance of nanofiltration membrane for water softening, *Journal of Membrane Science* **349**(2010), 411–420.

52. Yu, Y., Lee, S., Hong, S., Effect of solution chemistry on organic fouling of reverse osmosis membranes in seawater desalination, *Journal of Membrane Science* **351**(2010), 205–213.

53. Yang, J., Lee, S., Lee, E., Lee, J., Hong, S., Effect of solution chemistry on the surface property of reverse osmosis membranes under seawater conditions, *Desalination* **247**(2009), 148–161.

54. Mondal, S. and Wickramasinghe, S.R., Produced water treatment by nanofitration and reverse osmosis membranes, *Journal of Membrane Science* **322**(2008), 162–170.

55. Louie, J.S., Pinnau, I., Ciobanu I., Ishida, K.P., Ng, A., Reinhard, M., Effects of polyether-polyamide block copolymer coating on performance and fouling of reverse osmosis membranes, *Journal of Membrane Science* **280**(2006), 762–770.

56. Vrijenhoek, E.M., Seungkwan H., Elimelech, M., Influence of membrane surface properties on initial rate of colloidal fouling of reverse osmosis and nanofiltration membranes, *Journal of Membrane Science* **188**(2001), 115–128.

57. Elimelech, M. Zhu, X., Childress, A.E., Hong S., Role of membrane surface morphology in colloidal fouling of cellulose acetate and composite aromatic polyamide reverse osmosis membranes, *Journal of Membrane Science* **127**(1997), 101–109.

58. Rana, D. and Matsuura, T., Surface modifications for antifouling membranes, *Chemical Reviews* **110**(2010), 2448–2471.

59. Wilbert, M., Pellegrino, J., Zydney, A., Bench-scale testing of surfactant-modified reverse osmosis/nanofiltration membranes, *Desalination* **115**(1998), 15–32.

60. Brant, J.A. and Childress, A.E., Colloidal adhesion to hydrophilic membrane surfaces, *Journal of Membrane Science*, **241**(2004), 235–248.

61. Kwon, B., Lee, S., Cho, J., Ahn, H., Lee, D., Shin, H.S., Biodegradability, DBP formation, and membrane fouling potential of natural organic matter: characterization and controllability, *Environmental Science Technology*, **39**(2005), 732–739.

62. Hirose, M., Ito, H., Kamiyama, Y., Effect of skin layer surface structures on the flux behavior of RO membranes, *Journal of Membrane Science* **121**(1996), 209–215.

63. Kwak, S.-Y., Jung, S.G., Yoon, Y.S., Ihm, D.W., Details of surface features in aromatic polyamide reverse osmosis membranes characterized by scanning electron and atomic force microscopy, *Journal of Polymer Science: Part B: Polymer physics* **37**(1999), 1429-1440

64. Al-Jeshi, S. and Neville, A., An investigation into the relationship between flux and roughness on RO membranes using scanning probe microscopy, *Desalination* **189**(2006), 221–228.

65. Abdallah, S., Abu-Hilal, M., Mohsen, M.S., Performance of a photovoltaic powered reverse osmosis system under local climatic conditions, *Desalination*, **183**(2005), 95–104.

66. Goosen, M.F.A., Sablani, S.S., Al-Hinai, H., Al-Obeidani, S., Al-Belushi, R., Jackson, D., Fouling of reverse osmosis and ultrafiltration membranes; a critical review, *Separation Science and Technology* **39**(2004), 2261–2297.

67. Mattaraj, S., Phimpha, W., Hongthong, P., Jiraratananon, R., Effect of operating conditions and solution chemistry on model parameters in crossflow reverse osmosis of natural organic matter, *Desalination*, **253**(2010), 38–45.

68. Belfer, S., Purinson, Y., Fainshtein, R., Radchenko, Y., Kedem, O., Surface modification of commercial composite polyamide reverse osmosis membranes, *Journal of Membrane Science*, **139**(1998), 175–181.

69. Knyazkova, T.V. and Kavitskaya, A.A., Improved performance of reverse osmosis with dynamic layers onto membranes in separation of concentrated salt solutions, *Desalination* **131**(2000), 129–136.

70. Holmberg, K., Jönsson, B., Kronberg, B., Lindman, B., *Surfactants and polymers in aqueous solutions*, 2nd ed., John Wiley & Sons, England, 2003, 1– 36, 39–66, 337–355, 357–387, 389–402.

71. Kaya, Y., Aydiner, C., Barlas, H., Keskinler, B., Nanofiltration of single and mixture solutions containing anionics and nonionic surfactants below their critical micelle concentrations (CMCs) *Journal of Membrane Science* **282**(2006), 401–412

72. Kowalska, I., Kabsch-Korbutowicz, M., Majewska-Nowak, K., Winnicki, T., Separation of anionic surfactants on ultrafiltration membranes, *Desalination* **162**(2004), 33–40.

73. http://www.highbeam.com/doc/1G1-21188318.html, 9.10.2013, Karsa, D. R., Coming clean: the world market for surfactants, *Chemistry and Industry* **9**(1998), 685–691.

74. Byhlin, H., Jönsson, A.-S., Influence of adsorption and concentration polarization on membrane performance during ultrafiltration of a non-ionic surfactant, *Desalination* **151**(2002), 21–31.

75. Paria, S. and Khilar, K.C., A review on experimental studies of surfactant adsorption at the hydrophilic solid-water interface, *Advances in colloid and interface science* **110**(2004), 75–95.

76. Morell, S.P., Coatings technology handbook, 3rd ed., Taylor & Francis Group, 2006, 74-1–74-5.

77. Childress, A.E. and Elimelech, M., Relating nanofiltration membrane performance to membrane charge (electrokinetic) characteristics, *Environmental science and technology* **34**(2000), 3710–3716.

78. Childress, A.E. and Elimelech, Effect of solution chemistry on the surface charge of polymeric reverse osmosis and nanofiltration membranes, *Journal of Membrane Science* **119**(1996), 253–268.

79. Somasundaran, P., and Fuerstenau, D.W., Mechanisms of alkyl sulfonate adsorption at the alumina-water interface, *Journal of physical chemistry* **70**(1966), 90–96.

80. Cornelis, G., Boussu, K., Van der Bruggen, B., Devreese, I., Vandecasteele, C., Nanofiltration of nonionic surfactants: effect of the molecular weight cutoff and contact angle on flux behavior, *Industrial and Engineering Chemistry Research* **44**(2005), 7652–7658.

81. Maartens, A., Swart, P., Jacobs, E.P., Membrane pretreatment: a method for reducing fouling by natural organic matter, *Journal of colloid and interface science* **221**(2000), 137–142.

82. McCutcheon, J.R. and Elimelech, M., Influence of membrane support layer hydrophobicity on water flux in osmotically driven membrane processes, *Journal of Membrane Science* **318**(2008), 458–466.

83. Adamczyk, Z., Dabros, T., Czarnecki, J., Van De Ven, T.G.M., Particle transfer to solid surfaces, *Advances in Colloid and Interface Science*, **19**(1983), 183–252.

84. Gangolli, S., *Dictionary of Substances and Their Effects*, 3rd ed., Royal Society of Chemistry, 2005, http://app.knovel.com:80:80/hotlink/toc/id:kpDSTEDOS3/dictionary-substances, 18.1.2014.

85. Chemical Trading Guide,

a: http://www.guidechem.com/reference/dic-400143.html, 18.1.2014.
b: http://www.guidechem.com/cas-778/7786-30-3.html, 18.1.2014
c: http://www.guidechem.com/cas-748/7487-88-9.html, 18.1.2014
d: http://www.guidechem.com/cas-994/99400-01-8.html, 18.1.2014
e: http://www.guidechem.com/cas-764/7647-14-5.html, 18.1.2014.

86. Chemical Book, http://www.chemicalbook.com/ProductChemicalPropertiesCB9122608_EN.htm, 13.5.2014.

87. Freshwater systems, http://www.freshwatersystems.com/specifications/ag8040f-400-spec.pdf, 18.1.2014.

88. Lenntec Water treatment solutions, http://www.lenntech.com/Data-sheets/Dow-Filmtec-LE-4040.pdf, 18.1.2014.

89. Mänttäri, M., Pihlajamäki, A., Nyström, M., Comparison of nanofiltration and tight ultrafiltration membranes in the filtration of paper mill process water, *Desalination*, **149**(2002), 131–136.

90. Lotfi, M., Nejib, M., Naceur, M., Cell Adhesion to Biomaterials: Concept of Biocompatibility, *Advances in Biomaterials Science and Biomedical Applications*, http://www.intechopen.com/books/advances-in-biomaterials-science-and-biomedical-applications/cell-adhesion-to-biomaterials-concept-of-biocompatibility, 30.4.2014.

91. Luxbacher, T., Electrokinetic characterization of flat sheet membranes by streaming current measurement, *Desalination*, **199**(2006), 376–377.

92. Ariza, M.J. and Benavente, J., Streaming potential along the surface of polysulfone membranes: a comparative study between two different experimental systems and determination of electrokinetic and adsorption parameters, *Journal of Membrane Science*, **190**(2001), 119–132.

APPENDICES

APPENDIX I	The flow diagram of three-cell filter
APPENDIX II	Filtration procedure 1 with three-cell filter
APPENDIX III	Filtration procedure 1 with DSS Labstak M20 filter
APPENDIX IV	Filtration procedure 2
APPENDIX V	Filtration procedure 3 with surfactant 1
APPENDIX VI	Filtration procedure 3 with surfactant 2
APPENDIX VII	Filtration procedure 3 with surfactant 3
APPENDIX VIII	Filtration procedure 3 with pure water

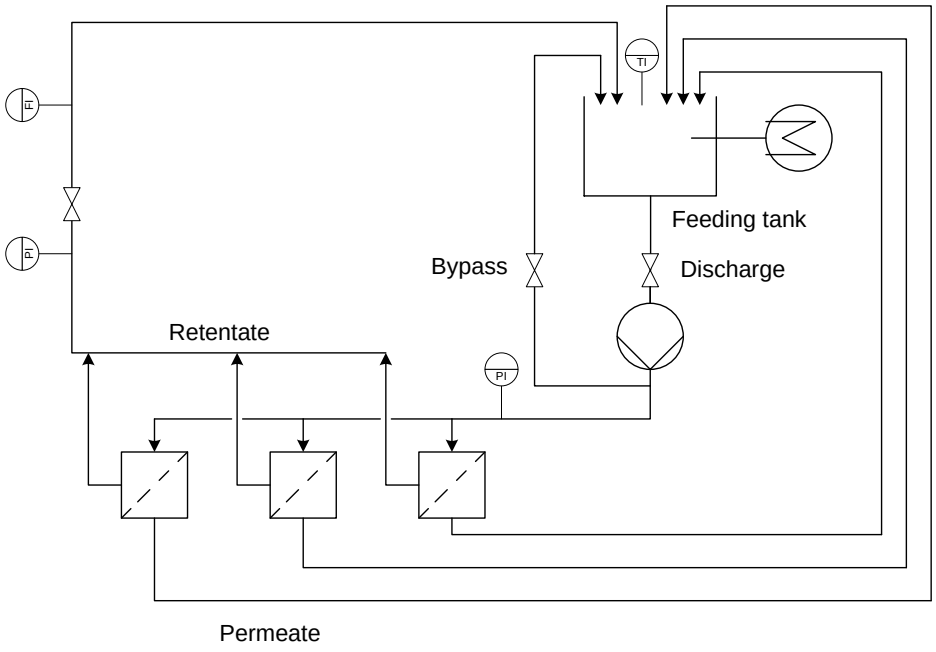

Figure 1. Flow diagram of the three-cell filter

Table I Permeability and flux of Desal AG membrane in the filtration of pure water and that with 20 ppm of surfactant 1 with three-cell filter (20–24 ˚C, 0.42 m/s) and the conductivity and pH of permeate.

filtration phase	pressure, bar	membrane module	time, min	flux, L/m^2h	permeability, L/m^2hbar	pH, -	conductivity, µS/cm
PW	15	1	40	69.92	4.56	-	-
			80	132.42	8.81	-	-
			120	123.55	8.13	-	-
surfactant	15	1					
1,			180	90.83	6.02	6.80	10.85
20 ppm			220	82.05	5.51	6.62	6.33
			260	80.03	5.35	6.57	6.70
			300	79.13	5.29	6.55	7.20
			340	79.34	5.29	6.52	6.40
PW	15	2	50	85.16	5.64	-	-
			90	85.17	5.70	-	-
			130	96.86	6.38	-	-
surfactant	15	2					
1,			190	50.67	3.36	6.91	13.60
20 ppm			230	45.11	3.04	6.64	4.85
			270	37.89	2.54	6.63	9.47
			310	42.69	2.84	6.56	4.95
			350	41.70	2.76	6.72	5.39
PW	15	3	60	131.57	8.68	-	-
			100	109.23	7.20	-	-
			140	120.98	8.03	-	-
surfactant	15	3					
1,			200	54.90	3.65	6.70	4.90
20 ppm			240	58.99	3.96	6.63	4.83
			280	55.01	3.64	6.59	5.28
			320	58.28	3.90	6.50	5.06
			360	56.97	3.80	6.61	5.83

Table II pH and conductivity of feed solution in the filtration of pure water and that with 20 ppm of surfactant 1 with three-cell filter (19–24 ˚C, 0.14 m/s).

filtration phase	pressure, bar	feed pH, -	feed conductivity, µS/cm
PW	at the start	6.53	2.30
	at the end	6.54	3.95
surfactant 1,	at the start	6.60	9.95
20 ppm	at the end	6.38	9.60

Table III Permeability and flux of Desal AG membrane in the filtration of pure water and that with 5 ppm of surfactant 1 with three-cell filter (20–24 ˚C, 0.42 m/s) and the conductivity and pH of permeate.

filtration phase	pressure, bar	membrane module	time, min	flux, L/m^2h	permeability, L/m^2hbar	pH, -	conductivity, µS/cm
PW	7	1	40	28.70	4.09	-	-
			80	32.56	4.54	-	-
			120	48.32	6.93	-	-
surfactant	7	1					
1,			180	183.86	26.74	6.64	3.06
5 ppm			220	238.92	34.88	6.59	3.22
			260	287.90	41.28	6.44	3.48
			300	274.63	39.66	6.29	3.35
			340	302.45	42.15	5.95	3.53
PW	7	2	50	29.89	4.32	-	-
			90	30.35	4.29	-	-
			130	53.17	7.62	-	-
surfactant	7	2					
1,			190	114.35	16.39	5.69	3.05
5 ppm			230	141.41	20.42	6.60	3.10
			270	162.63	23.23	6.17	3.30
			310	175.14	25.02	6.23	3.53
			350	185.96	26.10	5.83	3.63
PW	7	3	60	32.52	4.66	-	-
			100	38.01	5.61	-	-
			140	63.69	8.85	-	-
surfactant	7	3					
1,			200	255.91	36.82	5.69	3.05
5 ppm			240	295.13	42.77	6.51	3.18
			280	313.86	45.16	6.42	3.65
			320	317.51	44.56	6.04	3.48
			360	337.53	46.88	5.88	4.60

Table IV pH and conductivity of feed solution in the filtration of pure water and that with 5 ppm of surfactant 1 with three-cell filter (19–24 ˚C, 0.14 m/s).

filtration phase	pressure, bar	feed pH, -	feed conductivity, µS/cm
PW	at the start	6.34	1.90
	at the end	6.48	2.30
surfactant 1,	at the start	6.20	3.65
5 ppm	at the end	6.50	4.30

Table III Permeability and flux of Desal AG membrane in the filtration of pure water and pure water with 5 ppm of surfactant 1 with three-cell filter (20–24 ˚C, 0.42 m/s) and the conductivity and pH of permeate.

filtration phase	pressure, bar	membrane module	time, min	flux, L/m^2h	permeability, L/m^2hbar	pH, -	conductivity, µS/cm
PW	7	1	40	26..94	3.84	-	-
			80	32.21	4.77	-	-
			120	28.29	4.39	-	-
surfactant 1, 5 ppm	7	1	180	83.40	12.22	6.02	11.82
			220	113.99	16.40	5.99	8.55
			260	129.29	18.67	6.01	7.53
			300	108.19	15.79	6.05	6.66
			340	150.13	21.45	5.01	6.30
PW	7	2	60	22.15	3.22	-	-
			90	33.18	4.93	-	-
			130	41.83	6.39	-	-
surfactant 1, 5 ppm	7	2	190	68.27	9.75	6.08	12.64
			230	81.56	11.82	6.05	7.15
			270	93.32	13.24	6.06	10.19
			310	84.90	12.17	6.04	8.16
			350	99.59	14.43	6.05	3.89

Table IV pH and conductivity of feed solution in the filtration of pure water and that with 5 ppm of surfactant 1 with three-cell filter (19–24 ˚C, 0.14 m/s).

filtration phase	pressure, bar	feed pH, -	feed conductivity, µS/cm
PW	at the start	5.75	37.33
	at the end	5.89	19.12
surfactant 1, 5 ppm	at the start	6.03	21.7
	at the end	5.96	10.77

Table V Permeability and flux of Desal AG membrane in the filtration of pure water and that with 2 ppm of surfactant 1 with three-cell filter (20–24 ˚C, 0.42 m/s) and the conductivity and pH of permeate.

filtration phase	pressure, bar	membrane module	time, min	flux, L/m^2h	permeability, L/m^2hbar	pH, -	conductivity, µS/cm
PW	7	1	40	38.23	5.38	-	-
			80	53.43	7.72	-	-
			120	56.58	8.03	-	-
surfactant	7	1					
1,			180	62.70	9.09	6.09	68.75
2 ppm			220	76.39	11.03	5.80	165.55
			260	78.48	11.41	6.20	71.80
			300	79.05	11.29	6.18	66.25
			340	82.72	11.82	6.12	39.25
PW	7	2	50	45.80	6.76	-	-
			90	43.99	6.38	-	-
			130	28.21	3.97	-	-
surfactant	7	2					
1,			190	49.34	7.07	5.69	80.80
2 ppm			230	54.73	7.96	6.03	199.00
			270	47.74	6.97	6.44	85.90
			310	51.83	7.38	6.27	77.10
			350	50.11	7.18	6.18	82.45
PW	7	3	60	49.34	7.18	-	-
			100	57.29	8.18	-	-
			140	39.95	5.59	-	-
surfactant	7	3					
1,			200	61.04	8.57	5.44	81.30
2 ppm			240	63.95	9.34	5.74	79.20
			280	57.31	8.28	6.31	65.70
			320	58.24	8.32	6.39	85.00
			360	67.43	9.77	6.23	62.50

Table VI pH and conductivity of feed solution in the filtration of pure water and that with 2 ppm of surfactant 1 with three-cell filter (19–24 ˚C, 0.14 m/s).

filtration phase	pressure, bar	feed pH, -	feed conductivity, µS/cm
PW	at the start	5.88	27.00
	at the end	5.83	51.10
surfactant 1,	at the start	6.03	33.80
2 ppm	at the end	5.85	23.10

Table I Permeability and flux of Desal AG membrane in the filtration of pure water and that with 2 ppm of surfactant 1 with Labstak M20 filter unit (20–24 ˚C, 0.42 m/s) and the conductivity and pH of permeate. The conductivity and pH of used feed solution is presented in table IV.

filtration phase	pressure, bar	time, h	flux, L/m^2h	permeability, L/m^2hbar	pH, -	conductivity, µS/cm
PW	7	40	26.20	3.55	-	-
		45	25.05	3.59	-	-
		50	25.48	3.60	-	-
		55	25.50	3.62	-	-
		60	24.76	3.52	-	-
		65	24.41	3.52	-	-
		80	25.12	3.51	-	-
		85	24.25	3.44	-	-
		90	24.26	3.45	-	-
		95	25.38	3.52	-	-
		100	24.24	3.49	-	-
		105	24.19	3.39	-	-
		120	24.85	3.52	-	-
		125	24.84	3.52	-	-
		130	24.74	3.52	-	-
		135	24.90	3.52	-	-
		140	24.19	3.53	-	-
		145	24.85	3.54	-	-
surfactant 1, 2 ppm	7	185	25.25	3.61	5.64	2.06
		190	25.73	3.64	5.98	1.25
		195	25.78	3.60	5.74	2.37
		200	25.28	3.61	5.91	2.07
		205	25.20	3.60	5.95	1.42
		210	25.60	3.62	5.68	2.17
		225	25.02	3.64	6.03	2.57
		230	25.57	3.65	6.04	1.69
		235	25.27	3.61	5.40	2.38
		240	25.64	3.64	5.67	2.32
		245	25.19	3.60	6.15	4.03
		250	25.75	3.66	6.02	1.37
		265	25.33	3.64	6.05	1.27
		270	25.43	3.65	5.97	1.35
		275	24.89	3.66	5.80	1.82
		280	25.37	3.64	6.00	1.41
		285	25.62	3.66	6.11	1.45
		290	25.54	3.65	5.93	1.20
		305	25.47	3.65	5.71	1.83
		310	25.66	3.67	5.87	1.24
		315	24.67	3.52	6.14	1.33
		320	25.86	3.68	5.95	1.42
		325	25.62	3.66	6.12	1.37
		330	25.72	3.66	6.20	1.62
		345	25.37	3.66	6.05	2.24
		350	25.87	3.67	6.06	1.30
		355	25.76	3.68	5.99	1.11
		360	26.02	3.70	5.99	1.63
		365	25.57	3.67	6.14	1.49
		370	25.69	3.66	6.13	1.91

Table II Permeability and flux of Desal AG membrane in the filtration of pure water and that with 5 ppm of surfactant 1 with Labstak M20 filter unit (20–24 ˚C, 0.42 m/s) and the conductivity and pH of permeate. The conductivity and pH of used feed solution is presented in table V.

filtration phase	pressure, bar	time, h	flux, L/m^2h	permeability, L/m^2hbar	pH, -	conductivity, µS/cm
PW	7	40	24.06	3.42	-	-
		45	24.39	3.44	-	-
		50	24.26	3.44	-	-
		55	24.39	3.44	-	-
		60	24.72	3.46	-	-
		65	24.00	3.43	-	-
		80	23.85	3.42	-	-
		85	25.17	3.47	-	-
		90	23.78	3.43	-	-
		95	24.14	3.45	-	-
		100	24.06	3.43	-	-
		105	23.77	3.43	-	-
		120	23.42	3.38	-	-
		125	23.85	3.36	-	-
		130	23.38	3.31	-	-
		135	22.96	3.32	-	-
		140	23.33	3.34	-	-
		145	23.59	3.37	-	-
surfactant 1, 5 ppm	7	185	22.34	3.19	5.72	4.09
		190	22.46	3.19	5.62	4.86
		195	22.67	3.18	5.74	4.75
		200	22.61	3.13	5.56	4.42
		205	21.81	3.11	5.69	4.12
		210	21.81	3.14	5.78	10.03
		225	21.75	3.12	5.87	2.14
		230	22.31	3.15	5.92	7.43
		235	22.28	3.14	5.86	1.81
		240	21.80	3.12	5.99	1.23
		245	22.02	3.14	5.61	1.83
		250	22.17	3.17	5.89	4.69
		265	21.48	3.10	5.87	2.31
		270	21.79	3.14	5.72	1.27
		275	22.15	3.14	5.58	1.49
		280	21.40	3.05	5.75	3.64
		285	21.69	3.10	5.66	1.30
		290	21.89	3.13	5.91	1.49
		305	20.96	3.04	5.79	1.95
		310	21.57	3.07	5.85	1.38
		315	20.99	2.96	5.70	1.66
		320	21.03	3.03	5.80	2.05
		325	21.50	3.08	5.76	4.02
		330	21.57	3.07	5.79	1.29
		345	21.09	3.01	5.71	1.40
		350	21.34	3.05	5.61	3.18
		355	21.63	3.07	5.84	1.96
		360	21.54	3.07	5.70	1.86
		365	21.46	3.04	5.81	1.53
		370	21.54	3.07	5.75	5.64

Table III Permeability and flux of Desal AG membrane in the filtration of pure water and that with 5 ppm of surfactant 1 with Labstak M20 filter unit (20–24 ˚C, 0.42 m/s) and the conductivity and pH of permeate. The conductivity and pH of used feed solution is presented in table VI.

filtration phase	pressure, bar	time, h	flux, L/m^{2}h	permeability, L/m^{2}hbar	pH, -	conductivity, µS/cm
PW	3.5	40	12,67	3,64	-	-
		45	12,82	3,63	-	-
		50	12,99	3,69	-	-
		55	12,88	3,70	-	-
		60	13,02	3,69	-	-
		65	13,04	3,73	-	-
		80	13,27	3,78	-	-
		85	13,26	3,79	-	-
		90	13,57	3,79	-	-
		95	13,23	3,78	-	-
		100	13,45	3,80	-	-
		105	13,33	3,81	-	-
		120	13,32	3,79	-	-
		125	13,45	3,83	-	-
		130	13,40	3,84	-	-
		135	13,51	3,85	-	-
		140	13,50	3,84	-	-
		145	13,56	3,86	-	-
surfactant 1, 5 ppm	3.5	185	12.74	3.62	6.10	3.63
		190	12.60	3.65	6.16	2.13
		195	12.66	3.66	6.07	1.89
		200	12.81	3.67	6.23	2.03
		205	12.86	3.67	6.40	2.08
		210	12.87	3.67	6.41	2.38
		225	12.50	3.65	6.20	2.03
		230	12.75	3.64	6.20	2.05
		235	12.90	3.67	6.40	1.83
		240	12.76	3.67	6.32	2.12
		245	12.90	3.68	6.28	1.95
		250	12.63	3.60	6.41	2.10
		265	12.61	3.58	6.18	1.94
		270	12.43	3.59	6.28	1.90
		275	12.57	3.62	6.12	2.25
		280	12.64	3.61	6.20	2.38
		285	12.73	3.64	6.15	1.82
		290	12.57	3.56	5.70	2.15
		305	12.36	3.56	5.98	2.36
		310	12.46	3.56	6.12	1.78
		315	12.60	3.59	6.19	1.72
		320	12.63	3.57	5.99	1.86
		325	12.19	3.50	5.97	1.96
		330	12.09	3.44	6.18	1.84
		345	12.35	3.52	6.00	1.94
		350	12.58	3.57	5.99	1.64
		355	12.48	3.55	5.98	2.03
		360	12.58	3.56	6.01	1.87
		365	12.42	3.52	5.93	1.80
		370	12.37	3.53	5.85	1.70

Table IV pH and conductivity of feed solution in the filtration of pure water and that with 5 ppm of surfactant 1 Labstak M20 filter unit (19–24 ˚C, 0.14 m/s, 7 bar).and that with 2 ppm of surfactant 1 Labstak M20 filter unit (19–24 ˚C, 0.14 m/s, 7 bar).

filtration phase	pressure, bar	feed pH, -	feed conductivity, µS/cm
PW	at the start	6.15	3.16
	at the end	6.07	3.46
surfactant 1,	at the start	6.04	4.56
2 ppm	at the end	6.32	5.41

Table V pH and conductivity of feed solution in the filtration of pure water

filtration phase	pressure, bar	feed pH, -	feed conductivity, µS/cm
PW	at the start	6.30	2.65
	at the end	5.78	3.15
surfactant 1,	at the start	5.76	4.38
5 ppm	at the end	5.86	5.25

Table VI pH and conductivity of feed solution in the filtration of pure water and that with 5 ppm of surfactant 1 Labstak M20 filter unit (19–24 ˚C, 0.14 m/s, 3.5 bar).

filtration phase	pressure, bar	feed pH, -	feed conductivity, µS/cm
PW	at the start	6.09	1.45
	at the end	6.00	1.73
surfactant 1,	at the start	5.88	2.70
5 ppm	at the end	5.94	3.10

Table I Permeability and flux of LE-4040 membrane in the filtration of pure water and that with 2 ppm of surfactant 1, 2 and 3 with DSS Labstak M20 filter (pH ~6, 20–24 ˚C, 0.42 m/s).

filtration phase	pressure, bar	time, h	flux, L/m^2h	permeability, L/m^2hbar
pressurization	15	0.1	103.20	6.70
		0.5	97.28	6.40
		1.0	110.92	7.31
		1.5	92.16	6.12
		2.0	89.50	5.94
compression	25–30	2.1	146.97	5.67
		2.5	143.24	5.53
		3.0	141.12	5.31
		3.5	135.13	5.22
		4.0	135.49	5.21
PW_a	15	4.2	82.45	5.37
		5.0	80.50	5.35
		6.0	78.73	5.25
		20.1	75.84	5.05
		20.5	74.95	5.06
		21.0	76.17	5.03
surfactant 1 2 ppm	15	21.5	75.17	4.98
		22.0	74.82	4.96
		22.5	74.19	4.92
		23.0	73.46	4.86
PW_b	15	23.1	68.13	4.53
		23.5	72.13	4.78
		24.0	71.77	4.81
		24.5	73.88	4.86
		25.0	74.16	4.90
surfactant 2	15	25.5	71.69	4.75
		26.0	71.20	4.74
		26.5	71.31	4.72
		27.0	70.47	4.67
PW_c	15	27.1	68.57	4.56
		27.5	72.89	4.84
		28.0	75.16	4.97
		28.5	71.80	4.77
		29.0	72.82	4.85
surfactant 3	15	29.5	52.56	3.49
		30.0	47.86	3.17
		30.5	45.35	3.04
		31.0	44.76	2.99

Table II Permeability and flux of LE-4040 membrane in the filtration of pure water and that with 2 ppm of surfactant 1, 2 and 3 with DSS Labstak M20 filter (pH ~6, 20–24 ˚C, 0.14 m/s).

filtration phase	pressure, bar	time, h	flux, L/m^2h	permeability, L/m^2hbar
pressurization	15	0.1	83.26	5.53
		0.5	78.51	5.25
		1.0	75.13	4.88
		1.5	72.23	4.78
		2.0	70.92	4.70
compression	25–30	2.1	117.11	4.47
		2.5	109.28	4.20
		3.0	104.87	4.09
		3.5	103.56	3.96
		4.0	100.06	3.87
PW_a	15	4.1	60.19	3.96
		5.0	58.74	3.92
		6.0	59.81	3.97
		21.5	53.61	3.56
		22.0	52.94	3.56
		22.5	53.03	3.55
surfactant 1 2 ppm	15	23.0	51.75	3.50
		23.5	51.74	3.46
		24.0	51.84	3.46
		24.5	51.92	3.45
PW_b	15	24.6	54.34	3.57
		25.0	54.33	3.59
		25.5	53.56	3.56
		26.0	54.38	3.58
		26.5	53.71	3.56
surfactant 2	15	27.0	51.86	3.46
		27.5	51.63	3.45
		28.0	51.50	3.42
		28.5	51.49	3.42
PW_c	15	28.6	50.49	3.31
		29.0	50.64	3.38
		29.5	51.21	3.44
		30.0	52.31	3.47
		30.5	52.52	3.48
surfactant 3	15	31.0	41.24	2.73
		31.5	39.11	2.58
		32.0	37.93	2.53
		32.5	37.32	2.46

Table I Permeability and flux of LE-4040 membranes in the filtration of pure water and that with 2 ppm of surfactant 1 at pH 6 and pure water with marine salt (2 g/L) with DSS Labstak M20 filter (19–24 ˚C, 0.14 m/s).

filtration phase	pressure, bar	time, h	flux, L/m^2h	permeability, L/m^2hbar
surfactant 1	1	0.5	7.61	7.53
		1.0	7.77	7.77
		2.0	7.15	7.08
		17.0	6.02	5.84
		17.5	5.92	5.87
		18.0	5.92	5.86
compression	25–30	18.1	122.28	4.61
		18.5	112.64	4.33
		19.0	109.24	4.19
		19.5	106.20	4.05
		20.0	104.83	3.99
PW_a	15	20.1	64.42	4.25
		20.5	65.35	4.31
		21.0	64.60	4.31
		21.5	64.41	4.30
		22.0	65.41	4.33
marine salt 2000 ppm	15	22.1	52.22	3.45
		22.5	52.41	3.46
		23.0	51.35	3.41
		23.5	50.51	3.38
		24.0	51.21	3.37
PW_b	15	24.1	62.66	4.14
		24.5	63.21	4.19
		25.0	62.74	4.19
		25.5	62.19	4.17
		26.0	62.34	4.02

Table II pH and conductivity of the feed solution and the permeate and the determined membrane salt rejection with ion chromatography in the filtration of pure water with 2 ppm of surfactant 1 and pure water with marine salt (2 g/L) with DSS Labstak M20 filter (19–24 ˚C, 0.14 m/s).

		permeate			feed	
filtration phase	time, h	pH	conductivity, µS/cm (25 ˚C)	rejection, %	pH	conductivity, µS/cm (25 ˚C)
surfactant 1, 2 ppm	0.5	6.48	69.10		6.04	66.10
	18.0				6.10	119.50
compression	18.1	6.28	13.84		-	-
	20.0	6.06	37.73		6.06	17.95
marine salt 2000 ppm	22.1	5.70	513.00	86.89	5.59	3856.00
	22.5	5.68	380.10	91.39	5.63	4056.00
	23.0	5.81	389.00	91.08	-	-
	23.5	5.78	447.00	89.58	-	-
	24.0	5.71	368.10	91.62	5.72	4134.00

Table III Permeability and flux of LE-4040 membranes in the filtration of pure water and that with 2 ppm of surfactant 1 at pH 11 and pure water with marine salt (2 g/L) with DSS Labstak M20 filter (19–24 ˚C, 0.14 m/s).

filtration phase	pressure, bar	time, h	flux, L/m^2h	permeability, L/m^2hbar
surfactant 1	1	0.5	6.58	6.51
		1.0	6.45	6.39
		2.0	6.35	6.35
		17.0	5.13	5.13
		17.5	5.13	5.13
		18.0	5.04	5.04
compression	25–30	18.1	117.49	4.44
		18.5	103.52	3.99
		19.0	99.99	3.85
		19.5	95.49	3.68
		20.0	94.44	3.61
PW_a	15	20.1	59.32	3.92
		20.5	56.78	3.81
		21.0	57.09	3.79
		21.5	62.37	4.12
		22.0	57.70	3.84
marine salt 2000 ppm	15	22.0	46.28	3.02
		22.5	45.27	3.03
		23.0	43.66	2.92
		23.5	41.48	2.80
		24.0	41.30	2.77
PW_b	15	24.1	53.47	3.52
		24.5	51.62	3.45
		25.0	53.19	3.47
		25.5	51.76	3.46
		26.0	51.09	3.45

Table IV pH and conductivity of feed solution and permeate and the determined membrane salt rejection with ion chromatography in the filtration of pure water with 2 ppm of surfactant 1 and pure water with marine salt (2 g/L) with DSS Labstak M20 filter (19–24 ˚C, 0.14 m/s).

		permeate			feed	
filtration phase	time, h	pH	conductivity, µS/cm (25 ˚C)	rejection, %	pH	conductivity, µS/cm (25 ˚C)
surfactant 1, 2 ppm	0.5	10.16	92.12		10.70	217.00
	18.0	9.09	45.71		10.30	177.10
compression	18.1	9.03	26.11		-	-
	20.0	8.03	35.08		10.18	175.40
marine salt 2000 ppm	22.1	5.54	543.80	85.42	5.95	3.55
	22.5	5.68	406.00	91.15	5.94	4.26
	23.0	5.62	402.30	91.02	-	-
	23.5	5.72	398.00	91.31	-	-
	24.0	5.47	400.40	91.29	6.06	4.35

Table I Permeability and flux of LE-4040 membranes in the filtration of pure water and that with 2 ppm of surfactant 2 at pH 6 and pure water with marine salt (2 g/L) with DSS Labstak M20 filter (19–24 ˚C, 0.14 m/s).

filtration phase	pressure, bar	time, h	flux, L/m^2h	permeability, L/m^2hbar
surfactant 2	1	0.5	7.23	7.23
		1.0	7.37	7.37
		2.0	7.09	7.02
		17.0	6.44	6.31
		17.5	6.45	6.32
		18.0	6.40	6.27
compression	25–30	18.1	123.70	4.73
		18.5	111.07	4.26
		19.0	106.96	4.09
		19.5	103.13	3.98
		20.0	101.36	3.92
PW_a	15	20.1	66.98	4.43
		20.5	65.95	4.38
		21.0	67.35	4.50
		21.5	67.05	4.50
		22.0	67.77	4.49
marine salt 2000 ppm	15	22.1	54.54	3.64
		22.5	31.38	2.07
		23.0	27.04	1.79
		23.5	26.26	1.76
		24.0	26.34	1.76
PW_b	15	24.1	69.43	4.61
		24.5	67.64	4.55
		25.0	68.53	4.53
		25.5	67.17	4.48
		26.0	66.51	4.45

Table II pH and conductivity of feed solution and permeate and the determined membrane salt rejection with ion chromatography in the filtration of pure water with 2 ppm of surfactant 2 and pure water with marine salt (2 g/L) with DSS Labstak M20 filter (19–24 ˚C, 0.14 m/s).

		permeate			feed	
filtration phase	time, h	pH	conductivity, µS/cm (25 ˚C)	rejection, %	pH	conductivity, µS/cm (25 ˚C)
surfactant 2, 2 ppm	0.5	6.08	199.30		5.63	15.85
	18.0	6.26	16.06		5.74	34.17
compression	18.1	6.00	7.53		-	-
	20.0	6.37	21.34		5.72	10.79
marine salt 2000 ppm	22.1	6.10	478.30	88.78	6.30	4191.00
	22.5	6.00	438.50	89.95	5.85	4145.00
	23.0	5.89	420.00	90.33	-	-
	23.5	5.88	422.00	90.39	-	-
	24.0	5.84	428.40	90.17	5.71	4091.00

Table I Permeability and flux of LE-4040 membranes in the filtration of pure water and that with 2 ppm of surfactant 3 at pH 6 and pure water with marine salt (2 g/L) with DSS Labstak M20 filter (19–24 ˚C, 0.14 m/s).

filtration phase	pressure, bar	time, h	flux, L/m^2h	permeability, L/m^2hbar
surfactant 3	1	0.5	3.92	3.84
		1.0	3.66	3.66
		2.0	3.47	3.44
		17.0	2.60	2.65
		17.5	2.75	2.72
		18.0	2.68	2.65
compression	25–30	18.1	59.31	2.27
		18.5	54.88	2.12
		19.0	54.20	2.08
		19.5	53.69	2.07
		20.0	53.36	2.06
PW_a	15	20.1	34.99	2.29
		20.5	35.31	2.35
		21.0	35.56	2.37
		21.5	36.23	2.40
		22.0	35.84	2.39
marine salt 2000 ppm	15	22.1	31.04	1.97
		22.5	29.74	1.94
		23.0	28.69	1.92
		23.5	29.11	1.90
		24.0	28.54	1.90
PW_b	15	24.1	34.82	2.31
		24.5	35.95	2.39
		25.0	33.20	2.22
		25.5	36.29	2.43
		26.0	36.67	2.44

Table II pH and conductivity of feed solution and permeate and the determined membrane salt rejection with ion chromatography in the filtration of pure water with 2 ppm of surfactant 3 and pure water with marine salt (2 g/L) with DSS Labstak M20 filter (19–24 ˚C, 0.14 m/s).

		permeate			feed	
filtration phase	time, h	pH	conductivity, µS/cm (25 ˚C)	rejection, %	pH	conductivity, µS/cm (25 ˚C)
surfactant 3, 2 ppm	0.5	5.75	34.34		5.24	19.51
	18.0	5.90	36.06		5.55	9.39
compression	18.1	5.53	29.33		-	-
	20.0	5.36	23.28		5.56	6.30
marine salt 2000 ppm	22.1	5.38	476.30	90.43	5.65	4558.00
	22.5	5.48	421.70	91.04	5.69	4227.00
	23.0	5.30	406.50	91.06	-	-
	23.5	5.50	387.00	91.49	-	-
	24.0	5.58	393.50	91.55	5.60	4307.00

Table III Permeability and flux of LE-4040 membranes in the filtration of pure water and that with 2 ppm of surfactant 3 at pH 11 and pure water with marine salt (2 g/L) with DSS Labstak M20 filter (19–24 ˚C, 0.14 m/s).

filtration phase	pressure, bar	time, h	flux, L/m^2h	permeability, L/m^2hbar
surfactant 3	1	0.5	5.41	5.30
		1.0	4.99	4.94
		2.0	4.74	4.79
		17.0	3.15	3.09
		17.5	3.22	3.19
		18.0	3.28	3.17
compression	25–30	18.1	62.27	2.39
		18.5	56.08	2.17
		19.0	54.66	2.10
		19.5	53.27	2.04
		20.0	53.26	2.02
PW_a	15	20.1	36.04	2.38
		20.5	36.25	2.43
		21.0	36.52	2.45
		21.5	37.05	2.47
		22.0	36.89	2.47
marine salt 2000 ppm	15	22.1	30.81	1.99
		22.5	29.87	1.99
		23.0	29.16	1.97
		23.5	28.93	1.94
		24.0	30.25	1.94
PW_b	15	24.1	38.29	2.49
		24.5	37.45	2.48
		25.0	38.40	2.50
		25.5	36.90	2.49
		26.0	37.27	2.50

Table IV pH and conductivity of feed solution and permeate and the determined membrane salt rejection with ion chromatography in the filtration of pure water with 2 ppm of surfactant 3 and pure water with marine salt (2 g/L) with DSS Labstak M20 filter (19–24 ˚C, 0.14 m/s).

		permeate			feed	
filtration phase	time. h	pH	conductivity. µS/cm (25 ˚C)	rejection, %	pH	conductivity. µS/cm (25 ˚C)
surfactant 3. 2 ppm	0.5	10.06	86.99		10.76	202.60
	18.0	8.41	173.10		9.85	188.20
compression	18.1	8.14	116.80		-	-
	20.0	6.75	102.70		9.94	165.70
marine salt 2000 ppm	22.1	5.45	701.00	85.66	5.86	4492.00
	22.5	5.61	591.00	86.60	6.06	4279.00
	23.0	5.75	591.90	86.43	-	-
	23.5	5.50	598.40	86.27	-	-
	24.0	5.63	555.00	87.47	6.08	4190.00

Table V Permeability and flux of LE-4040 membranes in the filtration of pure water and that with 2 ppm of surfactant 3 at pH 4.4 and pure water with marine salt (2 g/L) with DSS Labstak M20 filter (19–24 ˚C, 0.14 m/s).

filtration phase	pressure, bar	time, h	flux, L/m^2h	permeability, L/m^2hbar
surfactant 3	1	0.5	4.68	4.68
		1.0	4.23	4.14
		2.0	3.81	3.61
		17.0	2.85	2.71
		17.5	2.78	2.72
		18.0	2.88	2.71
compression	25–30	18.1	58.24	2.22
		18.5	54.28	2.08
		19.0	52.93	2.03
		19.5	51.46	1.98
		20.0	51.42	1.97
PW_a	15	20.1	33.90	2.20
		20.5	33.75	2.28
		21.0	35.28	2.33
		21.5	35.95	2.39
		22.0	36.76	2.45
marine salt 2000 ppm	15	22.1	28.64	1.90
		22.5	30.04	2.00
		23.0	29.99	2.00
		23.5	30.50	2.03
		24.0	30.06	2.01
PW_b	15	24.1	37.21	2.47
		24.5	38.26	2.54
		25.0	38.49	2.55
		25.5	37.96	2.56
		26.0	38.39	2.59

Table VI pH and conductivity of feed solution and permeate and the determined membrane salt rejection with ion chromatography in the filtration of pure water with 2 ppm of surfactant 3 and pure water with marine salt (2 g/L) with DSS Labstak M20 filter (19–24 ˚C. 0.14 m/s).

		permeate			feed	
filtration phase	time. h	pH	conductivity. µS/cm (25 ˚C)	rejection, %	pH	conductivity. µS/cm (25 ˚C)
surfactant 3. 2 ppm	0.5	4.65	62.55		4.36	62.39
	18.0	4.91	70.85		4.60	247.50
compression	18.1	5.29	44.68		-	-
	20.0	5.33	72.85		4.63	59.83
marine salt 2000 ppm	22.1	5.30	696.40	79.06	5.61	3132.00
	22.5	5.51	479.30	90.67	5.58	4676.00
	23.0	5.52	419.30	91.95	-	-
	23.5	5.55	412.50	92.12	-	-
	24.0	5.36	423.00	91.01	5.56	4247.00

Table I Permeability and flux of LE-4040 membranes in the filtration of pure water and that with marine salt (2 g/L) with DSS Labstak M20 filter (19–24 ˚C, 0.14 m/s).

filtration phase	pressure, bar	time, h	flux, L/m^2h	permeability, L/m^2hbar
pure water	1	0.5	6.97	6.94
		1.0	6.99	6.75
		2.0	6.81	6.88
		17.0	6.27	6.34
		17.5	6.29	6.35
		18.0	6.77	6.77
compression	25–30	18.1	131.45	5.05
		18.5	122.53	4.69
		19.0	119.61	4.58
		19.5	116.64	4.53
		20.0	115.43	4.45
PW_a	15	20.1	71.92	4.62
		20.5	68.87	4.64
		21.0	72.69	4.63
		21.5	68.21	4.59
		22.0	68.15	4.59
marine salt 2000 ppm	15	22.1	53.22	3.57
		22.5	53.69	3.60
		23.0	53.49	3.55
		23.5	52.82	3.55
		24.0	52.29	3.49
PW_b	15	24.1	38.29	2.51
		24.5	37.45	2.50
		25.0	38.40	2.54
		25.5	36.90	2.48
		26.0	37.27	2.50

Table II pH and conductivity of feed solution and permeate and the determined membrane salt rejection with ion chromatography in the filtration of pure water with 2 ppm of surfactant 3 and pure water with marine salt (2 g/L) with DSS Labstak M20 filter (19–24 ˚C. 0.14 m/s).

		permeate			feed	
filtration phase	time. h	pH	conductivity. µS/cm (25 ˚C)	rejection, %	pH	conductivity. µS/cm (25 ˚C)
pure water, 2 ppm	0.5	6.11	10.62		5.79	8.86
	18.0	5.97	14.55		6.07	10.51
compression	18.1	-	-		-	-
	20.0	-	-		-	-
marine salt 2000 ppm	22.1	5.57	513.30	87.84	5.65	3997.00
	22.5	5.65	432.70	90.51	5.64	4174.00
	23.0	5.59	434.50	90.55		
	23.5	5.50	427.00	90.75		
	24.0	5.64	426.20	90.84	5.76	4273.00